NEUTRON THERMALIZATION IN SOLIDS

Thesis by

Kaye Don Lathrop

In Partial Fulfillment of the Requirements
For the Degree of
Doctor of Philosophy

California Institute of Technology
Pasadena, California

1962

ACKNOWLEDGEMENTS

The author is very grateful for the guidance and supervision of Dr. Harold Lurie, who directed the research of the thesis, and wishes to thank Dr. Milton Plesset for suggesting the basic oscillator model developed in the thesis and for numerous helpful discussions.

The author gratefully acknowledges financial support from the following sources: Atomic Energy Commission Special Fellowships in Nuclear Science and Engineering for 1958-61, and the R. C. Baker Foundation Fellowship for 1961-62.

A portion of the numerical computations of the thesis were made possible by the facilities of the Western Data Processing Center of the University of California at Los Angeles.

ABSTRACT

To describe neutron thermalization in solid media, two simplified models are formulated to describe the motions of atoms bound in solids. One atomic model postulates that the atoms of solids are linear, classical, randomly oriented, harmonic oscillators characterized by a single energy; and the other model postulates the same basic oscillator but permits a distribution of oscillator energies. With atom speed distributions derived from these models, energy exchange cross sections are evaluated analytically assuming a free particle neutron-atom interaction. With these energy exchange cross sections, integral equations are formulated describing thermalization of neutrons in infinite homogeneous media containing a 1/v absorber. The integral equations of both atomic models are solved numerically for the neutron density speed distribution. Numerical results for the single energy atomic oscillator of unit mass are compared with experimental results for neutron thermalization in zirconium hydride. Results for the averaged energy atomic oscillator of unit mass are compared with the neutron density calculated from the Wigner-Wilkins monatomic gas model. This comparison is made for three values of absorption. Numerical results for averaged energy atomic oscillators of masses 1, 2, 9, and 12 are examined to determine the effect of atomic mass upon the neutron density distribution.

NOTATION

σ_s	Microscopic scattering cross section
σ_a	Microscopic absorption cross section
N	Atomic density
n	Neutron density
Φ	Neutron flux
E	Neutron energy
w	Neutron speed before a collision (laboratory system)
v	Neutron speed after a collision (laboratory system)
y	Dimensionless w
x	Dimensionless v
U	Maximum oscillator speed
E_o	Oscillator energy
u	Atom speed
v_r	Neutron-atom relative speed
v_c	Neutron-atom center of mass speed
θ	Angle between $\vec{w}$ and $\vec{u}$
μ	$\cos^{-1}\theta$
φ	Spherical coordinates radial angle
Ω	Solid angle $d\Omega = d\mu d\varphi$
θ_c	Center of mass angle between $\vec{v}_c$ and neutron velocity after a collision
μ_c	$\cos^{-1}\theta_c$
φ_c	Radial angle in center of mass system
Ω_c	Solid angle in center of mass system: $d\Omega_c = d\mu_c d\varphi_c$

M_o	Maxwellian distribution
M	Distribution of atom speeds
$P(w \to v)$	Collision probability
$V(v)$	Average collision rate
m	Atomic mass measured in units of neutron mass
γ	$\frac{\sigma_a(v_r)v_r}{\sigma_s}$
Δ	Dimensionless γ
$c_o, c_1, \ldots$	Arbitrary constants
k	Boltzmann constant
T	Temperature
Θ_D	Debye characteristic temperature
Θ_E	Einstein characteristic temperature

ABBREVIATIONS

a	$\frac{m+1}{2m}$
c	$\frac{m-1}{2m}$
b	$1/\sqrt{2kT}$
α	$\sqrt{m}\,(av + cw)$
β	$\sqrt{m}\,(aw + cv)$
$\varkappa$	$\sqrt{m}\,(av - cw)$
λ	$\sqrt{m}\,(aw - cv)$

TABLE OF CONTENTS

INTRODUCTION

The primary analytical goal in the study of assemblies containing neutrons is the determination of the neutron density distribution, for all neutron-nucleus reaction rates are proportional to the neutron density. Neutron thermalization theory attempts to describe the neutron distribution when the neutrons have energies in the thermal range below one ev. In this energy range a neutron may gain as well as lose energy in a collision with a nucleus of the assembly, and the formulation of models to describe this energy interchange is fundamental to the theory of neutron thermalization.

Wigner and Wilkins (1), in the first work on neutron thermalization, postulated that the atoms of an infinite medium were a monatomic gas with a Maxwellian distribution of speeds. With this atom speed distribution they calculated the energy exchange cross sections necessary to formulate the integral equation expressing conservation of neutrons in the medium and numerically solved the balance equation for an infinite medium containing a monatomic hydrogen gas that had an absorption cross section inversely proportional to the neutron speed. Wilkins (2) subsequently simplified the equations for heavy monatomic gases. However, many of the materials of interest in nuclear reactors are not monatomic gases. In fact, crystalline solids such as graphite, beryllium and zirconium hydride are commonly used neutron moderators.

In media in which the atoms are chemically bound the

determination of the energy exchange cross sections is much more complicated than for gaseous media. In principle, the exact quantum mechanical energy exchange or scattering cross sections may be calculated for chemically bound atoms by means of the Fermi pseudo-potential approximation (3). This approximation replaces the actual interaction by a delta function interaction potential, V', which operates on $\partial(r\psi)/\partial r$ rather than on the wave function ψ, as would an ordinary potential. The calculation is described by Nelkin (4) who has applied this technique to water molecules (5), "To compute the scattering cross section it is necessary to calculate the matrix element of V' between initial and final plane wave neutron states, and initial and final states of the atomic system for a single scattering nucleus. This amplitude must then be summed over scattering nuclei, squared, and summed over final states of the scattering system consistent with energy conservation. Finally an average over a thermal equilibrium distribution of initial states must be performed. This is in general a complicated procedure and necessitates the use of powerful formal techniques as well as a certain number of approximations to carry out the calculation of the energy-transfer cross sections, even for systems in which the dynamical properties of the atomic motions are known exactly."

The work of this thesis is devoted to the development of idealized models for atomic motions to exhibit the effects of chemical binding in solid moderators. From these models, energy-transfer cross sections are derived and neutron conservation equations are formulated

and solved to determine the neutron density distributions.

Section I of the thesis contains a general discussion of the process of neutron thermalization and the development of the general equations determining the neutron density distributions.

Sections II and III are devoted to development of two different, but related, models of atomic motions, the calculation of the necessary energy exchange cross sections, and the formulation of specific equations governing the neutron density.

Section IV is a description of the numerical solution of the equations derived in Sections II and III. Section IV is supplemented by Appendix E which contains a description of less satisfactory attempts at numerical solution, and which displays the actual programs used for numerical solution. Section V is a discussion of the solutions and a comparison with experimental measurements.

Whenever extensive analysis is required in the derivation of results presented in the text of the thesis, the analysis is outlined in an appendix. Because the equation describing thermalization by monatomic gases served as a useful guide and standard of comparison throughout the analysis of the thesis, the Wigner-Wilkins (1) energy exchange cross sections are derived in Appendix A, and a brief summary of related work is given in Appendix B. Two simple descriptions of atomic motions and the resulting thermalization equations are discussed in Appendices F and G.

I. THE THERMALIZATION PROBLEM FOR AN ARBITRARY DISTRIBUTION OF ATOM SPEEDS

The Thermalization Process

If neutrons of a given energy distribution were introduced into an infinite, homogeneous, non-absorbing medium, the resulting neutron distribution at times sufficiently long after introduction would be an equilibrium Maxwellian distribution characterized by the final temperature of the medium. If the medium is absorbing or finite or inhomogeneous, however, there will usually be a deviation of the steady state neutron distribution from a Maxwellian distribution. (In the case of absorbing or finite media the source of neutrons is assumed to balance neutron losses so that a quasi-stationary distribution obtains.) If the medium is finite, neutrons of higher energy escape faster than neutrons of lower energy and the distribution is displaced towards lower energies. If the medium is inhomogeneous, either in temperature or composition, the distribution deviates from a Maxwellian due to transport of neutrons between the different regions of the medium. In both the finite and heterogeneous medium cases the neutron density distribution is a function of position in the medium as well as a function of the neutron energy. In the case of a neutron absorbing medium, the neutron distribution will deviate from an equilibrium distribution because of the finite time required for source neutrons to acquire the equilibrium distribution. With certain distributions of source neutrons there is no deviation from an equilibrium neutron distribution. This statement will be amplified subsequently.

Describing the neutron density in finite media, or in heterogeneous assemblies, necessitates the consideration of the spatial transport of neutrons. Several authors have attempted solutions of this complex problem using the Wigner-Wilkins scattering kernels. Kottwitz (6) solved the problem of an infinite non-absorbing medium with a temperature discontinuity using the heavy gas approximation of Wilkins. Michael (7) considered the general problem of finite media using the diffusion approximation for neutron spatial transport and carried out eigenfunction expansions for solutions using the heavy gas approximation. Hurwitz and Nelkin (8) investigated the problem of the effect of energy dependent escape probabilities on the neutron distribution in finite media, again using the heavy gas atomic model for quantitative results. More recently Honeck (9) computed numerical solutions for the neutron distribution in finite lattices using a variation of the Wigner-Wilkins scattering kernels. The variation, derived by Brown and St. John (10), assumes that the scattering mass of an atom in a chemically bound molecule can be represented by an effective mass assigned to a free atom and uses a three parameter fit of a calculated scattering cross section speed variation to match experimental data.

The consideration of neutron transport is essentially an extension, albeit an important one, of the neutron thermalization problem once suitable energy transfer cross sections are obtained. The analysis of the thesis is restricted to infinite homogeneous media in which the neutron density distribution is invariant with respect to position in the media.

Neutron Balance for an Infinite Homogeneous Medium

The neutron density distribution in speed and time in an infinite homogeneous absorbing medium is described, in the speed range dv, by a linearized* Boltzmann equation

$$\frac{\partial n(v,t)}{\partial t} = \int_0^\infty dw\, n(w,t) P_s(w \to v) + S(v,t)$$

$$-n(v,t)\left[\int_0^\infty dw P_s(v \to w) + P_a(v)\right], \qquad (1)$$

where $n(v,t)dv$ is the number of neutrons per unit volume in the speed range dv about v at time t. The quantity $P_s(w \to v)dv$ is defined as the average rate at which a neutron scattering event at w produces neutrons at speed v, so that the first term on the right of the equation represents the gain of neutrons at v due to scattering collisions at all other speeds w. $S(v,t)$ is the rate of production of neutrons at v from all sources, and the final two terms are the neutron loss rates from speed v due to scattering at v and absorption at v, respectively, $P_a(v)$ representing the average absorption rate per neutron. If the sources of neutrons are such that the neutron density is independent of time, conservation of neutrons requires that

$$\int_0^\infty dv \int_0^\infty dw\, n(w) P_s(w \to v) + \int_0^\infty dv S(v) = \int_0^\infty dv\, n(v) \int_0^\infty dw P_s(v \to w) + \int_0^\infty dv\, n(v) P_a(v), \qquad (2)$$

or upon interchanging the order of integration in the first term on the left

* The Boltzmann equation is linear due to neglect of neutron-neutron collisions (typical neutron densities are a factor of 10^7 less than atom densities) and due to the assumption that the neutrons do not appreciably affect the properties of the medium. See Wigner (11) page 91.

$$\int_0^\infty dv S(v) = \int_0^\infty dv\, n(v) P_a(v) . \tag{3}$$

Thus if the source distribution should be $P_a(v)M_o(v)$, where $M_o(v)$ is a Maxwellian distribution of speeds, then n(v) would be equal to $M_o(v)$. This is the exception to the previously mentioned deviation of the neutron distribution from a Maxwellian distribution in the presence of absorption. However, such a source is highly artificial. The spectrum of neutron speeds from the fission reaction source is not Maxwellian. Moreover the average energy of fission source neutrons is near 2 Mev, far higher than the average energies of Maxwellian distributions corresponding to material temperatures.

In the absence of absorption and a source the steady state neutron distribution is a Maxwellian, $M_o(v)$. The principle of microscopic reversibility imposes a condition on the scattering probabilities of equation 1 which holds in the presence of absorption. Known as detailed balancing, the condition is (see reference 12)

$$M_o(w)\, P_s(w \to v) = M_o(v)\, P_s(v \to w). \tag{4}$$

That is, the scattering rate from speed w to speed v is equal, in detail, to the scattering rate from speed v to speed w.

Energy Exchange Cross Sections

The rate at which neutrons of speed w interact with an atom of a medium is given by

$$n(w) v_r \sigma(v_r), \tag{5}$$

where n(w)dw is the number of neutrons per unit volume having speeds in

the range dw about w, and $\sigma(v_r)$ is an intrinsic atomic property, known as the microscopic cross section (it has the dimensions of area), which expresses the probability of an interaction. If the atoms have speed u, v_r is the neutron-atom relative speed,

$$v_r = \sqrt{w^2 + u^2 - 2uw\mu}, \tag{6}$$

where μ is the cosine of the angle θ between the neutron and atom velocity vectors $\vec{w}$ and $\vec{u}$. If an interaction results in a scattering of neutrons, the neutrons may transfer energy and momentum to the atoms of the medium or vice versa. In general the momentum of a neutron changes in a scattering collision, the neutron momentum after a collision depending upon the dynamics of collision. The dynamics of collision, if known, determine a conditional probability,

$$P(w \to v; u, \mu)dv, \tag{7}$$

that a neutron of initial speed w will acquire a final speed v in the range dv after undergoing a scattering interaction with an atom of speed u when the collision angle is θ. The rate per atom at which neutrons of initial speed w scatter to speed v is then

$$n(w)v_r\sigma_s(v_r)P(w \to v; u, \mu)dv, \tag{8}$$

where σ_s is the microscopic scattering cross section. The above expression is the scatter rate for specific u and μ. The average of equation 8 over possible atom speeds and orientations of $\vec{w}$ and $\vec{u}$ is the average scatter rate of neutrons from speed w to speed v,

$$n(w)P_s(w \to v)dv. \tag{9}$$

If any orientation of $\vec{w}$ and $\vec{u}$ is equally probable, then

$$P(\Omega)d\Omega = \frac{d\Omega}{4\pi} , \tag{10}$$

where $d\Omega$ is the differential solid angle from which $\vec{w}$ approaches $\vec{u}$,

$$d\Omega = d\varphi d\mu , \tag{11}$$

and φ is the radial angle of the orientation of $\vec{w}$ with respect to $\vec{u}$. If the motions of the atoms of the system can be characterized by a distribution of speeds M(u), then the average of expression 8 is

$$n(w)P_s(w\rightarrow v)dv = n(w)\int_0^{2\pi}\frac{d\varphi}{4\pi}\int_{-1}^{1}d\mu\int_0^{\infty}duM(u)v_r\sigma_s(v_r)P(w\rightarrow v;u,\mu)dv \tag{12}$$

so that

$$P_s(w\rightarrow v) = \int_{-1}^{1}\frac{d\mu}{2}\int_0^{\infty}duM(u)v_r\sigma_s(v_r)P(w\rightarrow v;u,\mu). \tag{13}$$

If it is assumed that scattering is isotropic in the center of mass system and that scattering is elastic (conservation of momentum and kinetic energy), $P(w\rightarrow v;u,\mu)$ may be derived as shown below.

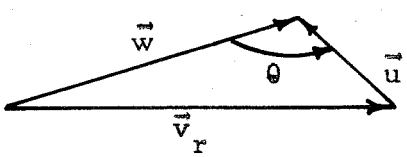

Laboratory System Before a Collision

Let the mass of the struck atom, m, be measured in units of neutron mass so that the mass of a neutron is unity. Conservation of momentum determines the velocity of the center of mass

$$(m+1)\vec{v}_c = \vec{w} + m\vec{u} . \tag{14}$$

The speed of the center of mass is seen from the diagram below

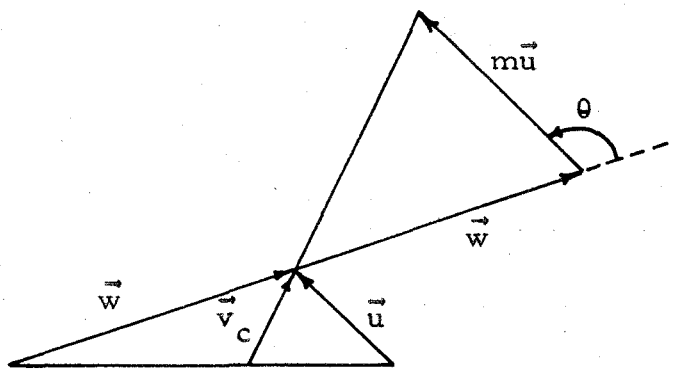

to be

$$v_c = |\vec{v}_c| = \frac{\sqrt{w^2+m^2u^2+2mwu\mu}}{m+1} . \qquad (15)$$

The assumption of an elastic collision means that in the center of mass system only the direction of the neutron and atom velocities will be changed by the collision.

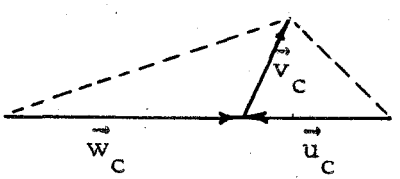

Center of Mass System Before a Collision

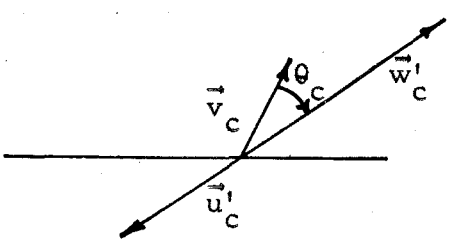

Center of Mass System After a Collision (The Primes Denote Velocities After a Collision)

The assumption of isotropic scattering in the center of mass provides that the probability of scatter into any solid angle Ω_c is equally likely, i.e.,

$$P(\Omega_c)d\Omega_c = \frac{d\Omega_c}{4\pi} \quad . \tag{16}$$

Since the scattering is axially symmetric about the direction of motion of the center of mass,

$$\int_0^{2\pi} P(\Omega_c)d\Omega_c = \int_0^{2\pi} \frac{\sin\theta_c d\theta_c d\varphi_c}{4\pi} = \frac{d\mu_c}{2} \quad , \tag{17}$$

where $\mu_c = \cos\theta_c$. The final velocity of the neutron is then $\vec{v} = \vec{w}_c' + \vec{v}_c$ where the prime indicates a velocity after the collision.

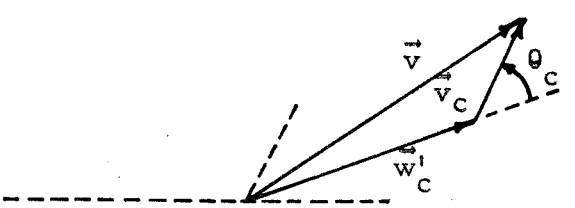

Neutron Speed in the Laboratory System After a Collision

From the above diagram,

$$v^2 = v_c^2 + w_c^2 + 2v_c w_c \mu_c \quad . \tag{18}$$

Since the neutron speed in the center of mass system before and after the collision is

$$w_c = \left|\vec{w} - \vec{v}_c\right| = \frac{mv_r}{m+1} \tag{19}$$

equation 18 becomes

$$v^2 = v_c^2 + \frac{m^2 v_r^2}{(m+1)^2} + \frac{2mv_c v_r \mu_c}{m+1} . \tag{20}$$

From this expression

$$\frac{d\mu_c}{2} = \frac{(m+1)vdv}{2mv_c v_r} = \frac{2vdv}{v_{max}^2 - v_{min}^2} . \tag{21}$$

Once the atom speed, u, and the cosine of the collision angle, μ, are specified and a collision occurs, a range of final neutron speeds, v, is possible. For a given μ and u, then, v_{max} in equation 21 is the maximum possible neutron speed after collision ($\theta_c = 0$, $\mu_c = 1$); and v_{min} is the minimum possible neutron speed after collision ($\theta_c = \pi$, $\mu_c = -1$). The values of these bounds on the final neutron speed are, from equation 20,

$$v_{max} = v_c + \frac{mv_r}{m+1} , \tag{22}$$

$$v_{min} = \left| v_c - \frac{mv_r}{m+1} \right| .$$

Expression 21 is the required conditional probability. It is properly normalized to unity.

$$\int_{-1}^{1} \frac{d\mu_c}{2} = \int_{v_{min}}^{v_{max}} \frac{2vdv}{v_{max}^2 - v_{min}^2} = 1. \tag{23}$$

Therefore, $P(w \to v; u, \mu)$ is defined by

$$P(w\to v;u,\mu) = \left\{ \begin{array}{ll} 0 & v < v_{min} \\ \dfrac{2v}{v_{max}^2 - v_{min}^2} & v_{min} \le v \le v_{max} \\ 0 & v_{max} < v \end{array} \right\} . \qquad (24)$$

When the struck atom is at rest this expression reduces to a probability customarily derived, (Ref. 13),

$$P(w\to v;0) = \left\{ \begin{array}{ll} 0 & v < \dfrac{m-1}{m+1} w \\ \dfrac{(m+1)^2 v}{2mw^2} & \dfrac{m-1}{m+1} w < v < w \\ 0 & w < v \end{array} \right\} . \qquad (25)$$

With the conditional probability determined, equation 13 becomes

$$P_s(w\to v) = \frac{(m+1)v}{4m} \int\int d\mu \frac{du\, M(u)\, \sigma_s(v_r)}{v_c} , \qquad (26)$$

where the limits of integration have been omitted because the vanishing of the conditional probability for the limits given in 24 restricts the domain of integration in the u-μ plane.

The term $\int_0^\infty dw\, P_s(v\to w)$ occurring in equation 1 may be evaluated by calculating $P_s(v\to w)$ from 26 and then integrating over w. However, it is simpler and more illuminating to carry out the integration over w first. From equation 13

$$\int_0^\infty dw P_s(v\to w) = \int_{-1}^{1} \frac{d\mu}{2} \int_0^\infty du\, M(u) v_r \sigma_s(v_r) \int_{w_{min}}^{w_{max}} dw P(v\to w;u,\mu) . \qquad (27)$$

But the only function containing w is the conditional probability since the neutron speed after these collisions is w and $v_r = \sqrt{v^2+u^2-2uvu}$. The conditional probability is normalized so that

$$\int_0^\infty dw P_s(v\to w) = \int_{-1}^{1} \frac{du}{2} \int_0^\infty du M(u) v_r \sigma_s(v_r) . \tag{28}$$

The above expression is an average, over all atom speeds and collision angles, of the scatter rate per neutron at speed v. A similar expression serves to define $P_a(v)$, the average absorption rate per neutron,

$$P_a(v) = \int_{-1}^{1} \frac{du}{2} \int_0^\infty du M(u) v_r \sigma_a(v_r) , \tag{29}$$

where σ_a is the microscopic absorption cross section of the medium.

Two further assumptions permit a considerable simplification. First the microscopic scattering cross section is taken to be constant, and second, the microscopic absorption cross section is assumed to be inversely proportional to the relative encounter speed. Equation 26 becomes

$$P_s(w\to v) = \frac{(m+1)v\sigma_s}{4m} \iint du\, du\, \frac{M(u)}{v_c} , \tag{30}$$

equation 28 becomes

$$\int_0^\infty dw P_s(v\to w) = \sigma_s \int_{-1}^{1} \frac{du}{2} \int_0^\infty du\, M(u) v_r , \tag{31}$$

and, because of the normalization of M(u), $P_a(v)$ is given by

$$P_a(v) = v\sigma_a(v),$$

which is a constant.

Except for the determination of the limits of integration in equation 30, a specification of an atom speed distribution permits the calculation of all the unknown terms in the neutron balance equation 1. Before examining the limits of integration, the validity of the assumptions made in the above derivation is discussed.

Validity of Assumptions

The assumption of random orientation of the neutron velocity $\vec{w}$ with respect to the direction of the atom velocity $\vec{u}$ is quite reasonable. Even if the motion of the atoms is constrained by chemical binding, the neutrons will, on the average, approach the atoms from all directions randomly. The properties assumed for the microscopic scattering and absorption cross sections are displayed experimentally in the thermal energy range for many materials of practical interest. Theoretical derivations of these properties are given by Weinberg and Wigner (14). There is an effective 1/v dependence of the scattering cross section on the neutron speed at thermal energies. This dependence is contained in equation 31, however, and will be displayed explicitly in Part II of the thesis. Scattering in the center of mass system here taken may not be isotropic for strongly bound systems. Precisely, the center of mass system should be that of the entire scattering assembly rather than that of the neutron-atom combination.

By far the poorest assumption is that of an elastic collision. At low neutron speeds the collisions with chemically bound molecules are inelastic. If the atom struck by a neutron is part of a molecule,

the neutron may excite rotational or vibrational states in the molecule. If the struck atom is part of a crystal lattice, the neutron may interact inelastically with the acoustical modes of vibration of the entire lattice (neutron-phonon interactions). The interactions described above are highly complex and not easily formulated theoretically (4). The approach of the work described in this thesis is to postulate an atom speed distribution to account for atomic binding, and then to treat the atoms as free particles. Once a free particle interaction is assumed the assumption of elastic scattering is completely valid in the neutron energy range 0-1 ev, and the center of mass system is that of the neutron and atom.

Domain of Integration in the u-μ Plane

In equation 24, the vanishing of P in certain ranges restricts the permissible values of u and μ. From a different viewpoint, only certain combinations of u and μ can produce neutrons of final speed v. This can most easily be seen for specific examples. Consider an overtaking collision ($\mu = +1$). $v \leq v_{max}$ of equation 22 then is

$$v \leq \frac{w+mu}{m+1} + \frac{m|w-u|}{m+1} \quad . \tag{33}$$

That is, $v \leq w$ if $w > u$ when $\mu = +1$. Therefore, if $\mu = +1$, and the initial speed of the neutron, w, is greater than the atom speed, u, the only final speeds of the neutron possible are less than the initial speeds. The expression $v = v_{max}$ is a hyperbola in the u-μ plane. (Once the square roots are rationalized $v = v_{min}$ is the same hyperbola.) The hyperbola is most easily recognized after the transformation of variables

$$u = u \tag{34}$$

$$v = 2mwu\mu + (m-1)(v^2-w^2) .$$

The Jacobian of the transformation is 2mwu. The hyperbola and the lines $\mu = \pm 1$ are shown in the u, v plane in figures 1 and 2. Arguments similar to those for the overtaking collision discussed above define the domain of integration as the shaded region shown in the figures. Two distinct cases arise, one for neutron speed gain in a collision, the other for neutron speed loss in a collision. The hyperbolas shown in the figures are conjugate with the equation

$$mu^2 - \frac{v^2}{4mv^2} = v^2 - w^2 . \tag{35}$$

The relative magnitude of w and v determines which hyperbola is applicable. For each main case ($v > w$ or $v < w$) there are three subregions of integration. These are indicated by the dotted lines in the figures. The lines $\mu = \pm 1$ have equal slopes of opposite sign in the u, v plane. When the atom mass is unity the lines intersect the origin and in each main case the subregions of integration labeled II disappear, considerably simplifying the integrations. If the atom mass is greater than unity only two subregions may exist for a different reason. In figure 1 the line $\mu = -1$ may intersect the u axis (point (e)) above the minimum value of the hyperbola (point (d)). In figure 2 the lines $\mu = \pm 1$ may intersect the v axis (point (f)) to the left of the left branch of the hyperbola. These special cases are significant as will be shown in Section III of the thesis.

With figures 1 and 2 and the equations of the lines and the

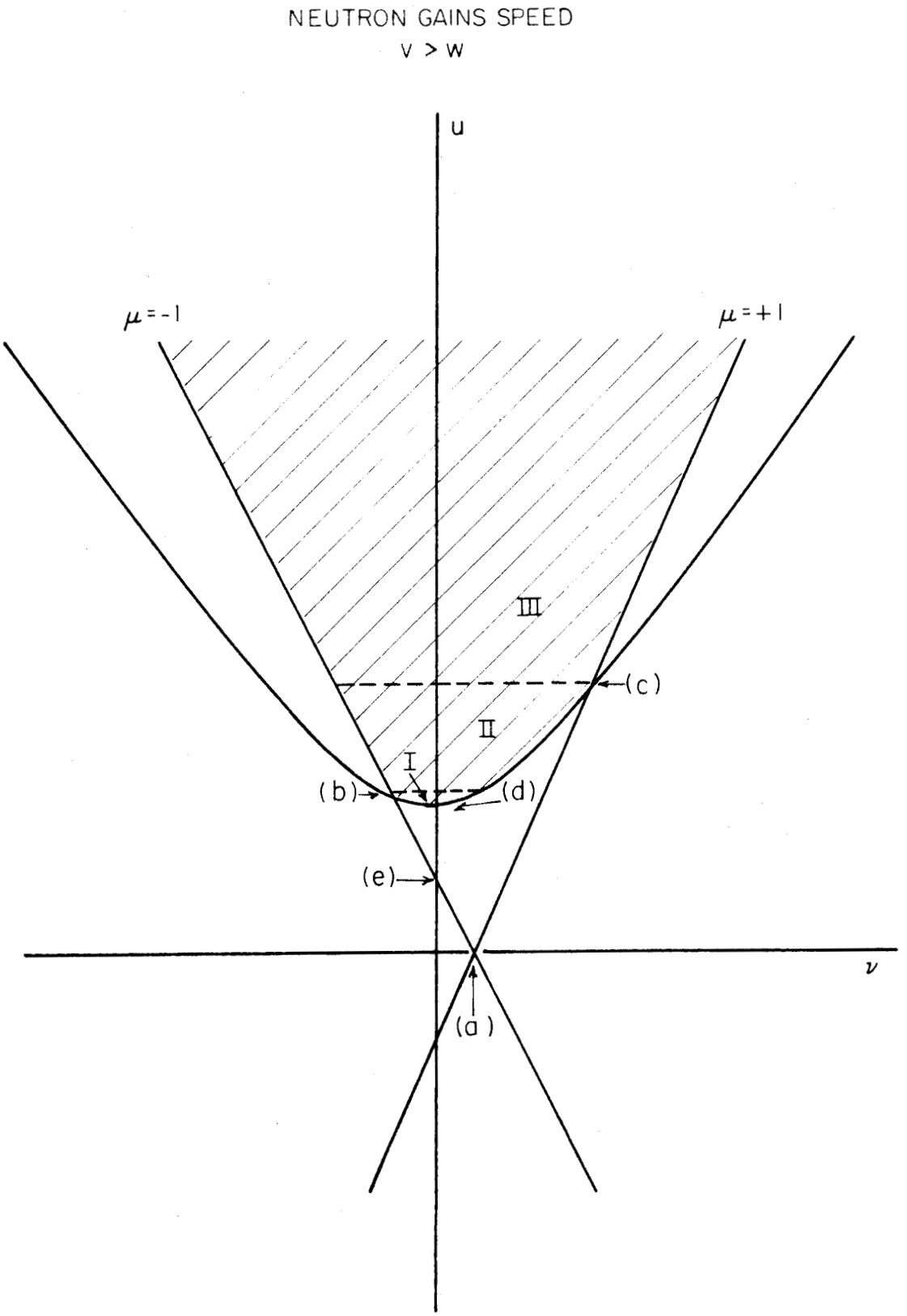

Figure 1. Domain of integration for neutron speed gain in a collision.

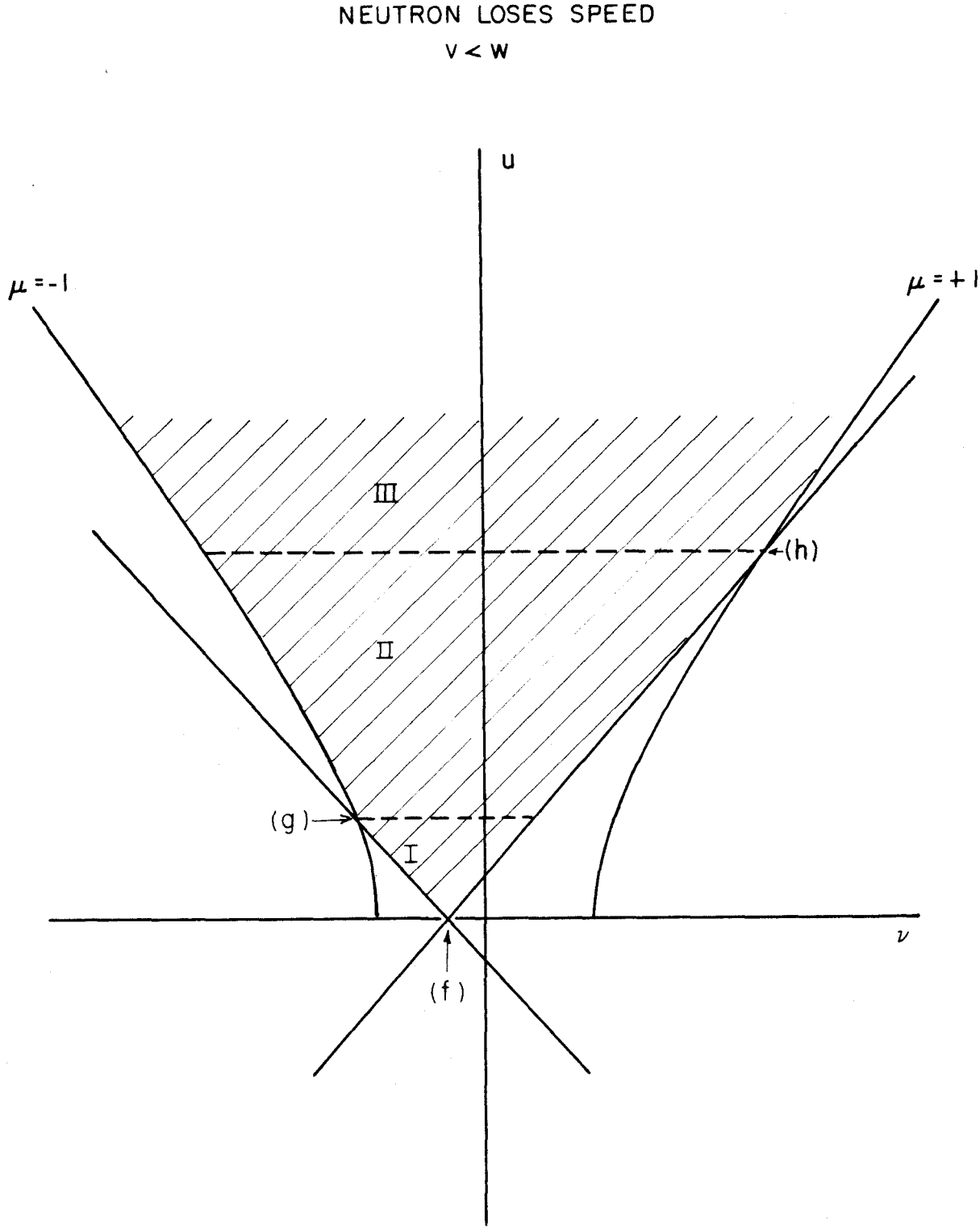

Figure 2. Domain of integration for neutron speed loss in a collision.

hyperbolas, the integration required for $P_s(w-v)$ may be accomplished. For reasonable $M(u)$ the actual integration is elementary, but very close attention must be paid to the magnitudes of u, w, v and m to ascertain the correct algebraic sign of the square roots of the integrands.

Details of the domain of integration, the intersections of the lines and hyperbola, and criteria for existence of subregions of integration are given in Appendix A.

Summary

The equation describing the steady state neutron distribution can now be expressed by substituting equations 30, 31 and 32 into equation 1:

$$\frac{(m+1)v\sigma_s}{4m}\int_0^\infty dw\, n(w)\int\int d\mu\, du\, \frac{M(u)}{v_c} + c_o S(v)$$

$$= n(v)\left[v\sigma_a(v) + \sigma_s \int_{-1}^{1}\frac{d\mu}{2}\int_0^\infty du\, M(u)v_r\right]. \qquad (36)$$

c_o is a suitable constant modifying the source so that neutrons are conserved. It is convenient to define

$$V(v) = \int_{-1}^{1}\frac{d\mu}{2}\int_0^\infty du M(u)v_r\,. \qquad (37)$$

The significance of this definition is explained by considering the atoms of the medium to be at rest. Then $M(u) = \delta(u)$ and $V(v) \equiv v$. In fact, if $M(u)$ is small for $u > u_{max}$, say, then

$$V(v) \approx \int_{-1}^{1}\frac{d\mu}{2}\int_0^{u_{max}} du M(u)v_r\,, \qquad (38)$$

and $V(v)$ will approach v for $v >> u_{max}$. It is also convenient to divide

equation 36 by σ_s and define the constant

$$\gamma = \frac{\sigma_a(v)v}{\sigma_s}. \tag{39}$$

With these definitions equation 36 becomes

$$\frac{(m+1)v}{4m}\int_0^\infty dw\, n(w) \iint du\, \frac{du M(u)}{v_c} + c_1 S(v) = n(v)\,[\gamma + V(v)], \tag{40}$$

where $c_1 = c_o/\sigma_s$. The combination now appearing in the first term of equation 40,

$$\frac{(m+1)v}{4m} \iint \frac{d\mu du M(u)}{v_c} = \frac{P_s(w\to v)}{\sigma_s}, \tag{41}$$

is henceforth designated by

$$P(w\to v) \equiv \frac{(m+1)v}{4m} \iint \frac{d\mu du M(u)}{v_c}. \tag{42}$$

$P(w\to v)$ is dimensionless and is the average probability that neutrons of initial speed w acquire final speed v in a scattering collision. The typical integral equation describing the neutron distribution is thus

$$\int_0^\infty dw\, n(w) P(w\to v) + c_1 S(v) = n(v)\,[\gamma + V(v)]. \tag{43}$$

Now only a specification of M(u) and S(v) is necessary to complete the formulation of the thermalization problem.

Portions of the above analysis were made from results given by Wigner and Wilkins (1). Since the analysis does not appear in the literature it was felt appropriate to produce it here.

Finally it should be noted that if M(u) is taken to be a Maxwellian distribution, the analysis is equivalent to the use of the Fermi pseudo-potential mentioned in the introduction. (See reference (15), pp. 98 and 103-4.)

II. THERMALIZATION BY SINGLE ENERGY HARMONIC OSCILLATORS

Oscillator Speed Distributions

As a model for the motions of atoms in solids it is assumed that each atom is an independent linear classical harmonic oscillator. Each atom is taken to have the same energy and to have a randomly oriented direction of oscillation. The speed of such an oscillator is given by

$$u = U\cos(\omega t + \xi), \tag{44}$$

where ω is the frequency of oscillation, ξ is an arbitrary phase angle and U is the maximum speed of the oscillator. U is determined by the energy E_o assigned the oscillator.

$$U = \sqrt{\frac{2E_o}{m}} \tag{45}$$

If the neutron-atom collision can be assumed to occur at any time with equal probability, any phase angle ξ is equally likely. That is, for a complete range of atom speeds u, this probability is given by

$$P(\xi)d\xi = \frac{d\xi}{\pi} . \tag{46}$$

The distribution of atom speeds u is then determined from the relation

$$M(u) = P(\xi)\left|\frac{d\xi}{du}\right| = \frac{1}{\pi}\left|\frac{d\xi}{du}\right| . \tag{47}$$

Since, from equation 44,

$$\left|\frac{d\xi}{du}\right| = \frac{1}{\sqrt{U^2 - u^2}},$$

M(u) is, when normalized to unity for positive atom speeds,

$$M(u, U) = \frac{2}{\pi\sqrt{U^2-u^2}} \qquad \text{if } 0 \leq u \leq U \tag{48}$$

$$= 0 \qquad \text{if } U < u.$$

This idealized model seems most suitable to describe thermalization by the hydrogen atoms in zirconium hydride. In this solid the hydrogen atoms are located in a spherically symmetric potential well inside a tetrahedron of zirconium atoms. Further, it has been reported that hydrogen atoms in zirconium hydride can be well characterized by the single energy, 0.137 ev (16). Almost all of the thermalization in zirconium hydride is performed by the hydrogen atoms, for a neutron can give up all its energy in a single collision with a proton, but only a very small fraction of its energy to a heavy atom such as zirconium (m=91). The model might also be applied to other solids if it is reasonable to assume interactions with a single atom. However, the assumption of a single atom energy is restrictive. For this reason, Part III of the thesis considers oscillators with a distribution of energies.

Energy Exchange Cross Sections

With M(u) as given by equation 48 the function V(v) of equation 37 may be readily calculated.

$$V(v) = \frac{1}{\pi}\int_0^U \frac{du}{\sqrt{U^2-u^2}}\int_{-1}^{1} d\mu \sqrt{u^2+v^2-2uv\mu} \tag{49}$$

$$= \frac{1}{3\pi v}\int_0^U \frac{du}{u\sqrt{U^2-u^2}}\left[(v+u)^3 - |v-u|^3\right].$$

At this point, a complexity arises which is typical of all subsequent calculations. A decision must be made about the relative size of u and v. Once this decision is made, the relative size of U and v must be argued to complete the integration. The latter decision is peculiar to the speed distribution 48 because there is a finite upper bound U on the atom speeds.

Assuming that $0 \le v \le U$ implies that u can be less than or greater than v. For this range of v the integrand of equation 49 changes form at u = v. That is,

$$V(v) = \frac{1}{3\pi v} \int_0^v \frac{du}{u\sqrt{U^2-u^2}}\left[(v+u)^3-(v-u)^3\right] \tag{50}$$

$$+ \frac{1}{3\pi v} \int_v^U \frac{du}{u\sqrt{U^2-u^2}}\left[(v+u)^3-(u-v)^3\right] \qquad \text{when } 0 \le v \le U.$$

When $U \le v$, u is always less than or equal to v. Thus equation 49 is

$$V(v) = \frac{1}{3\pi v} \int_0^U \frac{du}{u\sqrt{U^2-u^2}}\left[(v+u)^3-(v-u)^3\right] \qquad \text{when } U \le v \le \infty. \tag{51}$$

When these expressions are evaluated V is

$$V(v) = \frac{1}{3\pi}\left[5\sqrt{U^2-v^2} + \left(6v + \frac{U^2}{v}\right)\sin^{-1}\frac{v}{U} + \frac{2v^2}{U}\,\mathrm{sech}^{-1}\frac{v}{U}\right] \text{ if } 0 \le v \le U \tag{52}$$

$$= v + \frac{U^2}{6v} \qquad U \le v \le \infty. \tag{53}$$

The function is continuous at $v = U$. For $U = 0$, $V(v) = v$ and indeed, for $v >> U$, $V(v) \approx v$. For $v = 0$, $V(v) = \frac{2}{\pi} U$. The function is graphed in figure 3. The product $n(v)V(v)$ represents the neutron scatter rate for a unit, constant scattering cross section. Hence the function $V(v)/v$ represents an effective speed dependence of the scattering cross section. In figure 4 this function is compared with the scattering cross section computed by Fermi (3) for a quantum mechanical harmonic oscillator of mass one. Both functions are plotted in suitable dimensionless units. The discontinuities in the dotted curve are consequences of the discrete energy transfers allowed the quantum mechanical oscillator. The dotted curve is for the oscillator in its ground state. Zirconium hydride displays a scattering cross section very similar to this dotted curve. The similarity is enhanced if the presence of excited oscillator states is accounted for (16, 17).

The integrations for $P(w-v)$ (equation 42) are far more complex. A detailed argument for the various integrations is given in Appendix A. Only an illustrative example of the nature of the problem is outlined here.

Consider figure 1. Region I does not exist when the line $\mu = -1$ intercepts the u axis (point (e)) above the minimum of the hyperbola (point (d)). The criterion for this condition is $0 \leq w \leq \frac{m-1}{m+1} v$. With w in this range and v in the range $0 \leq v < \frac{2mU}{m+1}$ the integration may be carried out over both regions II and III if U is greater than the intercept of the line $\mu = +1$ and the hyperbola (point (c)). This requires $U \geq [(m+1)v + (m-1)w]/2m$. This condition implies $w \leq \frac{2mU-(m+1)v}{m-1}$.

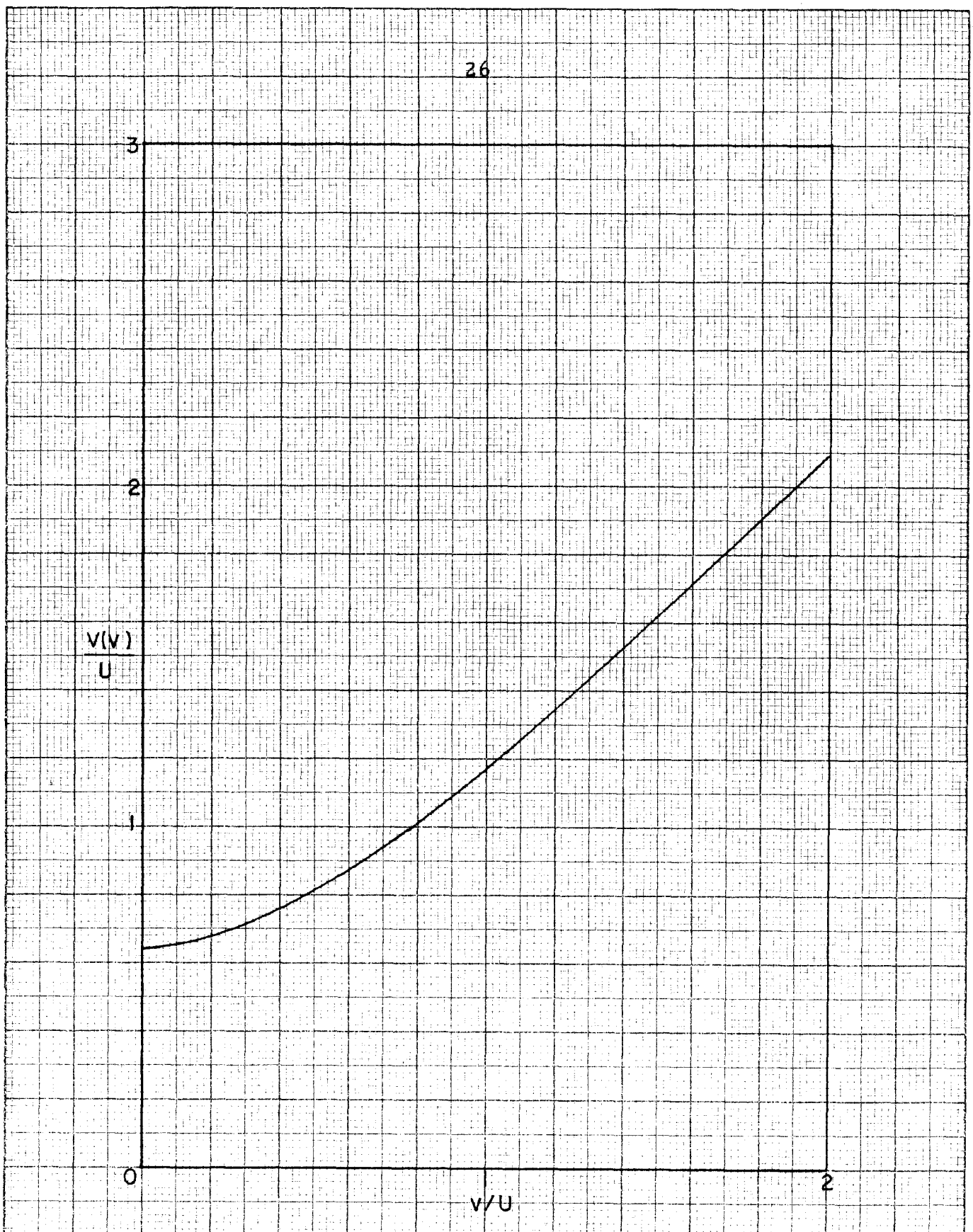

Figure 3. Variation of the function V(v)

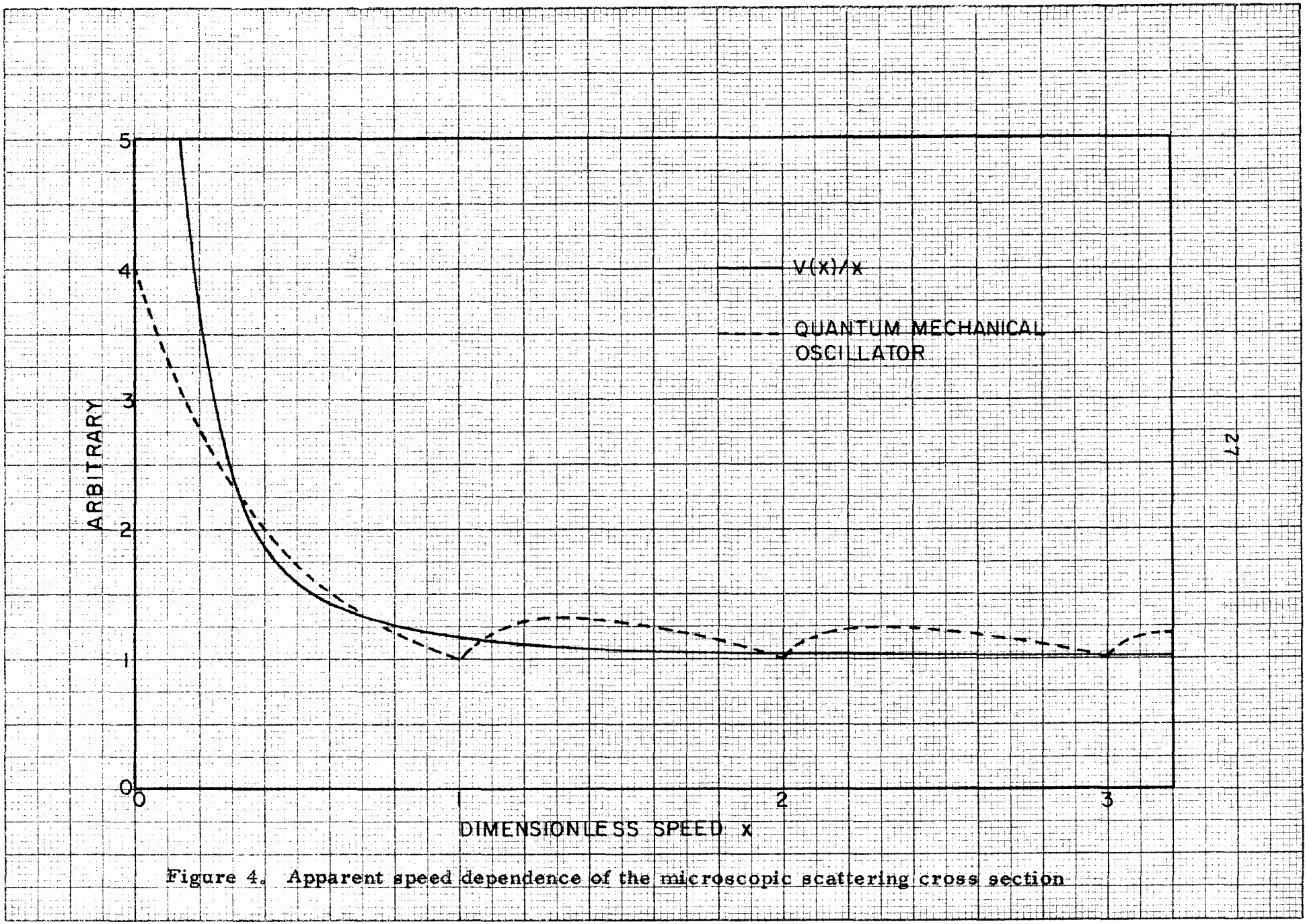

Figure 4. Apparent speed dependence of the microscopic scattering cross section

The latter quantity is greater than zero when $v < \frac{2mU}{m+1}$ which is in the range of v considered. Now for w, $\frac{2mU-(m+1)v}{(m-1)}$ is greater than $\frac{m-1}{m+1}v$ when $v \leq \frac{2m(m+1)U}{(m-1)^2+(m+1)^2}$ which is less than $\frac{2mU}{m+1}$. Therefore the integration on ν and u is in regions II and III when the integration on w is in the range $0<w<\frac{(m-1)v}{(m+1)}$ and when $0 < v < \frac{2m(m+1)U}{(m-1)^2+(m+1)^2}$. In effect, not only the limits of integration for ν and u are determined, but also the limits of integration for w. In addition, separate integral equations are found for different ranges of the neutron speed v. Or in other words, the kernel of the equation is highly fractionated.

Rather surprisingly, the results of the analysis of Appendix A show that P(w-v) of equation 42 can be written in six fundamental forms although there are potentially ten different regions of integration. Some short hand notation is adopted to make the expressions concise. Defining

$$
\begin{aligned}
a &= \frac{m+1}{2m} & c &= \frac{m-1}{2m} \\
\alpha(v,w) &= \sqrt{m}\,(av+cw) & Q &= \sqrt{m}\,U \\
\beta(v,w) &= \sqrt{m}\,(aw+cv) & R(v,w) &= \sqrt{Q^2-\varkappa^2} \\
\varkappa(v,w) &= \sqrt{m}\,(av-cw) & S(v,w) &= \sqrt{Q^2-\alpha^2} \\
\lambda(v,w) &= \sqrt{m}\,(aw-cv) & T(v,w) &= \sqrt{v^2-w^2},
\end{aligned}
\tag{54}
$$

then

$$P(w\to v) = \frac{2a^2 mv}{\pi w}\left[tg^{-1}\frac{\lambda}{R} + tg^{-1}\frac{\varkappa}{R} + tg^{-1}\frac{\beta}{S} - tg^{-1}\frac{a}{S} \right.$$

$$- \frac{T}{Q}\left(tg^{-1}\frac{Q\lambda}{TR} + tg^{-1}\frac{Q\beta}{TS}\right) \qquad (55)$$

$$\left. + \frac{v+w}{Q\sqrt{m}}\,\mathrm{sech}^{-1}\frac{\varkappa}{Q} + \frac{w-v}{Q\sqrt{m}}\,\mathrm{sech}^{-1}\frac{a}{Q}\right]$$

when $Q \geq a$ and $0 \leq w \leq v$

$$P(w\to v) = \frac{2a^2 mv}{\pi w}\left[tg^{-1}\frac{\lambda}{R} + tg^{-1}\frac{\varkappa}{R} - \frac{T}{Q}\left(tg^{-1}\frac{Q\lambda}{TR} + \frac{\pi}{2}\right) + \frac{v+w}{Q\sqrt{m}}\,\mathrm{sech}^{-1}\frac{\varkappa}{Q}\right]$$

when $\varkappa \leq Q \leq a$ and $0 \leq w \leq v$ (56)

$$P(w\to v) = \frac{2a^2 mv}{w}\left(1 - \frac{T}{Q}\right) \qquad \text{when } \sqrt{v^2 - mU^2} \leq Q \leq \varkappa \text{ and } 0 \leq w \leq v \qquad (57)$$

$$P(w\to v) = \frac{2a^2 mv}{\pi w}\left[tg^{-1}\frac{\lambda}{R} + tg^{-1}\frac{\varkappa}{R} + tg^{-1}\frac{a}{S} - tg^{-1}\frac{\beta}{S}\right.$$

$$\left. + \frac{T}{Q}\left(tg^{-1}\frac{Q\beta}{TS} - tg^{-1}\frac{Q\lambda}{TR}\right) + \frac{v+w}{Q\sqrt{m}}\,\mathrm{sech}^{-1}\frac{|\varkappa|}{Q} + \frac{v-w}{Q\sqrt{m}}\,\mathrm{sech}^{-1}\frac{a}{Q}\right] \qquad (58)$$

when $Q \geq a$ and $v \leq w \leq \infty$

$$P(w\to v) = \frac{2a^2 mv}{\pi w}\left[tg^{-1}\frac{\lambda}{R} + tg^{-1}\frac{\varkappa}{R} - \frac{T}{Q}\left(tg^{-1}\frac{Q\lambda}{TR} - \frac{\pi}{2}\right) + \frac{v+w}{Q\sqrt{m}}\,\mathrm{sech}^{-1}\frac{|\varkappa|}{Q}\right]$$

when $\varkappa \leq Q \leq a$ and $v \leq w \leq \infty$ (59)

$$P(w\to v) = \frac{2a^2 mv}{w} \qquad \text{when } 0 \leq Q \leq \varkappa \text{ and } v \leq w \leq \infty. \qquad (60)$$

Specific Thermalization Equations

The integral equation itself (equation 43) has five different forms depending upon the magnitude of the neutron speed v. The analysis determining the forms is given in Appendix A. The integral equations are displayed symbolically in Table I where the numbers in parentheses correspond to formulae in the text. The equations given are continuous at the boundaries of v. For a particular equation the kernels are continuous at the boundaries of w. If the maximum oscillator speed U is allowed to go to zero, the whole system collapses to a single equation,

$$\frac{(m+1)^2 v}{2m} \int_{v}^{\frac{(m+1)v}{(m-1)}} \frac{dw\, n(w)}{w} + c_1 S(v) = n(v)[\gamma+v], \tag{61}$$

which is a form of a known result (13) for the neutron density in an infinite homogeneous medium containing a 1/v absorber when the neutron speeds are such that the atoms of the medium can be assumed to be at rest. The only gain in the number of neutrons at v due to collisions at w is from neutrons that lose speed in a collision. This is the only possible situation when the atoms are at rest and is indicated by the limits of integration in equation 61. If the medium is non-absorbing ($\gamma=0$) and the source vanishes for a range of v being considered, the equation becomes

$$\frac{(m+1)^2}{2m} \int_{v}^{\frac{(m+1)v}{m-1}} \frac{dw\, n(w)}{w} = n(v), \tag{62}$$

TABLE I

Integral equation for thermalization by single energy harmonic oscillators.

Range of v	Neutron Gain Terms			Neutron Loss Terms
$0 \le v \le U$	$\int_0^v dw\, n(w)$ (55)	$+ \int_v^{\frac{U-av}{c}} dw\, n(w)$ (58)	$+ \int_{\frac{U-av}{c}}^{\frac{U+av}{c}} dw\, n(w)$ (59)	$+ c_1 S(v) = n(v)[\gamma +$ (52)$]$
$U \le v \le \frac{U}{a}$	$\int_0^{\frac{U-av}{c}} dw\, n(w)$ (55)	$+ \int_{\frac{U-av}{c}}^{v} dw\, n(w)$ (56)	$+ \int_v^{\frac{U+av}{c}} dw\, n(w)$ (59)	$+ c_1 S(v) = n(v)[\gamma +$ (53)$]$
$\frac{U}{a} \le v \le amU$	$\int_{\frac{av-U}{c}}^{v} dw\, n(w)$ (56)		$+ \int_v^{\frac{U+av}{c}} dw\, n(w)$ (59)	$+ c_1 S(v) = n(v)[\gamma +$ (53)$]$
$amU \le v \le mU$	$\int_{\frac{av-U}{c}}^{\frac{av-U}{c}} \frac{dw\, n(w)}{\sqrt{v^2 - mU^2}}$ (57)	$+ \int_{\frac{av-U}{c}}^{v} dw\, n(w)$ (56)	$+ \int_v^{\frac{U+av}{c}} dw\, n(w)$ (59)	$+ c_1 S(v) = n(v)[\gamma +$ (53)$]$
$mU \le v \le \infty$	$\int_{\sqrt{v^2 - mU^2}}^{v} \frac{dw\, n(w)}{\sqrt{v^2 - mU^2}}$ (57)	$+ \int_v^{\frac{av-U}{c}} dw\, n(w)$ (60)	$+ \int_{\frac{av-U}{c}}^{\frac{U+av}{c}} dw\, n(w)$ (59)	$+ c_1 S(v) = n(v)[\gamma +$ (53)$]$

with solution

$$n(v) = \frac{c_2}{v^2} \ , \tag{63}$$

which is a standard result for the neutron density (for atoms of any mass) in a speed range far from the source.

In a physical situation of great practical importance the neutron source is the fission source. As mentioned, the fission source produces neutrons of very high energy. In the thermal energy (or speed) range, then, the only source of neutrons is the neutrons which arrive in the range as a result of collisions at higher speeds. At this point of the analysis it is assumed that the only source is a fission source at a single very large speed. The explicit display of the source is discontinued and the region of validity of the balance equation is restricted to the thermal speed range. When absorption appears in the equations it is to be understood that a sufficient number of neutrons arrive at thermal speeds by speed loss collisions from higher speeds to balance the absorption loss. Thermalization by hydrogen is a slightly anomalous situation. Neutrons may arrive at thermal speeds as a result of collisions at source speed. This is indicated by the infinite integration limit in equation 62 when m = 1. In this case the source may be thought of as at infinity or simply at some very large speed v_o. In subsequent equations infinite integration limits are interpreted in this fashion.

Equation 61, for m = 1 with absorption is

$$2v \int_v^\infty \frac{dw\, n(w)}{w} = n(v)[v+\gamma] \ , \tag{64}$$

with solution

$$n(v) = \frac{c_3 v}{\left(v + \frac{\sigma_a v}{\sigma_s}\right)^3} , \qquad (65)$$

where the constant c_3 contains the source strength. Equation 65 is another solution which is given by the theory of neutron slowing down when $\sigma_a v$ is a constant.

Because the integral equations of Table I contain the finite maximum speed of the oscillator, their solutions should exhibit the behavior of the rest atom solutions 63 and 65 when the neutron speeds v are much larger than the maximum atom speed U.

The equations of Table I include the possibility of neutron speed gain in a collision because of the atomic motions. In addition, it is interesting to note that the range of speeds in which a neutron may lose speed is broadened by a factor U2m/(m-1) compared to the rest atom assumption. This effect is also due explicitly to the atomic motions. However, it is not possible for all neutrons to lose speed and contribute to the neutron density. Moreover, in certain ranges it is not possible for a neutron to gain speed in a collision and contribute to the neutron density. Therefore the principle of detailed balance (equation 4) cannot be satisfied. For example, with $v \geq mU$, no neutrons of initial speed less than $\sqrt{v^2 - mU^2}$ gain-scatter to speed v. Also, no neutrons with initial speeds greater than $[2mU+(m+1)v]/(m-1)$ will loss-scatter to speed v. These observations imply that the neutron density predicted by the equations of Table I will not be a Maxwellian in the absence of absorption

which, again, is a consequence of the finite maximum oscillator speed. Therefore, the oscillator model is, at best, an approximation to the actual physical situation. The non-equilibrium c_o/v^2 distribution for large v persists in the absence of absorption. However, absorption is always present in a physical situation and experimental neutron distributions display the c_o/v^2 "tail" for large v. A quantum mechanical atomic model using a perfect harmonic oscillator does not predict an equilibrium neutron distribution, either, because of the restriction of energy transfer to multiples of $h\nu$. In addition a scattering function may satisfy detailed balance and yet not represent a physical situation. This is illustrated in Appendix F. Finally, although it is not evident from Table I, the deviation from a Maxwellian in the absence of absorption is not great, especially for m=1. (See figure 9.)

Thermalization by Hydrogen

The remainder of the analysis for the single energy model is restricted to thermalization by hydrogen (m=1). As indicated previously, the model is deemed most suitable for thermalization by the hydrogen in zirconium hydride. A refinement of the model is applied to media with mass greater than unity in Part III.

The equations of Table I are much simpler for m = 1, for then a = 1, c = 0, $\alpha = \varkappa = v$ and $\beta = \lambda = w$. Introduction of the dimensionless variables

$$x = v/\sqrt{2E_o} = v/\sqrt{m}\,U \qquad (66)$$
$$y = w/\sqrt{m}\,U,$$

is useful in further simplifying the expressions. (The unit mass of the neutron is understood to be present in $\sqrt{2E_o}$ so that the quantity has the dimensions of speed.)

When m = 1, equations 52 and 53 become

$$UV(x) = \frac{U}{3\pi}\left[5\sqrt{1-x^2} + \left(6x+\frac{1}{x}\right)\sin^{-1}x + 2x^2\,\mathrm{sech}^{-1}x\right] \quad \text{if } 0 \le x \le 1 \qquad (67)$$

$$= U\left(x + \frac{1}{6x}\right) \quad \text{if } 1 \le x \le \infty .$$

When m=1, only 4 of equations 55-60 defining P(w→v) are applicable. These are

$$\left\{\begin{array}{ll} \text{equation 55:} & \text{if } 0 \le w \le v \\ \text{equation 58:} & \text{if } v \le w \le \infty \end{array}\right\} \quad \text{when } 0 \le v \le U, \qquad (68)$$

and

$$\left\{\begin{array}{ll} \text{equation 57:} & \sqrt{v^2-U^2} \le w \le v \\ \text{equation 60:} & \text{if } v \le w \le \infty \end{array}\right\} \quad \text{when } U \le v \le \infty . \qquad (69)$$

These equations become, with a=1, c=0, $\alpha=\chi=xU$, and $\beta=\lambda=yU$,

$\underline{0 \le x \le 1}$

$$(55):\ P(y\to x) = \frac{4x}{\pi y}\left(\mathrm{tg}^{-1}\frac{y}{\sqrt{1-x^2}} - \sqrt{x^2-y^2}\,\mathrm{tg}^{-1}\frac{y}{\sqrt{x^2-y^2}\sqrt{1-x^2}} + y\,\mathrm{sech}^{-1}x\right)$$

$$\text{if } 0 \le y \le x \qquad (70)$$

$$(58):\ P(y\to x) = \frac{4x}{\pi y}\left(\mathrm{tg}^{-1}\frac{x}{\sqrt{1-x^2}} + x\,\mathrm{sech}^{-1}x\right) \quad \text{if } x \le y \le \infty , \qquad (71)$$

$1 \le x \le \infty$

(57): $$P(y \to x) = \frac{2x}{y}\left(1 - \sqrt{x^2 - y^2}\right) \qquad \text{if } \sqrt{x^2-1} \le y \le x \qquad (72)$$

(60): $$= \frac{2x}{y} \qquad \text{if } x \le y \le \infty . \qquad (73)$$

The integral equation 43 is, after changing to dimensionless variables, and omitting the source,

$$\int_0^\infty dy\, n(y)\, P(y \to x) = \frac{n(x)}{U}\left[UV(x) + \gamma\right], \qquad (74)$$

which is properly dimensionless. The quantity γ/U is called

$$\Delta = \frac{\gamma}{U} = \frac{\sigma_a(v)v}{\sigma_s\sqrt{2E_o}} , \qquad (75)$$

and is a dimensionless constant. Equation 74 then may be written for the two ranges of x as

$$\frac{4x}{\pi}\int_0^x dy \frac{n(y)}{y}\left(\mathrm{tg}^{-1}\frac{y}{\sqrt{1-x^2}} - \sqrt{x^2-y^2}\ \mathrm{tg}^{-1}\frac{y}{\sqrt{x^2-y^2}\sqrt{1-x^2}} + y\ \mathrm{sech}^{-1}x\right)$$

$$+ \frac{4x}{\pi}\left(\sin^{-1}x + x\ \mathrm{sech}^{-1}x\right)\int_x^\infty dy\,\frac{n(y)}{y} \qquad (76)$$

$$= \frac{n(x)}{3\pi}\left[5\sqrt{1-x^2} + \left(6x + \frac{1}{x}\right)\sin^{-1}x + 2x^2\ \mathrm{sech}^{-1}x + 3\pi\Delta\right]$$

if $0 \le x \le 1$,

and as

$$2x \int_{\sqrt{x^2-1}}^{x} dy \frac{n(y)}{y} \left(1 - \sqrt{x^2-y^2} \right) + 2x \int_{x}^{\infty} dy \frac{n(y)}{y} = n(x) \left[x + \frac{1}{6x} + \Delta \right] \qquad (77)$$

$$\text{if } 1 \leq x \leq \infty .$$

The two equations above are continuous at x = 1. The kernel P in each equation is a continuous function at its boundaries. In fact, in a given range P is a monotonic function of y for a given x. The y variation of P is displayed for three values of x in figure 5. The two equations 76 and 77 are coupled. Neutrons with initial speeds $x > 1$ may scatter to speeds below x = 1. Similarly neutrons with initial speeds $x < 1$ may scatter to speeds above x = 1. However, for $x \geq \sqrt{2}$ speed gain scattering from below x = 1 is not possible and equation 77 is uncoupled from equation 76. The equation determining the neutron density is then

$$2x \int_{\sqrt{x^2-1}}^{x} dy \frac{n(y)}{y} \left(1 - \sqrt{x^2-y^2} \right) + 2x \int_{x}^{\infty} dy \frac{n(y)}{y} = n(x) \left[x + \frac{1}{6x} + \Delta \right] . \qquad (78)$$

$$x > \sqrt{2}$$

For sufficiently large x the energy gain scattering term may be neglected and the equation is approximately

$$2x \int_{x}^{\infty} dy \frac{n(y)}{y} = n(x)(x+\Delta) , \qquad (79)$$

with solution

$$n(x) = \frac{c_4 x}{(x+\Delta)^3} . \qquad (80)$$

This is the expected rest atom solution of equation 65, which n approaches for large x. It has not been found possible to reduce

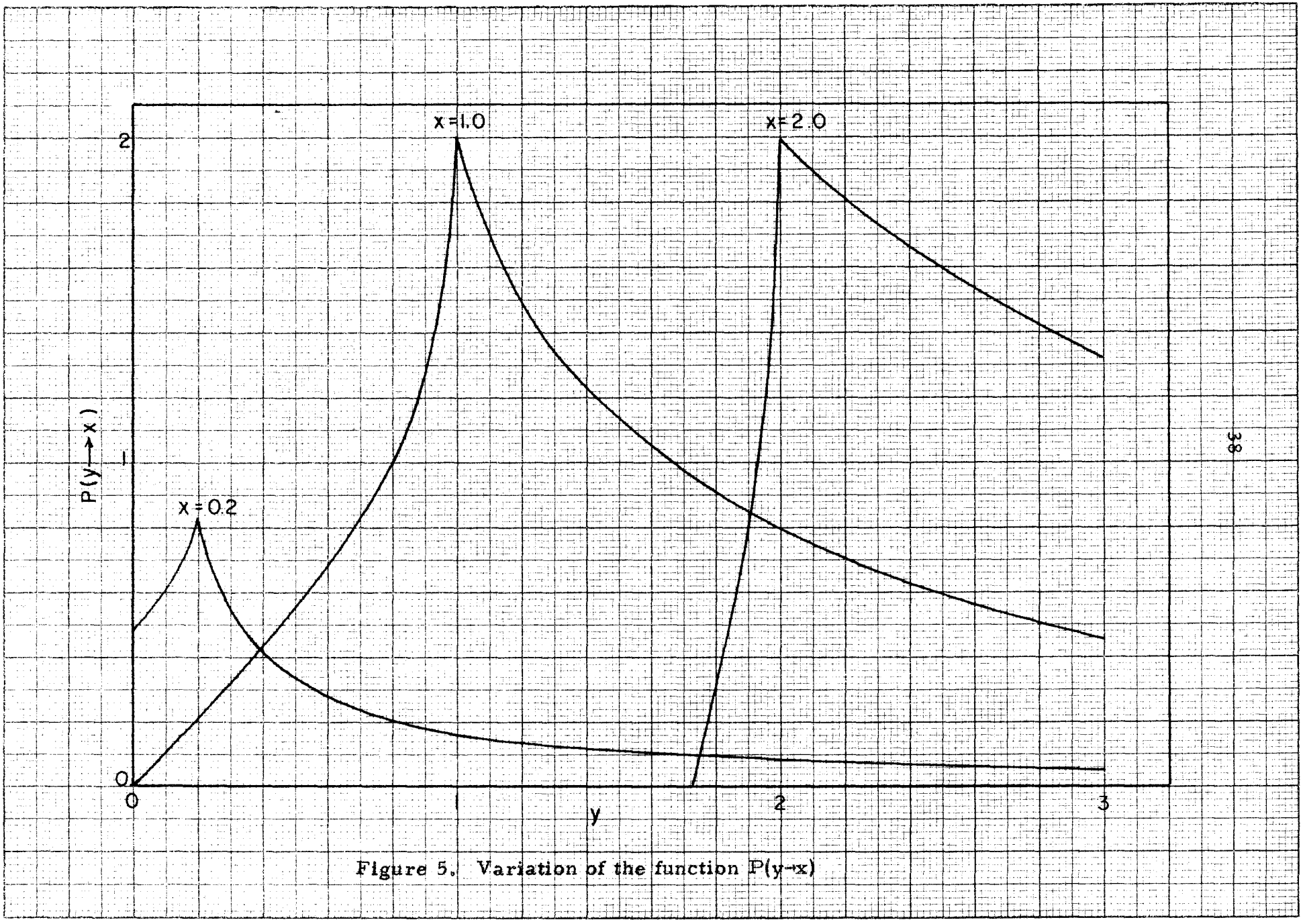

Figure 5. Variation of the function P(y-x)

equation 78 to a differential equation, primarily because of the square root in the equation. Integrations in a method of successive approximations starting from equation 80 rapidly become intractable. However, if $n(y)/y$ can be taken to be a slowly varying function in the range $\sqrt{x^2-1} \le y \le x$ for large x, equation 78 may be approximated by

$$2n(x)\int_{\sqrt{x^2-1}}^{x} dy\left(1-\sqrt{x^2-y^2}\right)+2x\int_{x}^{\infty} dy\frac{n(y)}{y} = n(x)\left[x+\frac{1}{6x}+\Delta\right], \qquad (81)$$

which is, neglecting terms of $O\left(\frac{n}{x^2}\right)$,

$$2x\int_{x}^{\infty} dy\frac{n(y)}{y} = n(x)\left[x-\frac{1}{6x}+\Delta\right], \qquad (82)$$

with solution

$$n(x) = \frac{16c_4x^2\left(2x+\Delta-\sqrt{\Delta^2+\frac{2}{3}}\right)^{\frac{\Delta}{\sqrt{\Delta^2+\frac{2}{3}}}-2}}{\left(2x+\Delta+\sqrt{\Delta^2+\frac{2}{3}}\right)^{\frac{\Delta}{\sqrt{\Delta^2+\frac{2}{3}}}+2}} . \qquad (83)$$

This solution has the following limiting forms:

$$n(x) \to \frac{c_4}{x^2} \qquad x \gg \Delta , \qquad (84)$$

$$n(x) \to \frac{c_4x}{(x+\Delta)^3} \qquad \Delta \gg 1 , \qquad (85)$$

$$n(x) = \frac{c_4x^2}{\left(x^2-\frac{1}{6}\right)^2} \qquad \Delta = 0 . \qquad (86)$$

Equation 86 is larger than $1/x^2$ for a given x, an effect due to the atomic motions and in qualitative agreement with results derived (Ref. 18) for the Wigner-Wilkins equation (1). The effect is due to the energy of atomic motions which is transferred to the neutrons, causing the rate at which neutrons lose speed to be decreased.

If an inverse power series in x

$$\sum_{r=1}^{\infty} \frac{a_r}{x^r}, \tag{87}$$

is substituted in equation 78, a determination of the coefficients a_r as given in Appendix C produces the relations

$$\begin{aligned} a_1 &= 0 \\ a_2 &= \text{arbitrary} \end{aligned} \tag{88}$$

$$(r-1)a_{2r} = -\Delta r\, a_{2r-1} + \frac{r}{6} a_{2r-2} + \sum_{j=2}^{r-1} \frac{a_{2r-2j}}{(2j+1)!} \binom{r}{j}, \qquad r \geq 2 \tag{89}$$

$$(2r-1)a_{2r+1} = -\Delta(2r+1)\, a_{2r} + \frac{(2r+1)a_{2r-1}}{6} + 2 \sum_{j=2}^{r-1} \frac{a_{2r-2j+1}}{(2j+1)!} \binom{r+\frac{1}{2}}{j} \qquad r \geq 1. \tag{90}$$

with empty sums zero. The first few terms of the series are

$$n(x) = a_2 \left(\frac{1}{x^2} - \frac{3\Delta}{x^3} + \frac{\frac{1}{3} + 6\Delta^2}{x^4} - \frac{5\Delta\left|\frac{5}{18} + 2\Delta^2\right|}{x^5} + \frac{\frac{23}{60} + \frac{43}{12}\Delta^2 + 15\Delta^4}{x^6} - \cdots \right). \tag{91}$$

The coefficients of the largest powers of Δ are just those of

$$\frac{a_2 x}{(x+\Delta)^3} = a_2\left(\frac{1}{x^2} - \frac{3\Delta}{x^3} + \frac{6\Delta^2}{x^4} - \frac{10\Delta^3}{x^5} + \frac{15\Delta^4}{x^6} - \ldots\right). \qquad (92)$$

An expansion of the approximate solution of equation 83 agrees with equation 91 through terms of order $1/x^4$. For $\Delta = 0$ in equation 91, only even powers of x appear

$$n(x) = a_2\left(\frac{1}{x^2} + \frac{1}{3x^4} + \frac{23}{60x^6} + \frac{773}{1890x^8} + \ldots\right), \qquad (93)$$

indicating that the neutron density is a function of the neutron energy only. Convergence of the expansion of equation 91 has not been shown. However, for $x = 2.0$ and $\Delta = 0.01$, the first six terms of equation 91 give $n(x) = 0.2725$ ($a_2=1$), while the numerically computed value is found to be $n(x) = 0.2717$.

For very small x, equation 76 may be written approximately as

$$2\int_0^x dy\, h(y)\left(y - \sqrt{x^2-y^2}\sin^{-1}\frac{y}{x} + y\ell n\frac{2}{x}\right) + 2(x + x\ell n\frac{2}{x})\int_x^\infty dy\, h(y) = h(x)\Delta', \qquad (94)$$

where $h(x) = n(x)/x$ and $\Delta' = 1 + \frac{\pi}{2}\Delta$. Solution of this equation is complicated by two factors: 1) although the relation is valid only for small x, all values of the unknown function are required for the integration from x to infinity and 2) $\ell n\frac{2}{x}$ is singular at the origin. An approximate solution is determined below.

Equation 94 is treated as an exact relationship. Upon differentiation it becomes

$$-2x \int_0^x \frac{dy\, h(y)}{\sqrt{x^2-y^2}} \sin^{-1}\frac{y}{x} + 2\ell n \frac{2}{x} \int_x^\infty dy\, h(y) = \Delta' \frac{dh}{dx} . \tag{95}$$

If h(y) is a slowly varying function compared to the remainder of the integrand in the integral from zero to x, equation 95 may be approximated by

$$\Delta' \frac{dh}{dx} + \frac{\pi^2}{4} xh - 2\ell n \frac{2}{x} \int_x^\infty dy\, h(y) = 0. \tag{96}$$

Substituting

$$f(x) = \int_x^\infty dy\, h(y) , \tag{97}$$

so that

$$h(x) = -\frac{df}{dx} , \tag{98}$$

equation 96 becomes

$$\Delta' \frac{d^2 f}{dx^2} + \frac{\pi^2}{4} x \frac{df}{dx} + 2\ell n \frac{2}{x} f = 0. \tag{99}$$

When the variable $z = \ell n \frac{2}{x}$ is introduced, equation 99 becomes

$$\frac{d^2 f}{dz^2} + \left(1 - \frac{\pi^2}{\Delta'} e^{-2z}\right) \frac{df}{dz} + \frac{8}{\Delta'} z e^{-2z} f = 0. \tag{100}$$

The transformation

$$f(z) = g(z)\, e^{-\frac{z}{2} - \frac{\pi^2}{4\Delta'} e^{-2z}} , \tag{101}$$

reduces equation 100 to

$$\frac{d^2 g}{dz^2} + p(z) g = 0, \tag{102}$$

where

$$p(z) = -\frac{1}{4}\left[1-\frac{32}{\Delta'}ze^{-2z}+\frac{2\pi^2}{\Delta'}e^{-2z}+\frac{\pi^4}{\Delta'^2}e^{-4z}\right]. \tag{103}$$

When z is large (x small), p(z) satisfies the criterion

$$\left|\frac{dp}{dz}\right| \ll \left|p^{3/2}\right| \tag{104}$$

so that the WKB approximation (19) may be used. That is,

$$g(z)\approx \frac{e^{\pm i\int^z dz'\sqrt{p(z')}}}{p^{1/4}}. \tag{105}$$

Expanding $\sqrt{p}$ and $p^{1/4}$ and integrating gives

$$g(z)\approx a_0\left[1+O(ze^{-2z})\right]e^{\pm\frac{1}{2}\left[z+\frac{8ze^{-2z}}{\Delta'}+\frac{4}{\Delta'}e^{-2z}-\frac{\pi^2}{2\Delta'}e^{-2z}-O(z^2e^{-4z})\right]}, \tag{106}$$

and thus, using equation 101,

$$f(z)\approx a_1'\left[1+O\ (ze^{-2z})\right]e^{\frac{4ze^{-2z}}{\Delta'}+\frac{2}{\Delta'}e^{-2z}-\frac{\pi^2}{2\Delta'}e^{-2z}-O(z^2e^{-4z})}$$
$$+a_2'\left[1+O(ze^{-2z})\right]e^{-z-\frac{4ze^{-2z}}{\Delta'}-\frac{2}{\Delta'}e^{-2z}+O(z^2e^{-4z})}. \tag{107}$$

Returning to $x = 2e^{-z}$, f(x) is, for small x,

$$f(x)\approx a_1\left[1+O(x^2\ell n\frac{2}{x})\right]e^{\frac{x^2\ell n\frac{2}{x}}{\Delta'}+\frac{x^2}{2\Delta'}\left(1-\frac{\pi^2}{4}\right)-O\left(x^4(\ell n\frac{2}{x})^2\right)}$$
$$+a_2\left[1+O(x^2\ell n\frac{2}{x})\right]xe^{\frac{-x^2\ell n\frac{2}{x}}{\Delta'}-\frac{x^2}{2\Delta'}+O\left(x^4(\ell n\frac{2}{x})^2\right)}. \tag{108}$$

For x near zero, then, f behaves qualitatively either as a constant or as x. For either behavior, h(o) as determined from equation 94 is zero provided h(x) is not as singular as 1/x for small x. But h(x) is proportional to df/dx which is zero or a constant at x equal to zero. Therefore a_2 in equation 108 must be chosen to be zero so that h(o) will equal zero. Then, for small x, the most significant term in n(x) is

$$n(x) = xh(x) = -x\frac{df}{dx} \approx a_3 x^2 \ell n \frac{2}{x} . \tag{109}$$

To this approximation the integral

$$-2x \int_0^x dy \frac{h(y)\sin^{-1}(y/x)}{\sqrt{x^2-y^2}} , \tag{110}$$

which was approximated by

$$-2x \frac{\pi^2}{8} h(x), \tag{111}$$

is

$$-2x \int_0^x dy \frac{y\,\ell n(2/y)\sin^{-1}(y/x)}{\sqrt{x^2-y^2}} , \tag{112}$$

or

$$-2x \left(x\ell n \frac{2}{x} + 2x - x \int_0^{\pi/2} \frac{\theta d\theta}{\sin\theta} \right) , \tag{113}$$

or

$$-2x\,h(x) - 4x^2 \left(1 - \frac{1}{2} \int_0^{\pi/2} \frac{\theta\, d\theta}{\sin\theta} \right) . \tag{114}$$

The remaining integral is equal to 0.916 (page 216, reference (20)),

so that equation 114 is

$$-2x\,h(x) - 0.336x^2, \tag{115}$$

which is sufficiently accurate to be consistent with the remainder of the approximations.

The above results serve only as a qualitative description of the behavior of n for small x because of the crudeness of the various assumptions. A comparison of numerically calculated values of n(x) and the functions $240\,x^2 \ln \frac{2}{x}$ and $237.5\,x^2 \ln \frac{2}{x} \exp\left[\frac{x^2 \ln \frac{2}{x}}{\Delta'} + \frac{x^2}{2\Delta'}\left(1 - \frac{\pi^2}{4}\right)\right]$ is given below. For the values below $\Delta = 0.01$ or $\Delta' = 1.0157$.

TABLE II

x	n(x) (numerical)	$240\,x^2 \ln \frac{2}{x}$	$237.5\,x^2 \ln \frac{2}{x}\, e^{\frac{x^2 \ln \frac{2}{x}}{\Delta'} + \frac{x^2}{2\Delta'}\left(1 - \frac{\pi^2}{4}\right)}$
0.05	2.21	2.21	2.21
0.10	7.33	7.20	7.27
0.15	14.27	13.99	14.42
0.20	22.18	22.10	23.27

A method of numerical solution of equations 76 and 77 is discussed in Section IV and solutions are presented in Section V.

III. THERMALIZATION BY HARMONIC OSCILLATORS WITH A DISTRIBUTION OF ENERGIES

Oscillator Speed Distribution

The distribution of atom speeds derived in Section II contains the energy of the harmonic oscillator as a parameter.

$$M(u, E) = \frac{2}{\pi\sqrt{\frac{2E_o}{m} - u^2}} \qquad 0 \le u \le \sqrt{2E_o/m}$$

$$= 0 \qquad \sqrt{2E_o/m} < u. \tag{48}$$

To ease the restrictive assumption that each oscillator has the same energy, a distribution of atom energies is postulated. Several choices of energy distributions are possible. For example, experimental measurements may suggest that atom energies are statistically distributed about a single energy, in which case a Gaussian distribution of E_o might be used. The distribution chosen to particularize the following analysis is an equilibrium distribution of atomic energies

$$P(E_o)dE_o = c_5\sqrt{E_o}\, e^{-E_o/kT}\, dE_o , \tag{116}$$

where c_5 is a normalizing constant, k is Boltzmann's constant and T is the material temperature. With this distribution the effect of atomic binding is yet contained in equation 48 while the temperature of the medium is introduced.

The atom speed distribution to be used is the average of equation 48 over the energy distribution 116. That is,

$$M(u) = \frac{2c_5}{\pi} \int_{\frac{mu^2}{2}}^{\infty} \frac{dE_o \sqrt{E_o} e^{-E_o/kT}}{\sqrt{\frac{2E_o}{m} - u^2}} \qquad 0 \le u \le \infty \ . \tag{117}$$

Making the change of variable

$$st + s = \frac{E_o}{kT} \ , \qquad s = \frac{mu^2}{2kT} \ , \tag{118}$$

equation 117 becomes

$$M(u) = c_6 s e^{-s} \int_0^{\infty} \frac{dt e^{-st} \sqrt{t+1}}{\sqrt{t}} \ . \tag{119}$$

Using the results that

$$\int_0^{\infty} \frac{dt\, e^{-st(t+\frac{1}{2})}}{\sqrt{t}\ \sqrt{t+1}} = \frac{1}{2} e^{s/2} K_1\left(\frac{s}{2}\right) \qquad \text{(ref. 21)}, \tag{120}$$

$$\int_0^{\infty} \frac{dt e^{-st}}{\sqrt{t}\ \sqrt{t+1}} = e^{s/2} K_0\left(\frac{s}{2}\right) \qquad \text{(ref. 22)}, \tag{121}$$

where K_0 and K_1 are modified Bessel functions, the integral in equation 119 is, by adding 1/2 of equation 121 to equation 120,

$$\int_0^{\infty} \frac{dt e^{-st} \sqrt{t+1}}{\sqrt{t}} = \frac{1}{2} e^{s/2} \left[K_0\left(\frac{s}{2}\right) + K_1\left(\frac{s}{2}\right) \right] . \tag{122}$$

The resulting atom speed distribution is thus

$$M(u) = c_7 z e^{-z} \left[K_0(z) + K_1(z) \right] \qquad 0 \le u \le \infty \tag{123}$$

$$z = \frac{mu^2}{4kT} \ .$$

This function is compared to a Maxwellian distribution of u in figure 6. Each curve is normalized to unit area for the scale employed. The integral (page 331, reference (21))

$$\int_0^\infty dx\, x^{s-1}\, e^{-ax}\, K_\nu(ax) = \frac{\sqrt{\pi}\,\Gamma(s+\nu)\Gamma(s-\nu)}{2^s a^s \Gamma(s+\tfrac{1}{2})}\ , \tag{124}$$

is used to normalize equation 123. Using the relation of 124 the average atom energy represented by equation 123 is

$$\langle E_o \rangle = \frac{\int_0^\infty E_o M(E_o(u))\,dE_o}{\int_0^\infty M(E_o(u))\,dE_o} = \frac{3kT}{4}\ , \tag{125}$$

or one-half the average energy of a Maxwellian distribution of atom speeds. Therefore if a temperature is chosen to characterize the medium, it must be an effective temperature rather than the measured temperature.

Specific Thermalization Equation

If the speed distribution 123 is used, the terms of the thermalization equation may be calculated in exactly the same manner as indicated in Section II. It is also possible to calculate the terms by averaging the expressions of equations 52-3 and 55 through 60 over the energy distribution 116 above. As a check of the accuracy of the resulting expressions both methods were employed to calculate V(v). It proves to be decidedly simpler to average the existing functions than to use the speed distribution 123 ab initio.

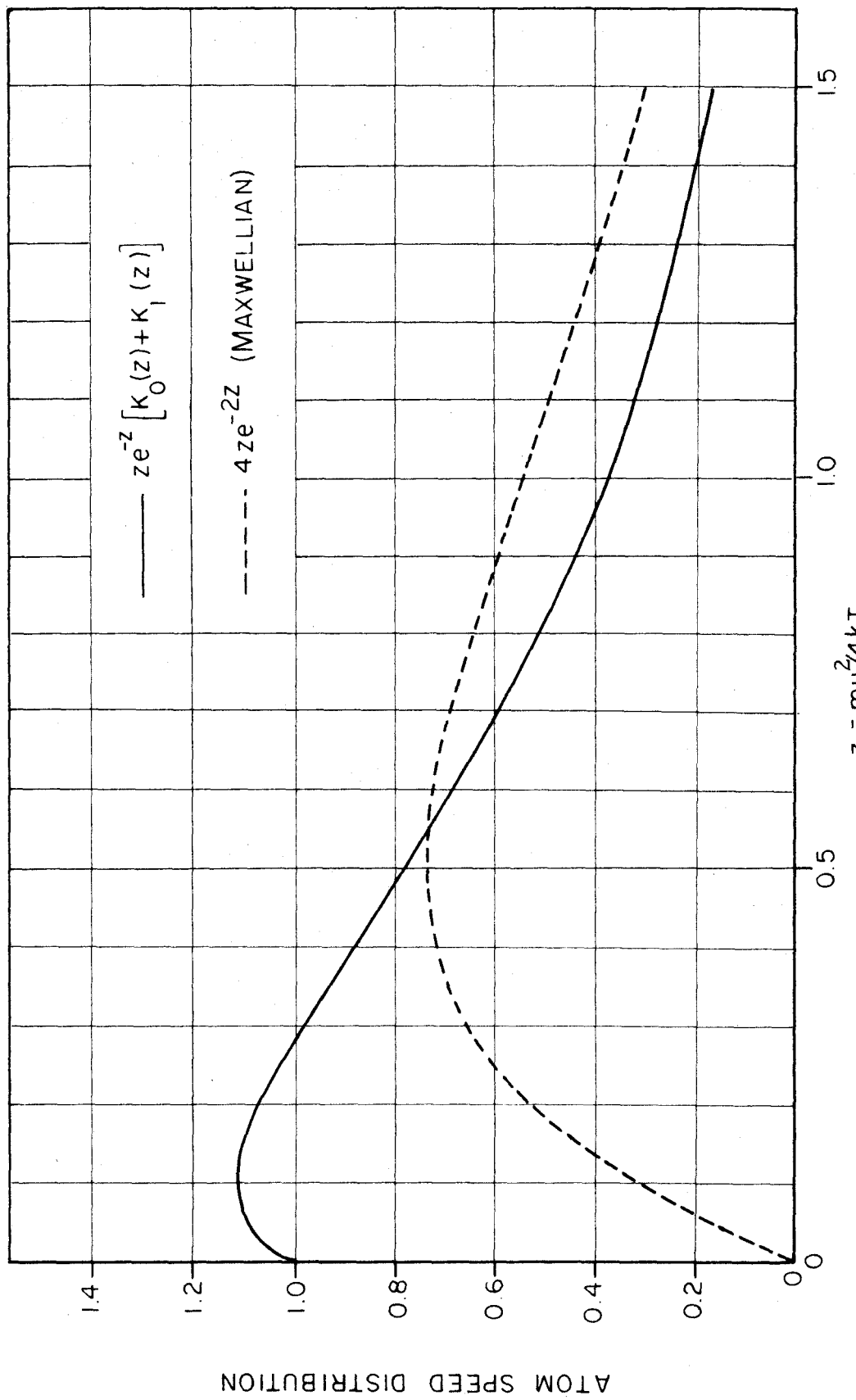

Figure 6. Comparison of the atom speed distribution of equation 123 with a Maxwellian speed distribution

With the atom speed distribution of 123, the function V defined by equation 37 is, as derived in Appendix A,

$$V(x) = \frac{\sqrt{\pi}}{2}\left(x + \frac{1}{4mx}\right) + \frac{\sqrt{m}}{\pi}\int_x^\infty dt\, e^{-mt^2}\left[3\sqrt{t^2-x^2} - (2x+t^2/x)\cos^{-1}\frac{x}{t}\right], \tag{126}$$

with x the dimensionless speed

$$x = v/\sqrt{2kT}\ . \tag{127}$$

Here the mass of the neutron is again present to provide the correct dimensions for $\sqrt{2kT}$. V(x) may be expressed in terms of Bessel functions, but for numerical calculations the integral representations appearing in V above and P(y→x) below are more practical. For large x (compared to one), V behaves as x as it should for the assumed atom speed distribution.

The integral equation is

$$\int_0^\infty dy\, n(y)P(y\to x) = n(x)\left[\frac{\sqrt{\pi}}{2}\Delta + V(x)\right], \tag{128}$$

where now

$$x = v/\sqrt{2kT}, \quad y = w/\sqrt{2kT}, \quad \Delta = v\sigma_a(v)/\sigma_s\sqrt{2kT}\ , \tag{129}$$

and the expression P(y→x) is defined below. Because, with this model, M(u) contains all atom speeds in the range zero to infinity, there is but a single integral equation for all neutron speeds x, for any mass of the thermalizing atoms. P(y→x) is considerably more complex. Defining, as in Section II,

$$a = \frac{m+1}{2m} \qquad c = \frac{m-1}{2m}$$

$$\begin{aligned} \alpha(x,y) &= \sqrt{m}\,(ax + cy) \\ \beta(x,y) &= \sqrt{m}\,(ay + cx) \\ \varkappa(x,y) &= \sqrt{m}\,(ax - cy) \\ \lambda(x,y) &= \sqrt{m}\,(ay - cx), \end{aligned} \tag{54}$$

and the integrals

$$I_1(x,y) = \frac{1}{\pi}\int_{\alpha}^{\infty} dt\, e^{-t^2}\left(tg^{-1}\frac{\beta}{\sqrt{t^2-\alpha^2}} - tg^{-1}\frac{\alpha}{\sqrt{t^2-\alpha^2}}\right)$$

$$I_2(x,y) = \frac{1}{\pi}\int_{\varkappa}^{\infty} dt\, e^{-t^2}\left(tg^{-1}\frac{\varkappa}{\sqrt{t^2-\varkappa^2}} + tg^{-1}\frac{\lambda}{\sqrt{t^2-\varkappa^2}}\right) \tag{130}$$

$$I_3(x,y) = \int_{0}^{\varkappa} dt\, e^{-t^2}$$

$$I_4(x,y) = \int_{\sqrt{x^2-y^2}}^{\varkappa} dt\, e^{-t^2},$$

P(y→x) may be written as

$$P(y\to x) = 2ma^2\frac{x}{y}(I_1 + I_2) \qquad \text{if} \quad 0 \le y \le \frac{c}{a}x \tag{131}$$

$$= 2ma^2\frac{x}{y}(I_1 + I_2 + I_4) \qquad \text{if} \quad \frac{c}{a}x \le y \le x \tag{132}$$

$$= 2ma^2\frac{x}{y}(I_2 - I_1 + I_3) \qquad \text{if} \quad x \le y \le \frac{ax}{c} \tag{133}$$

$$= 2ma^2\frac{x}{y}(I_2 - I_1) \qquad \text{if} \quad \frac{ax}{c} \le y \le \infty\,. \tag{134}$$

The calculation of the above expressions for $P(y \to x)$ is outlined in Appendix A.

It is in this formulation of P that the special subregions of integration mentioned in Section I are important. The quantities $\varkappa$ and λ may be negative for appropriate values of x and y. λ is negative when subregion I does not appear in figure 1. $\varkappa$ is negative when subregion I does not appear in figure 2. The criterion for negative λ is $y < cx/a$. The vanishing of the subregion corresponds to the disappearance of I_4 between 132 and 131. Similarly $\varkappa$ is negative when $y > ax/c$ and I_3 disappears from 133 in 134. As a consequence, the magnitude of $\varkappa$ must be used for the integration limit of I_2 in 134. A physical interpretation of this situation may be given. Suppose $\varkappa$ is negative and the subregion I vanishes from figure 2. Then for certain values of the atom speed $u \geq 0$, no collision is possible in which a neutron has final speed v less than its initial speed w. That is, just as in the rest atom assumption the range of speed loss scattering is restricted. However, since all atom speeds are present in the distribution 123, the restriction is expressed as an attenuation of $P(y \to x)$ for $y >> x$, rather than an abrupt vanishing of P for $y > \frac{a}{c} x$ as in the rest atom case. It can be seen that $I_2 - I_1$ is very small compared to unity when $y >> ax/c$. The arctangents of the integrands in both I_1 and I_2 are of opposite sign. The lower limits of integration are large, and, finally, the integrals subtract. For dimensionless speeds, $P(2.0 \to 0.2) = 0.0128$ compared to $P(0.2 \to 0.2) = 0.6839$ (m=2). Here $ax/c = 0.6$ and $y = 2.0$.

Thermalization by Hydrogen

Thermalization by hydrogen is again simpler. The integral equation 128 becomes, with m=a=1, c=0, $\alpha=\kappa=x$ and $\beta=\lambda=y$,

$$2x\int_0^x dy\frac{n(y)}{y}\left[\int_{\sqrt{x^2-y^2}}^{\infty} dt\, e^{-t^2} - \frac{2}{\pi}\int_x^{\infty} dt\, e^{-t^2} tg^{-1}\frac{\sqrt{t^2-x^2}}{y}\right]$$

$$+2x\left[\frac{\sqrt{\pi}}{2} - \frac{2}{\pi}\int_x^{\infty} dt\, e^{-t^2}\cos^{-1}\frac{x}{t}\right]\int_x^{\infty} dy\,\frac{n(y)}{y} = n(x)\left[V(x)+\frac{\sqrt{\pi}}{2}\Delta\right], \qquad (135)$$

with V(x) defined in equation 126. For $x \gg 1$ the speed gain term ($y<x$) is very small unless y is very near x. Neglecting this term and the smaller terms of the remainder of the equation, 135 is approximately

$$2x\int_x^{\infty}\frac{n(y)dy}{y} = n(x)[x+\Delta] \qquad x \gg 1. \qquad (136)$$

This is, once again, the equation describing the neutron density in a medium with atoms at rest. Its solution is

$$n(x) = \frac{c_8 x}{(x+\Delta)^3}\,. \qquad (137)$$

For any atom mass the expression $P(y\to x)$ does not satisfy detailed balance even for this averaged energy model. The distribution of atom speeds 123 is such that there are yet motionless atoms present (see figure 6). In a sense, however, the averaged energy model is closer to satisfying detailed balance than the single energy model. A consequence of detailed balance is that $P(y\to x)$ can be made symmetric

under interchange of x and y if the dependent variable n(x) is modified. P(y→x) from equation 135 may be written as

$$P(y\to x) = \frac{2x}{y} e^{y^2-x^2}\left[\int_0^\infty \frac{dt\, e^{-t^2} t}{\sqrt{t^2+x^2-y^2}} - \frac{2}{\pi}\int_y^\infty \frac{dt\, e^{-t^2} t}{\sqrt{t^2+x^2-y^2}} \operatorname{tg}^{-1}\frac{\sqrt{t^2-y^2}}{y}\right]$$

$$\text{if } 0 \le y \le x, \qquad (138)$$

$$= \frac{2x}{y}\left[\frac{\sqrt{\pi}}{2} - \frac{2}{\pi}\int_x^\infty dt\, e^{-t^2} \operatorname{tg}^{-1}\frac{\sqrt{t^2-x^2}}{x}\right] \qquad \text{if } x \le y \le \infty.$$

Only the terms in the square brackets need be considered since the substitution $\nu(x) = n(x)e^{x^2/2}/x$ will symmetrize the remaining terms. In the square brackets, only the term x^2-y^2 in the square roots ($y<x$) prevents the expressions from being symmetric. Since this term is always greater than zero, speed gain scattering is attenuated compared to a speed loss scattering. As a result, relatively more neutrons scatter from x to y than from y to x when x is larger than y. The effect of this imbalance is, qualitatively, to shift the peak of the neutron distribution to lower speeds than would result if P could be symmetrized. This conclusion might be expected, for the distribution of atom speeds 123 is biased in favor of small atom speeds compared to a Maxwellian atom speed distribution for which P can by symmetrized.

Numerical solutions to equations 128 and 135 are discussed in Section IV. Results are displayed in Section V.

IV. NUMERICAL SOLUTION OF THE THERMALIZATION EQUATIONS

Neutron Source and Conservation of Neutrons

The typical integral equation solved is

$$\int_0^\infty dy\, n(y)\, P(y\to x) = n(x)\left[V(x) + \Delta\right]. \tag{139}$$

As indicated in Section II, the presence of absorption requires a source of neutrons, and the above equation is valid only in a limited range of x. The upper limit of this range is designated x_o. The source of neutrons is taken to be those neutrons which undergo collisions at speeds greater than x_o which produce neutrons of speed less than x_o. That is

$$S(x) = \int_{x_o}^\infty dy\, n(y)\, P(y\to x) \ . \tag{140}$$

x_o is also assumed to be large enough that n(x) assumes its asymptotic form as given in equations 63, 80 and 137. This is tantamount to saying that x_o is large enough that the rate of speed gain scattering is negligible. x_o is a speed which is asymptotic in two senses. It is large enough so that the neutron density described in 139 assumes an asymptotic form and it is small enough so that neutrons arriving from the true source (assumed to be at very high speeds) have an asymptotic distribution. Both these distributions have the same form as has been described previously. With n(x) known (within an arbitrary constant), S(x) is determined within an arbitrary constant. Rather than adjust the source constant to conserve neutrons for varying absorption, the source constant is chosen to be unity. Then, conservation of neutrons

is maintained by adjusting the normalization of the neutron density. Such a normalization adjusts the amplitude of the neutron distribution to display graphically the effect of absorption.

With n(x) known for $x \geq x_o$, S(x) is known and equation 139 is now

$$\int_0^{x_o} dy\, n(y)P(y\to x) + S(x) = n(x)[V(x)+\Delta] \qquad \text{if } 0 \leq x \leq x_o. \tag{141}$$

Integrating the equation over x provides an approximate conservation relation,

$$\int_0^{x_o} dx S(x) = \Delta \int_0^{x_o} dx\, n(x) + \int_0^{x_o} dx\, n(x)V(x) - \int_0^{x_o} dx \int_0^{x_o} dy\, n(y)P(y\to x) = \Delta \int_0^{x_o} dx\, n(x) . \tag{142}$$

The relation is approximate because $x_o \neq \infty$. For the case of the single energy hydrogen oscillator this approximation may be estimated analytically. By actually integrating equations 76 and 77, it is shown in Appendix D that $\int_0^{x_o} dx \int_0^{x_o} dy\, n(y)P(y\to x)$ differs from $\int_0^{x_o} dx\, n(x)V(x)$ by a single term which is

$$\epsilon = \frac{\int_0^{x_o} dy\, n(y)}{\sqrt{x_o^2-1}} \int_{x_o}^{\sqrt{1+y^2}} dx \left(\frac{2x}{y} - \frac{2x}{y}\sqrt{x^2-y^2} \right), \tag{143}$$

or

$$\epsilon = \frac{\int_0^{x_o} dy\, n(y)}{\sqrt{x_o^2-1}} \left[y - \frac{x_o^2}{y} + \frac{1}{3y} + \frac{2}{3y}\left(x_o^2-y^2 \right)^{3/2} \right]. \tag{144}$$

but for x_o large, $\sqrt{x_o^2-1}$ is large and n(y) may be approximated by

$1/y^2$. Using this value, integrating, and expanding in inverse powers of x_o, the error is

$$\epsilon = \sum_{n=0}^{\infty} \frac{1}{(2n+4)(2n+5)x_o^{2n+4}} , \tag{145}$$

with the first term

$$\frac{1}{20x_o^4} . \tag{146}$$

With $x_o = 5$, (a value used in most calculations)

$$\epsilon = 0.00008156.... \tag{147}$$

In this instance the integrated source of equation 140 is

$$\int_0^{x_o} dx S(x) = \left(\frac{x_o^2}{2} - \frac{1}{12}\right) \frac{1}{(x_o+\Delta)^2} , \tag{148}$$

which for the largest value of Δ employed ($\Delta=4$) is equal to 0.153 at $x_o=5$ so that ϵ is a negligible correction. A typical integrated source for all problems is near one half for small absorptions. The term ϵ of equation 143 is due to the speed gain scattering of neutrons (of equation 77). The term is small because relatively few neutrons can gain scatter when the neutron speed is much larger than the maximum oscillator speed. That is, $P(y \to x) \ll 1$ when $x \gg y$. The gain scatter terms for the averaged energy oscillator model are also very small for sufficiently large neutron speeds. For $m=1$ this can be seen directly from equation 90. For $m > 1$, $P(y \to x)$ was numerically shown to be small (for small y and large x) compared to $P(y \to x)$ for nearly equal y and x. For example, $P(0.2 \to 2.0) = 0.00917$ compared to $P(2.0 \to 2.0) = 1.965$ (m=2).

In view of the above discussion, the approximation of equation 142 is felt to be very good for sufficiently large x_o. In fact, it is the neglect of the speed gain scattering terms which leads to the asymptotic forms of n(x) for $x >> 1$, so that if numerical solutions approach these asymptotic forms for $x < x_o$, the validity of the approximation is confirmed.

Numerical Analysis of the Thermalization Equation

Equation 139 is solved by reducing it to a set of linear equations in r unknowns. n(o) is zero as may be determined directly from the specific equations. Choosing a uniform integration mesh spacing h and defining

$$x = ih, \qquad y = jh, \qquad i, j = 1, 2, \ldots r, \tag{149}$$

$$S_i = S(ih), \quad V_i = V(ih), \quad n_i = n(ih),$$

$$P_{ij} = w_j P(jh \rightarrow ih),$$

$$w_j = h \quad j \neq r,$$

$$w_r = h/2,$$

the system becomes

$$\sum_{j=1}^{r} P_{ij} n_j + S_i = n_i [V_i + \Delta] \qquad i=1, 2, \ldots r. \tag{150}$$

The algebraic equations 150 are solved iteratively. An initial guess (a Maxwellian) is assumed

$$n_i^{(k)} = (ih)^2 \, e^{-(ih)^2} \qquad i=1, 2, \ldots r. \tag{151}$$

and normalized to satisfy neutron conservation (the tilde representing normalization),

$$\tilde{n}_i^{(k)} = n_i^{(k)} \sum_{j=1}^{r} w_j S_j \Big/ \left(\Delta \sum_{j=1}^{r} w_j n_j^{(k)} \right) \qquad i=1, 2, \ldots r. \qquad (152)$$

Successive approximations are generated by the scheme

$$n_i^{(k+1)} = \frac{\sum_{j=1}^{r} P_{ij} n_j^{(k)} + S_i}{V_i + \Delta} \qquad i=1, 2, \ldots r, \qquad (153)$$

and the normalization of equation 152 is performed as each new iterate is computed. Iteration is continued until

$$\text{Max}_i \left| \frac{n_i^{(k+1)} - n_i^{(k)}}{n_i^{(k+1)}} \right| \leq 10^{-5} \quad . \qquad (154)$$

The integrals appearing in $P(y \to x)$ and $V(x)$ for the averaged energy model (equations 131-4 and 126) are also computed numerically. All the integrals may be cast in the form

$$I(x, y) = \int_{f(x, y)}^{\infty} dt\, e^{-t^2} g(x, y, t), \qquad (155)$$

and the mean value theorem used to truncate the integration. For actual computation the value of the upper limit of integration was chosen to be $f(x, y) + 4$ for $m=1$, and $f(x, y) + 3$ for masses greater than one. Simpson's rule is used for the quadrature. For $m=1$ all the integrands are well behaved and a mesh spacing of 0.1 suffices for four decimal accuracy. The accuracy was verified experimentally by varying the mesh spacing and using known value of error functions as a control. For masses greater than one, some of the integrands of the integrals of $P(y \to x)$ are

rapidly varying functions. Fortunately, in the instances where the integrands vary rapidly the integrals are small compared to other terms. All integrations were ultimately performed with a mesh spacing of 0.05 over the ranges given above.

Modified Source for Atoms Other than Hydrogen

For masses greater than one in the averaged energy model, computation of the source from 140 with the known P(y-x) is as lengthy as the computation of the entire matrix P_{ij}. To conserve computing time, a modified source is used. From the known theory of neutron slowing down (14) the asymptotic neutron density is given by (in the notation of the thesis)

$$n(x) = \frac{S_o}{\xi \sigma_s x[x+\Delta]} e^{-\int_x^{x_s} \frac{2\Delta dx}{\xi x[x+\Delta]}}, \qquad (156)$$

where S_o is the true source strength, and x_s is the source speed (very large compared to x and Δ). ξ is the mean logarithmic energy decrement of a neutron in a collision with an atom of mass m, if the atom is at rest.

$$\xi = 1 + \frac{(m-1)^2}{2m} \ln\left(\frac{m-1}{m+1}\right). \qquad (157)$$

For m = 1, ξ = unity; and ξ decreases with increasing m, approaching 2/m.

The solution for n(x) given by 156 is

$$n(x) = \frac{S_o x^{\frac{2}{\xi}-1}}{\xi \sigma_s (x+\Delta)^{\frac{2}{\xi}+1}}, \qquad (158)$$

which has the following special forms:

$$n(x) = \frac{S_o}{\sigma_s} \frac{x}{(x+\Delta)^3} \qquad m=1, \tag{159}$$

$$n(x) = \frac{S_o}{\xi\sigma_s x^2} \qquad \Delta=0,$$

$$n(x) \to \frac{S_o}{\xi\sigma_s x^2} \qquad x >> \Delta.$$

The approximation of $P(y\to x)$ is taken from the theory of rest atom scattering (see equation 61).

$$P(y\to x) = \frac{2x}{y} \frac{(m+1)^2}{4m} \qquad x_o \le y \le \frac{(m+1)x}{m-1} \quad . \tag{160}$$

The approximate source then is, from equation 140,

$$S(x) = \frac{(m+1)^2 x}{2m} \int_{x_o}^{\frac{m+1}{m-1}x} dy \frac{n(y)}{y} \qquad \frac{m-1}{m+1} x_o \le x \le x_o. \tag{161}$$

Thus the source feeds neutrons into a limited range of x below x_o except for m=1. The evaluated source is then

$$S(x) = \frac{(m+1)^2 x}{2m\xi} \left[\left(\frac{y}{y+\Delta} \right)^{2/\xi} \frac{y\xi^2+2\Delta\xi}{2\Delta^2(2-\xi)y} \right]_{x_o}^{\frac{m+1}{m-1}x} \qquad \text{if } \frac{m-1}{m+1} x_o < x \le x_o, \tag{162}$$

$$= 0 \qquad \text{if } 0 \le x \le \frac{m-1}{m+1} x_o ,$$

where S_o has been chosen to absorb certain constants* so that the

* In actual numerical calculations S is multiplied by $\sqrt{\pi}/2$ because the source free equation has been multiplied by this constant.

neutron distribution should asymptotically approach $1/\xi x^2$ for large x. The integrated source is near one half for sufficiently small absorption. As an example, the numerically integrated source for $\Delta = 0.01$, m=9, is 0.4900.

The assumptions used in calculating the approximate source are qualitatively consistent with the actual integral equation. For m=1, n(x) asymptotically approaches (within a constant) the form given by equation 158. The form of P(y→x) of 160 appears in the equation multiplied by integrals which are slowly varying in the range of y, $x < y < \frac{m+1}{m-1} x$, and which are small $\frac{m+1}{m-1} x < y$. The attenuation of P for these latter values of y has been discussed in Section III. The ultimate test for the validity of the assumptions, which are applied for $x > x_o$, is the asymptotic behavior of calculated values of n(x) for $1 \ll x < x_o$.

Numerical Errors

Actual computations were accomplished with the aid of an IBM 7090 computer. FORTRAN programming was used to translate the numerical problem into machine language.

In a sense, the numerical solution of the type of equations occurring in the thesis is an experiment. Assumptions made to permit numerical computation produce errors which compound with the inherent limitations of the machine to produce further errors. A precise estimate of the deviation of the numerical solutions from the actual solutions is not possible. To test the accuracy of a given approximation it is possible to vary the approximation and observe the effect upon the solution. In effect, an experiment is performed.

The fundamental errors in the computation are:

1) The replacement of the integral equation by a discrete system of equations.

2) The assumption of an asymptotic form of neutron density for large speeds.

3) The solution of the system of algebraic equations by an iterative technique.

4) For the averaged energy model,

   a) the assumption of a known form of $P(x \rightarrow y)$ in a range of calculation,

   b) and the numerical calculation of the integrals of $P(x \rightarrow y)$.

5) Machine errors.

The errors of 4) b) have been discussed. The errors of 4) a) and 2) are related. It is felt that the strongest test of the assumptions producing these particular errors is the computed behavior of $n(x)$ in regions of x where $n(x)$ should assume its asymptotic form. The normalization is such that the amplitude of n is "floating". That is, the neutron density function is adjusted to conserve neutrons and the final computed amplitude of the function is free. If the final amplitude for $x >> 1$ is that as predicted by the assumed asymptotic forms, then a strong confirmation of the assumed forms is given. That is, the equation is such that the actual behavior of $n(x)$ is the assumed behavior. In all actual computations the neutron density in the range $4 < x < x_o$ is found to agree very well with the assumed forms:

$$n(x) = \frac{x}{(x+\Delta)^3} \qquad \text{if } m = 1, \tag{163}$$

$$n(x) = \frac{1}{\xi x^2} \qquad \text{if } m > 1,\ \Delta \ll 1.$$

The iterative technique is a powerful tool for the solution of large systems of equations. The convergence of the final iterate to satisfy the criterion 154 means that the final iterate satisfies the formulated equations to that degree of accuracy. Conventional row reduction methods of solving linear equations are highly susceptible to round off error because of numerous subtractions. Because the elements of P_{ij} are all positive, the iterative method consists entirely of additions and multiplications. Such manipulations are performed by the machine in floating decimal arithmetic so that a minimum of eight significant figures are always retained. The division by $V_i+\Delta$ does not involve small numbers (cf. figure 3). To check a possible dependence on the initial guess, a test run was performed with several different guesses including a partially negative guess. In all cases the final answers agreed to the order of accuracy specified by equation 154. In fact, in varying the parameter Δ, solutions for a previous value of Δ were used as initial guesses for the next value of Δ. Final solutions for the same value of Δ again agreed to five significant figures, independent of the initial value of Δ from which the computation began.

The reduction of the integral equation to a system of algebraic equations is essentially a numerical integration. As the scheme of equation 119 indicates, a trapezoidal integration is performed. Analytic estimation of the integration error is not possible, for at best n(x) is

known only numerically. The effect of varying the mesh spacing, h, was determined to be small once a sufficiently small h was chosen. A practical lower limit of h is determined by machine storage capabilities. $h = 0.01$ for the range $0 \leq x \leq 5.0$ produces 500 equations and P_{ij} then has 250,000 elements. For the two values of $h = 0.10, 0.05$, the solution for the averaged energy model for mass one varied only in the fourth significant figure.

Compared with other errors, machine errors are not deemed significant. Machine programs compute elementary functions, e.g., square roots, arctangents, exponentials, etc., to eight significant figures. All arithmetic is performed with floating decimal point location which minimizes round off error except for the subtraction of nearly equal quantities. As mentioned, the iterative technique avoids subtractions. Elsewhere in the computation, a very small number is the desired result for subtraction of nearly equal numbers. Only in the computation of the integrals for $m > 1$ is subtraction of nearly equal small numbers likely, and the computation of the integrals was performed separately to insure their smooth variation. (Round off errors typically display a statistical variation which produces a characteristic "meander" in a function which is actually smoothly varying.)

As an additional check on the entire numerical procedure and to provide comparison values of the neutron distribution, the Wigner-Wilkins equation was solved ($m=1$) using the methods of this section.

It is felt (although not proved) that final numerical values of

n(x) are accurate to three significant figures. This accuracy is more than sufficient for qualitative comparisons with contemporary experimental and theoretical work. If greater accuracy were needed for a specific calculation using the computed values of n(x), the accuracy of the above procedure could be refined by using more sophisticated quadrature schemes and finer integration meshes.

Representative Parameters of a Typical Computation

Typical values of parameters used in solving the integral equations representing the various models are given below. Maximum capabilities of the programs written are given in parentheses.

Range of solutions	$0 < x \leq 5.0$		
Mesh spacing h	0.05	m = 1	
	0.10	m > 1	
Resultant matrix size	100 x 100	m = 1	(150 x 150)
	50 x 50	m > 1	
Values of Δ	10		(unlimited)

Other information:

Number of iterations for convergence	10
Computing time	0.2 min/value of Δ, m=1 1.0 min/value of Δ, m>1.

The numerical procedures outlined in this section are the result of the refinement of much cruder initial attempts to solve the neutron balance equation. Numerical methods that were less satisfactory are discussed in Appendix E. In addition, Appendix E contains the final form of the actual programs used to compute n(x).

RESULTS AND CONCLUSIONS

Single Energy Harmonic Oscillator Model

For the single energy oscillator model the neutron density distribution is shown in figure 7. The curves represent thermalization by hydrogen for three values of Δ. The attenuation of the curves with increasing Δ is a direct result of the absorption of neutrons. There is also a slight displacement of the peak of the distribution towards larger speeds with increasing absorption. This displacement is more pronounced in figure 8, where the effect of larger Δ upon the distribution is displayed. The vertical scale in figure 8 is a continuation of the vertical scale in figure 7.

The displacement of the neutron distribution to higher speeds with increasing Δ, sometimes called "absorption hardening", is a result of the finite time required for the source neutrons to acquire thermal speeds. For large Δ, this time is large, since the absorption rate is high. For very large Δ, as in figure 8, the resemblance of the neutron distribution to an equilibrium distribution disappears almost entirely. This effect for the model of the thesis is in qualitative agreement with numerically computed distributions reported by Hurwitz (23) for the heavy monatomic gas model.

The approach of the neutron distribution to the asymptotic distribution for large x is clearly shown in figure 7. Although the exact equation was computed for $0 \leq x \leq 5.0$, the computed value at $x = 3.0$ is 0.1134 for $\Delta = 0.01$ while the value of

$$n(x) = \frac{x}{(x+\Delta)^3}, \qquad \Delta = 0.01, \qquad x = 3.0, \tag{164}$$

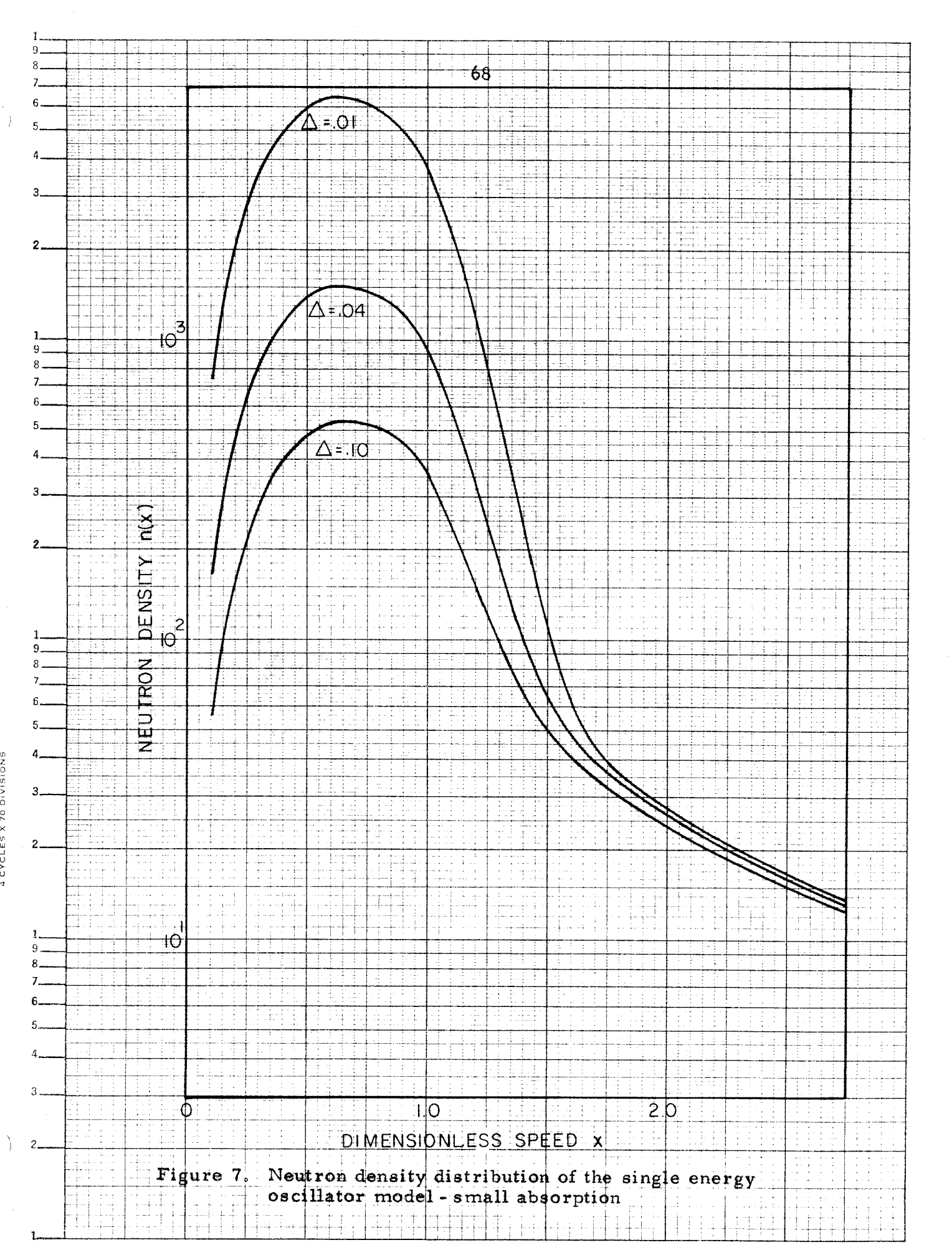

Figure 7. Neutron density distribution of the single energy oscillator model - small absorption

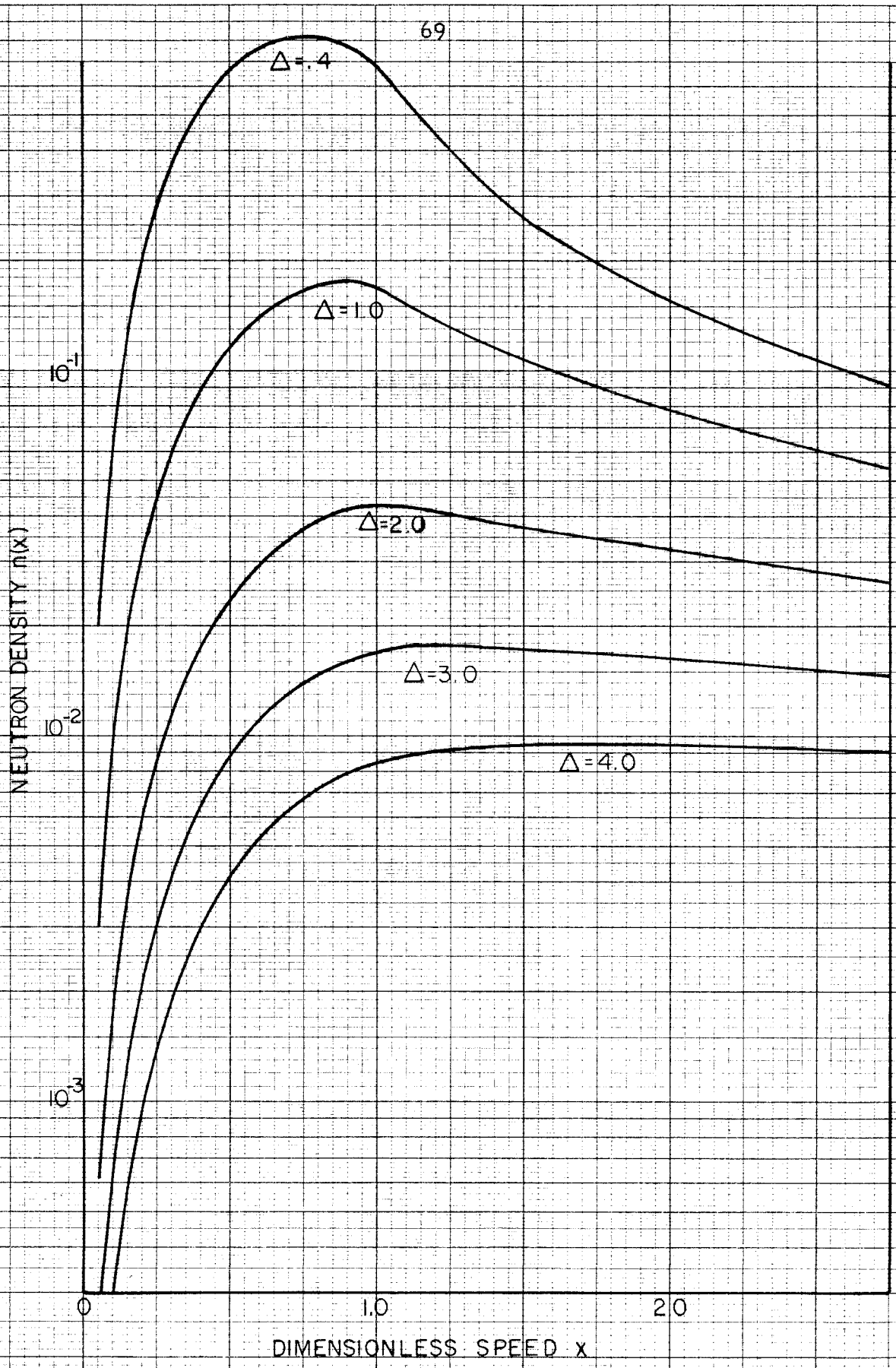

Figure 8. Neutron density distribution of the single energy oscillator model - large absorption

is 0.1100.

Figure 9 displays the neutron distribution for $\Delta = 0$. The appearance of the non-equilibrium "tail" is shown clearly. The actual values of n(x) in this curve are not as reliable as the values computed for non-zero Δ. The neutron conservation normalization of iterates is not possible for $\Delta = 0$ because of division by Δ. For the computation of figure 9, iterates were normalized to maintain the maximum value of n(x) constant. A Maxwellian is drawn on figure 9 to illustrate the qualitative deviation from an equilibrium distribution.

Comparison with Experiment

Two experimental values of neutron distributions for thermalization by zirconium hydride are reported in the literature by Beyster et al., (24). Both experimental values are measurements in $ZrH_{1.5}$. One measurement is for an unpoisoned assembly $\sigma_a = 0.49$ barns per hydrogen atom and the second measurement is for a boron poisoned assembly, $\sigma_a = 4.95$ barns per hydrogen atom.

Using large scale plots of the experimental observations furnished by Beyster, a comparison of the single energy oscillator model (m=1) is possible. The experimental quantity measured is the neutron flux per unit energy,

$$\phi(E) = vn(E). \tag{165}$$

Because of the Jacobian of the transformation from energy to speed variables

$$\phi(E) = \frac{n(v)}{m_n}, \tag{166}$$

where m_n is the neutron mass which is unity in the system of units

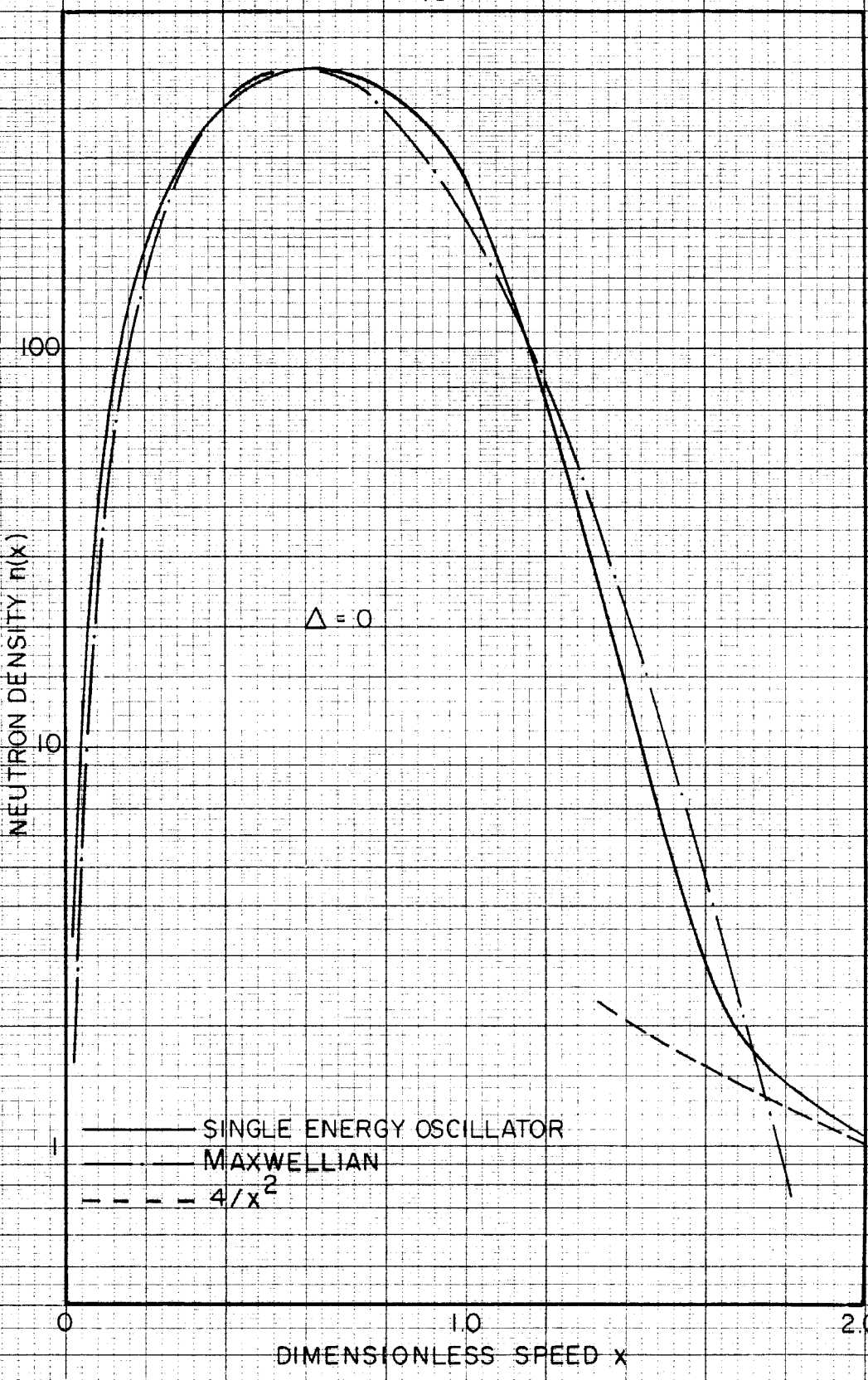

Figure 9. Neutron distribution of the single energy oscillator model. (Non-absorbing medium.)

employed in the thesis. In terms of dimensionless variables used for the single energy oscillator model

$$\phi(E) = c_9 n(x) \tag{167}$$

$$E = E_o x^2,$$

where E_o is the oscillator energy. The constant c_9 is not relevant, for the neutron distributions may be arbitrarily normalized. Therefore the distributions of figure 7 or 8 may be compared with experimental neutron flux distributions by plotting them versus $E_o x^2$ and adjusting the amplitude. For zirconium hydride the experimental value of E_o is 0.137 ev (16). For $\Delta = \sigma_a(v)v/\left|\sigma_s\sqrt{2E_o}\right| = 0.10$, figure 10 shows a comparison of the computed distribution of the single energy oscillator model with the experimental distribution. The amplitude of the single energy oscillator model neutron distribution was adjusted to coincide with the experimental results at 3.425 ev. The computed value of Δ, using a scattering cross section of 20.36 barns for hydrogen and the reported value $\sigma_a = 4.95$ barns/hydrogen atom, is 0.104. The effect of an addition of 0.004 to Δ is not discernible on the plot of figure 10. Thermalization by zirconium atoms is neglected. A measure of the effectiveness of a material in slowing down neutrons is a quantity known as the moderating power (13),

$$N\xi\sigma_s , \tag{168}$$

where N is the atomic density and ξ is defined in equation 157. The ratio of this quantity for hydrogen and zirconium is, in $ZrH_{1.5}$,

$$\frac{N_H \xi_H \sigma_{s_H}}{N_{Zr}\xi_{Zr}\sigma_{s_{Zr}}} = \frac{1.5(1)(20.36)}{(1)(2/91)(6)} = 231.6 , \tag{169}$$

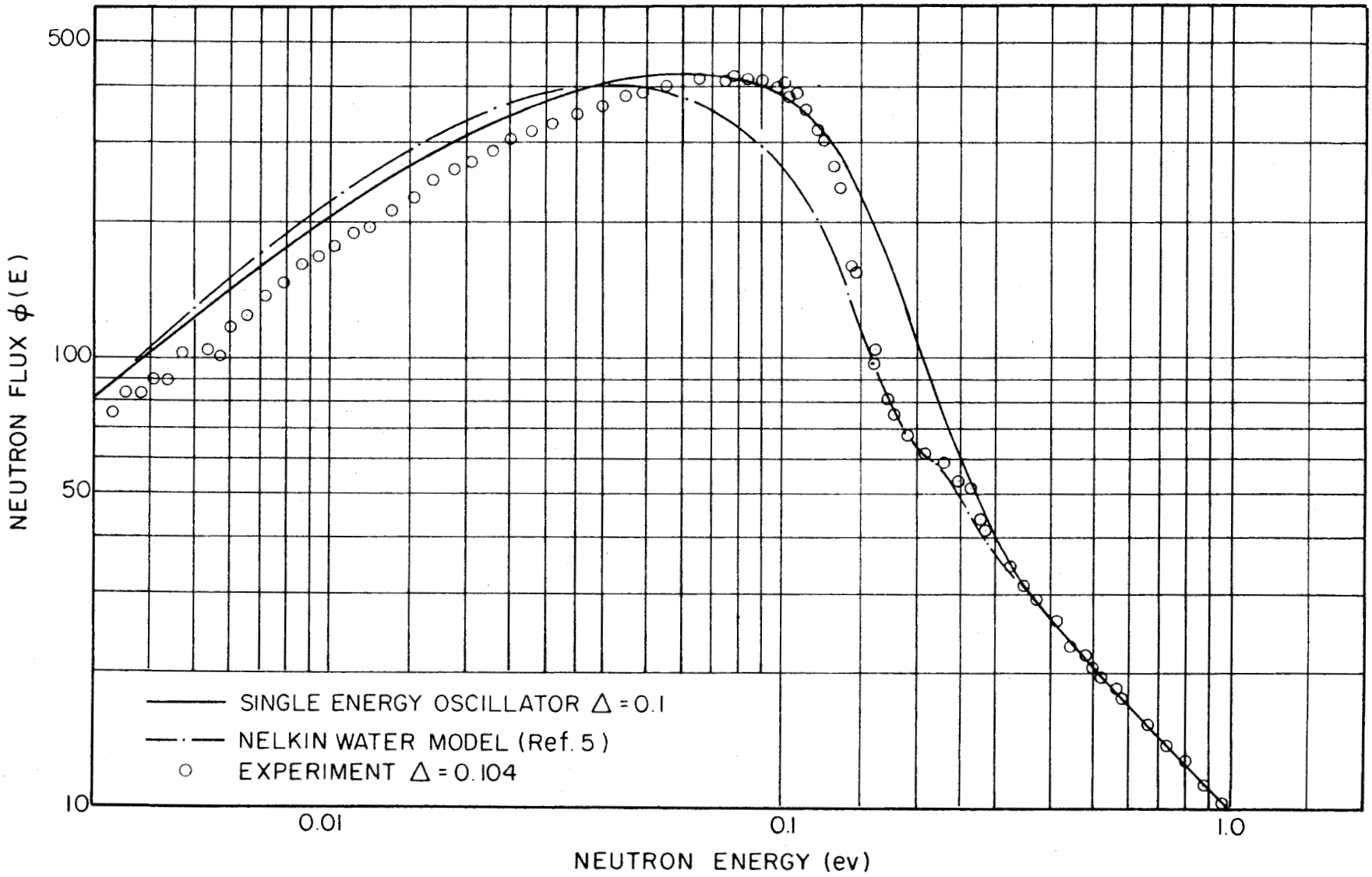

Figure 10. Comparison of single energy oscillator neutron distribution with experimental results for $Z_r H_{1.5}$

so that hydrogen is much more effective in the thermalizing process than zirconium.

The broken curve in figure 10 is the neutron distribution calculated from a modification of Nelkin's water model scattering kernel (5). In the computer program calculating thermalization using the Nelkin scattering kernel (25), thermalization by zirconium is neglected.

The dip of the experimental curve near 0.14 ev is the quantum mechanical effect of restricted energy transfer which the classical oscillator model cannot display. Similar distortions of the experimental curve are barely visible at 0.27 ev and 0.41 ev. Such effects might be simulated with the classical oscillator model by superposing the single energy oscillator solutions for nE_o, $n=1, 2, \ldots$, with the amplitude of the individual solutions weighted by the Boltzmann factor $\exp(-nE_o/kT)$ and the statistical weight of each state. This procedure could be accomplished by using a single solution of figure 7 and appropriately adjusting the dimensionless speed x.

Figure 11 shows a single energy oscillator model neutron density curve compared with the other experimental curve given by Beyster ($\sigma_a = 0.49$ barns/hydrogen atom). The calculated experimental value of Δ is 0.130 and the value of $\Delta = \sigma_a v/\sigma_s\sqrt{2E_o}$ used for the single energy oscillator fit is also 0.130. But in this case E_o was not taken to be 0.137 ev. Instead a value of $E_o = 0.091$ ev was used. It is felt that in this case the experimental neutron spectrum is not representative of an infinite medium. Beyster acknowledges the effect of a finite assembly

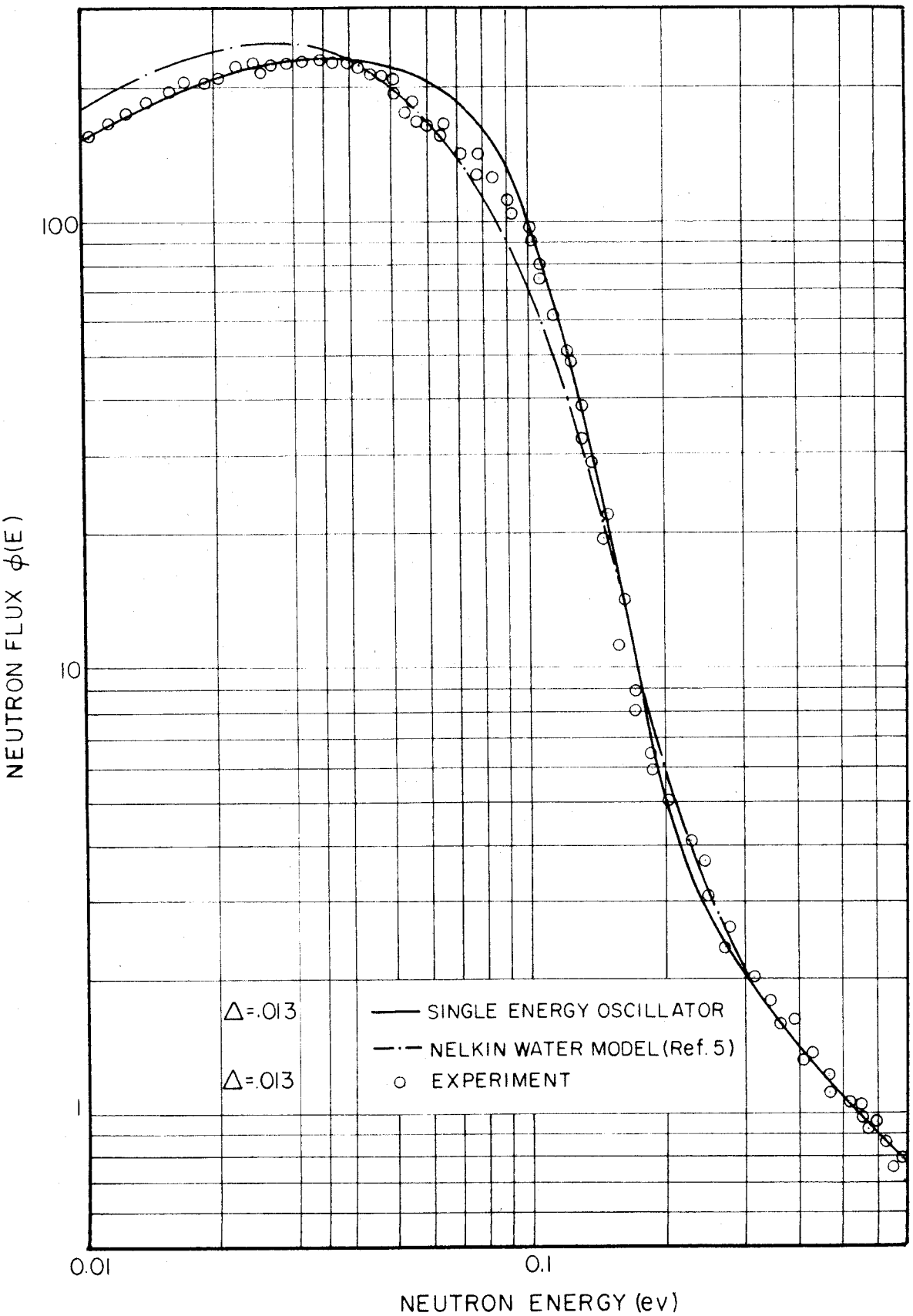

Figure 11. Comparison of single energy oscillator model neutron distribution with experimental results for $ZrH_{1.5}$

on the distribution in his article. No existing theory can account for the shift of the neutron distribution for the order of magnitude difference of absorption between the two experiments. The effects of a finite assembly are more pronounced for small absorption. In the less absorbing experiment the mean free path to absorption for a neutron is ten times as great as in the experiment containing more absorption. Consequently, the escape of neutrons from the assembly is much more important. The qualitative effect of neutron escape is to "cool" the distribution, that is, to shift it in favor of lower speeds. This shift is reflected in the smaller value of E_o used to fit the experimental curve with the single energy oscillator model. The good qualitative fit obtained indicates that application of the oscillator model may be regarded from another viewpoint. The model may be regarded as a single parameter (E_o) fit to experimental data. (If the dependence of Δ upon E_o is ignored a two parameter fit is possible.) The availability of only two experimental distributions does not permit testing of this potentiality.

Averaged Energy Harmonic Oscillator Model

Figure 12 displays the computational results for thermalization by the averaged energy oscillator model with a hydrogen oscillator. For comparison, the dotted curves represent solutions of the monatomic hydrogen gas model equations (reference (1), Appendix B) for the same values of absorption. Both sets of curves approach the same values for large x. The monatomic gas model curves are peaked near $x = 1.0$ as is a Maxwellian.

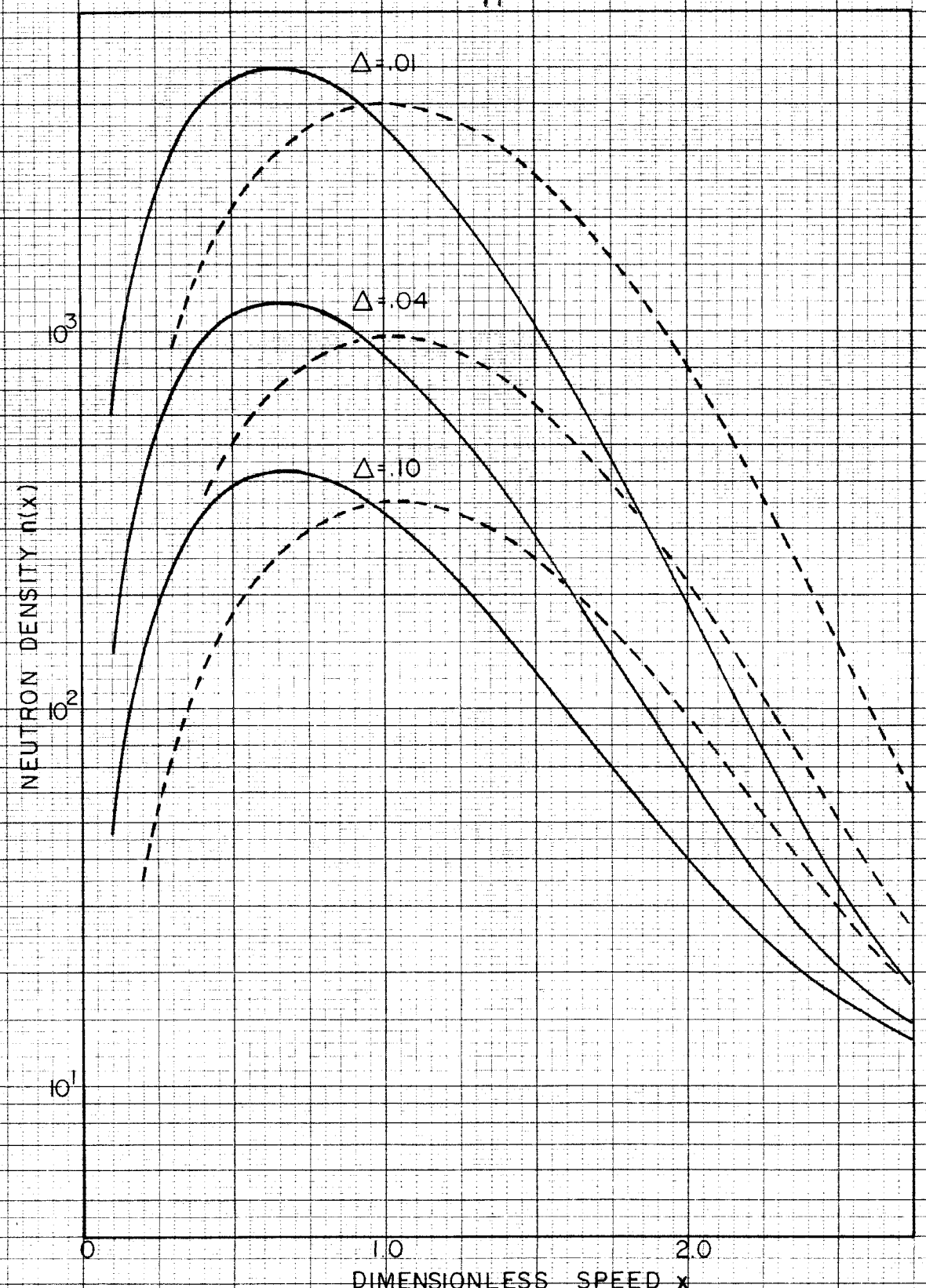

Figure 12. Neutron distribution of the averaged energy oscillator model, m=1. Dashed curves are neutron distributions for a monatomic hydrogen gas.

Figure 13 shows the variation of the neutron distribution computed with the averaged energy model for atoms of different masses. The masses 2, 9 and 12 represent deuterium, beryllium, and carbon, respectively, corresponding to materials actually used in nuclear reactors. The main variation of the curves is in the asymptotic approach to $1/\xi x^2$ (fig. 13b). This implies that if the quantity $\Delta_o = \Delta/\xi$ were held constant in a calculation the curves should be practically identical after suitable normalization.* If this supposition be true, the mass dependence of equation 128 is effectively restricted to the mass dependence of ξ (equation 157). That this observation is valid is surprising when the detailed mass dependence of equation 128 is examined. Some support for the conclusion is given by considering the constant

$$\Delta_o = \frac{\sigma_a(x)x}{\xi\sigma_s} , \qquad (170)$$

which contains the three intrinsic parameters describing the thermalzing medium. However, ξ is the mean logarithmic energy decrease for neutron scattering by motionless atoms. And it is the effective decrease of ξ due to thermal atomic motions which increases the amplitude of the neutron distribution in the thermal range.

In the approximate differential equation describing thermalization by a heavy monatomic gas (2), Δ_o is the only parameter appearing. This approximate equation is derived by an expansion in inverse powers

---

* The quantity appearing in equation 128 is then $\xi\Delta_o$. Instead of $\Delta = 0.01$ for all m, $\Delta_o = 0.01$ for all m and $\xi\Delta_o = 0.01$ for m=1, $\xi\Delta_o = 0.00725$ for m=2, etc. In effect decreasing values of Δ are used for increasing m. Decreasing Δ increases the value of the maximum of n(x) relative to the asymptotic value of n(x).

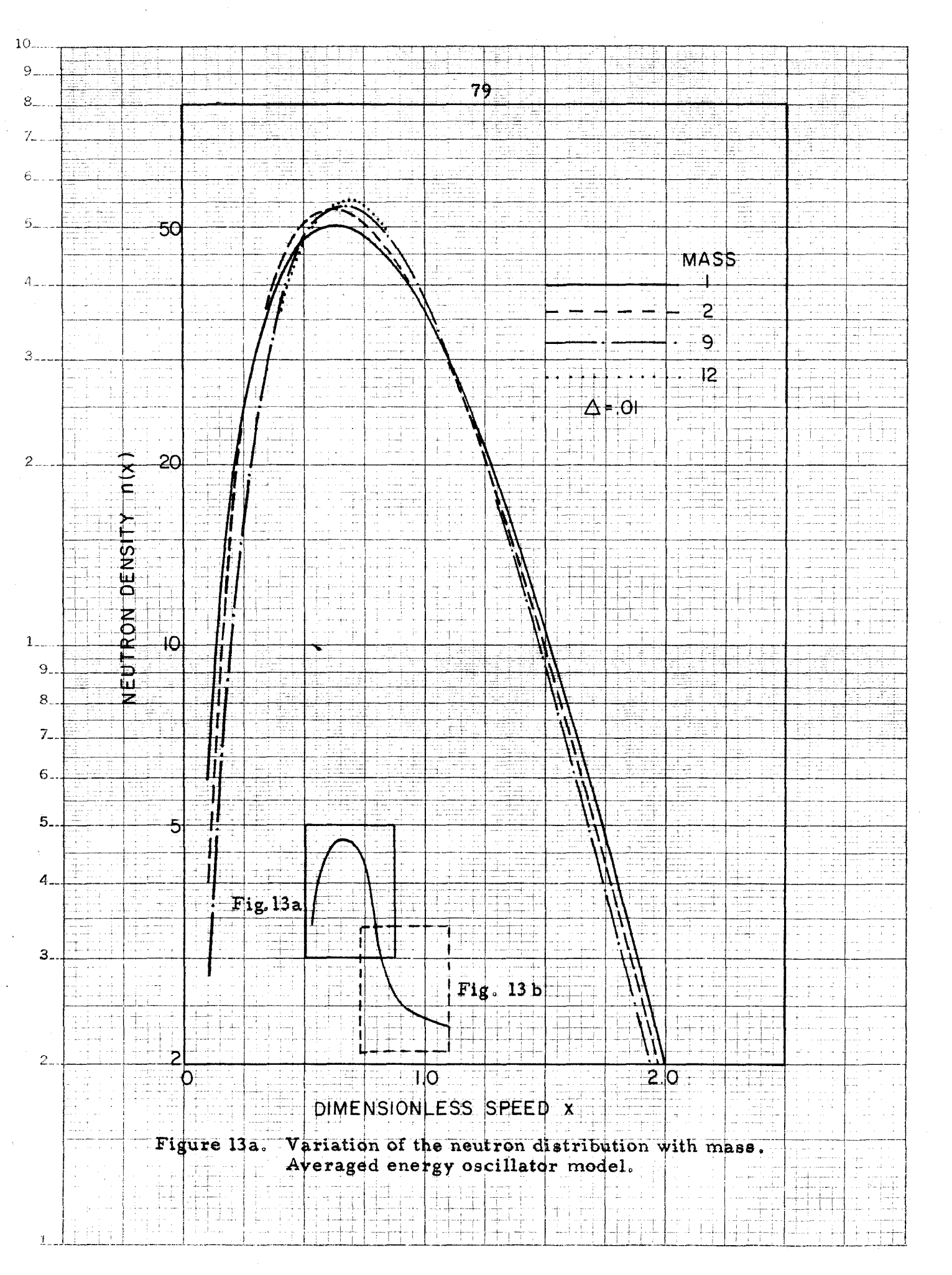

Figure 13a. Variation of the neutron distribution with mass. Averaged energy oscillator model.

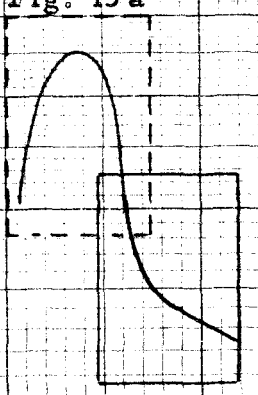

Figure 13b. Variation of the neutron distribution with mass. Averaged energy oscillator model.

of the atomic mass, neglecting terms of $O\left(\frac{1}{m^2}\right)$. (See Appendix B.) For the results of figure 13, the dependence upon Δ_o seems to hold even for m=2 which is not a large mass.

The shift of the peak of the distributions of figure 13 to larger x with increasing mass is in qualitative agreement with comparisons of the monatomic gas model for m=1 and m>>1 made by Hurwitz and Nelkin (23).

Effective Temperatures

As indicated in Section III, if the neutron distributions of the averaged energy oscillator model are to be characterized by a material temperature, an effective temperature must be used. That is, if for very small absorptions the neutron distribution is a Maxwellian, the peak of the distribution corresponding to the most probable neutron speed is near x=1. In the scale employed for figures 12 and 13, x=1 represents an energy kT, or 0.025 ev for $T = 300^{\circ}K$. The distributions of figure 13, however, are peaked in the neighborhood of x = 0.72 (m=9 and 12) corresponding to 0.013 ev at $T = 300^{\circ}K$. If the effective temperature suggested by the average energy of the oscillator speed distribution is chosen,

$$T^* = 2T, \tag{171}$$

the peaks of the two distributions of figure 13 correspond to neutron energies of 0.026 ev. The effective temperature chosen in 171 makes the average energy of the oscillator speed distribution (equation 123) correspond to the average energy of a Maxwellian atom speed distribution.

A different choice of an effective temperature is perhaps more physically plausible. For the Einstein and Debye models of crystalline solids, characteristic temperatures are defined for the prediction of specific heats. The motion of atoms in the Einstein and Debye models is Maxwellian, but the temperature characterizing the distribution is not the material temperature (Lamb (26)). The relations between this temperature, the material temperature and the characteristic Einstein or Debye temperature are given by Dresner (27).

$$T_E^* = \frac{1}{2}\Theta_E \coth(\Theta_E/2T) \tag{172}$$

$$T_D^* = \frac{3\Theta_D}{2}\int_0^1 dx\, x^3 \coth\left(\frac{x\Theta_D}{2T}\right), \tag{173}$$

where Θ_E and Θ_D are the Einstein and Debye characteristic temperatures. For material temperatures large compared to Θ_E or Θ_D these effective temperatures approach the material temperature. For materials with small Θ_E or Θ_D, then, the effective temperatures of 172 and 173 would be near the material temperature. But beryllium and graphite have anomalously high Einstein and Debye temperatures near 1000° K (14). Taking $\Theta_E = 1000^\circ$K, T= 300°K, gives $T_E^* = 537^\circ$K. With this temperature the peak of the distributions (m=9 and 12) of figure 13 corresponds to E = 0.023 ev.

Thus for beryllium and graphite, the use of an effective material temperature for the averaged energy oscillator atomic model places the most probable neutron energy near the most probable neutron energy of a thermal equilibrium distribution. (As long as the material

temperature is not much larger than 1000°K.) Such a conclusion is not true of the heavy gas atomic model (2) which predicts a most probable energy near kT using the material temperature. If the Einstein or Debye atomic model were used to provide an effective temperature for a Maxwellian atom speed distribution in beryllium or graphite, kT^* would be too large in the heavy gas model unless the material temperature were large compared with the Einstein or Debye temperature.

Although the use of an effective temperature may be used to interpret the most probable energy of the neutron distributions of the averaged energy oscillator model in the above manner, the detailed nature of the distribution differs from a thermal equilibrium distribution. This difference may be seen for m=1 in figure 12, where for small values of Δ the dotted curves are nearly Maxwellian in the range $0 \leq x \leq 2.0$. It is this detailed difference in the distribution that represents the internal structure of the averaged energy oscillator model.

Conclusions

The oscillator models developed in the thesis represent atomic motions which are only crude approximations to actual atomic motions. The energy exchange scattering cross sections derived from the models do not satisfy the principle of detailed balance so that the equilibrium neutron distribution described by the models is not Maxwellian. Nevertheless, the models represent an attempt to account for the effects of chemical binding. The attempt seems most successful in matching the experimental neutron distribution in zirconium hydride, a material for

which the effect of chemical binding is pronounced. The apparent success in zirconium hydride may, however, be coincidental. The experimental data may be unreliable, particularly because of neutron leakage from the finite assembly. The prediction of the neutron distribution in another metal hydride for which the hydrogen atom energy is well defined would be a much more satisfying test of the single energy oscillator model. Unfortunately experimental results are not available.

More experimental results are needed, too, to test the possibility that the single energy oscillator model could be considered a parametric fit to observed distributions. At least three measurements would be needed to calibrate parameters.

The averaged energy model developed may not represent the most suitable choice of oscillator energy distributions. The distribution chosen in the thesis is used to illustrate the method. The actual model used provides neutron distributions which are qualitatively interpreted in terms of effective material temperatures. Again, experimental measurements are needed to test the appropriateness of these temperatures.

In either the case of a parametric fit or the choice of an effective temperature to compare theoretical distributions with experimental distributions, the advantage to be gained from the models of the thesis would depend upon the prediction of a yet unmeasured distribution. For once a representative distribution were obtained, it might prove more advantageous to fit an analytic function to it rather than to use the models of the thesis.

A disadvantage of the models of the thesis is that they are not more amenable to analytic solution. Although this disadvantage is inherent in all thermalization models except the heavy gas model, a simple model to account for chemical binding which could be handled analytically would be of great practical utility. For the estimation of reactor characteristics dependent upon the thermal neutron distribution, e.g., the temperature coefficient of reactivity, numerical solutions are of limited usefulness because the dependence upon parameters is disguised. An extension of the models of the thesis to the problem of spatially dependent distributions would necessarily require numerical solutions.

The models of the thesis seem most applicable to systems in which the thermalizing atoms are strongly bound. It is in these systems that the neutron distribution deviates most markedly from an equilibrium distribution even for small absorption. Consequently the actual neutron distribution is most important in these systems. The models of the thesis, despite the numerous, and sometimes crude, approximations made, provide a means by which strong binding can be taken into account.

APPENDIX A

DETAILS OF THE CALCULATION OF P(w→v)

With the assumptions made in the text of the thesis P(w→v) is defined by

$$P(w\rightarrow v) = \frac{(m+1)v}{4m} \int\int \frac{du\,du\,M(u)}{v_c} \quad . \tag{A-1}$$

In this appendix, the above expression is evaluated for a variety of atom speed distributions M(u) and the details of the integration in the u-ν plane are given. Integrations on ν can be performed without knowledge of M(u) and the first section of the appendix is devoted to this evaluation. The second section contains a completion of the evaluation for a monatomic gas atom speed distribution. The integrations for the gas atom speed distribution are given here for three reasons: 1) the integrations do not appear in the literature, 2) the general technique employed is applicable to the atomic models of the thesis, and 3) there is an essential complication introduced by the models of the thesis which is highlighted by comparison with the integrations of the gas model. The third and fourth sections of the appendix are devoted to the evaluation for the two models of the thesis.

I-A. INTEGRATION OF $\int du/v_c$

When the change of variable

$$\begin{aligned} u &= u \\ \nu &= 2mwu_{\perp} + (m-1)(v^2 - w^2), \end{aligned} \tag{A-2}$$

is made, the condition that $v = v_{max}$ is the hyperbola

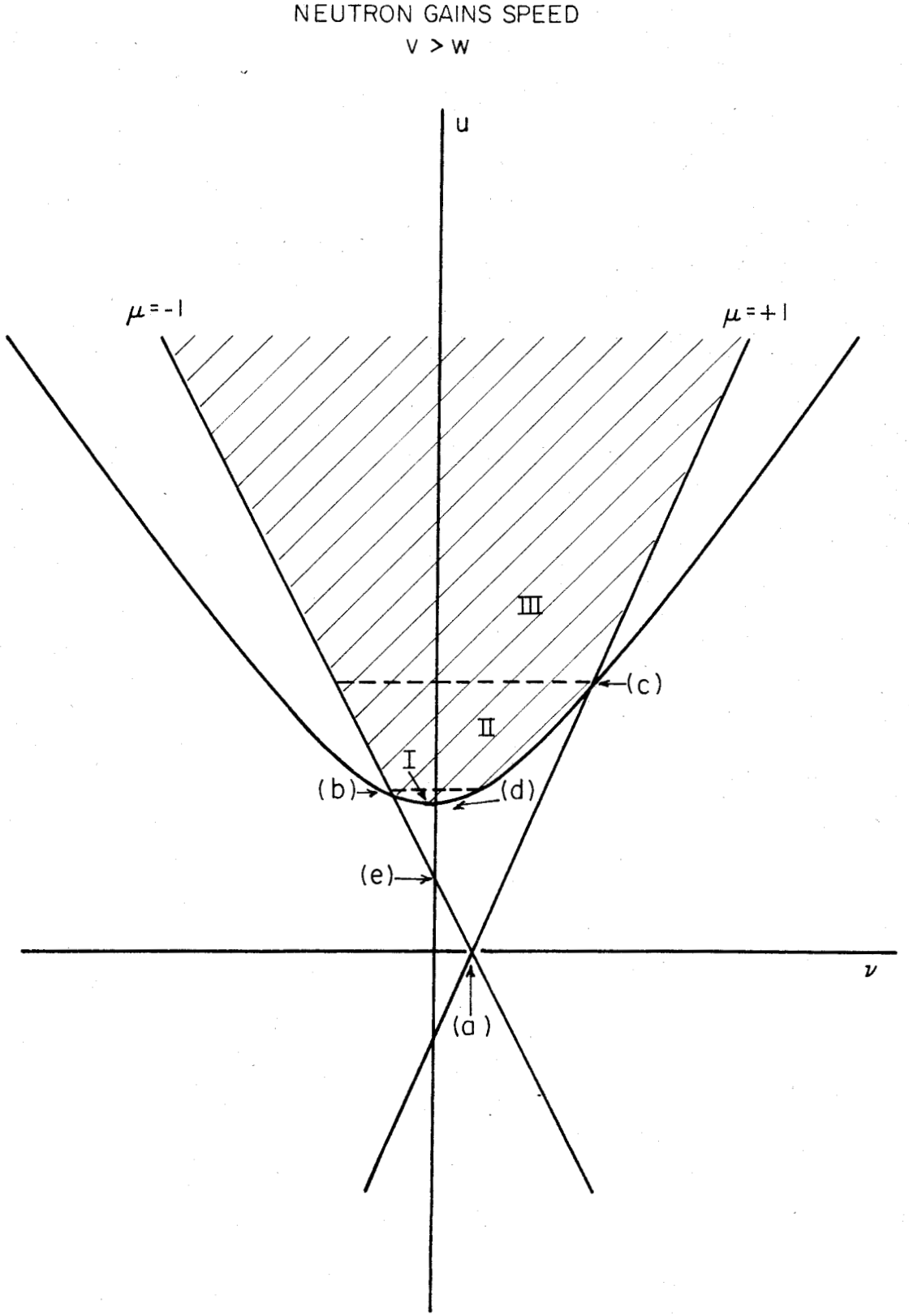

Figure 1. Domain of integration for neutron speed gain in a collision.

$$mu^2 - \frac{v^2}{4mv^2} = v^2 - w^2 , \qquad (A-3)$$

and the lines $\mu = \pm 1$ become the lines

$$\mu = +1 \qquad v = 2mwu + (m-1)(v^2 - w^2)$$
$$\mu = -1 \qquad v = -2mwu + (m-1)(v^2 - w^2). \qquad (A-4)$$

The cases of $v > w$ and $v < w$ are considered separately.

Neutron Speed Gain: $v > w$

When $v > w$ the positive branch of equation A-3 is shown in figure 1. The lines $\mu = \pm 1$ intersect the v axis at $v \geq 0$ (Point (a)). The lines (A-2) intersect the hyperbola (A-3) at

$$\text{point (b)} \quad \mu = -1 \qquad u = \frac{(m+1)v - (m-1)w}{2m}$$
$$\text{point (c)} \quad \mu = +1 \qquad u = \frac{(m+1)v + (m-1)w}{2m} , \qquad (A-5)$$

which are positive values of u when $v > w$. The minimum point (d) of the hyperbola is

$$u = \sqrt{\frac{v^2 - w^2}{m}} . \qquad (A-6)$$

The u value of the intercept of the line $\mu = -1$ (point (e)) is

$$u = \frac{(m-1)(v^2 - w^2)}{2mw} . \qquad (A-7)$$

This value is less than the minimum point (d) of the hyperbola when

$$(m-1)^2(v^2 - w^2) < 4mw^2 ,$$

or

$$(m-1)v < (m+1)w. \qquad (A-8)$$

When this criterion is satisfied there are three subregions of integration as indicated in figure 1. The u boundaries of these regions are, introducing the notation $a = (m+1)/2m$, $c = (m-1)/2m$,

$$\begin{aligned} &\text{I:} && \sqrt{\frac{v^2-w^2}{m}} \le u \le av-cw \\ &\text{II:} && av-cw \le u \le av+cw \\ &\text{III:} && av+cw \le u \le \infty . \end{aligned} \tag{A-9}$$

When criterion A-8 is not satisfied, that is when

$$cv > aw, \tag{A-10}$$

subregion I vanishes. The u boundaries of regions II and III remain the same. The boundaries on ν are the hyperbola in subregion I, the line $\mu = -1$ and the hyperbola in subregion II, and the lines $\mu = \mp 1$ in subregion III. These values of ν are

$$\begin{aligned} &\text{I:} && -2v\sqrt{m^2u^2-m(v^2-w^2)} \le \nu \le 2v\sqrt{m^2u^2-m(v^2-w^2)} \\ &\text{II:} && 2m[c(v^2-w^2)-wu] \le \nu \le 2v\sqrt{m^2u^2-m(v^2-w^2)} \\ &\text{III:} && 2m[c(v^2-w^2)-wu] \le \nu \le 2m[c(v^2-w^2)+wu] . \end{aligned} \tag{A-11}$$

In terms of the variables of equation A-2 the relation of equation A-1 is

$$P = \frac{(m+1)^2 v}{4m^2 w} \int \frac{du M(u)}{u} \int \frac{d\nu}{2\sqrt{w^2+m^2u^2-(m-1)(v^2-w^2)+\nu}} , \tag{A-12}$$

where v_c contributes the extra factor of m+1 and the Jacobian of the variable change produces a factor 2mwu. The indefinite integral of the ν integration of A-12 is

$$\sqrt{w^2+m^2u-(m-1)(v^2-w^2)+\nu} \quad . \tag{A-13}$$

Evaluating this term with the ν limits of equation A-11 gives, after some algebra,

$$\begin{aligned} \text{I:} \quad & v + \sqrt{m^2u^2-m(v^2-w^2)} - \left|v-\sqrt{m^2u^2-m(v^2-w^2)}\right| \\ \text{II:} \quad & v + \sqrt{m^2u^2-m(v^2-w^2)} - \left|mu-w\right| \\ \text{III:} \quad & mu+w - \left|mu-w\right| \quad . \end{aligned} \tag{A-14}$$

The relative magnitudes of the quantities in A-14 which may be negative are determined below. In subregion I, when it exists, the assumption of the inequality

$$v > \sqrt{m^2u^2-m(v^2-w^2)} \text{ implies that } u^2 < \frac{v^2+m(v^2-w^2)}{m^2} . \tag{A-15}$$

But when subregion I exists, integration on u contributes in the range

$$u < av-cw, \tag{A-16}$$

and if this upper bound of u is less than the value of u of equation A-15 then the assumed inequality of equation A-15 is valid. Now

$$(av-cw)^2 < \frac{v^2+m(v^2-w^2)}{m^2} \tag{A-17}$$

is

$$(cv-aw)^2 < 4v^2. \tag{A-18}$$

When subregion I exists, $cv < aw$, so equation A-18 is

$$aw-cv < 2v,$$

or

$$w < v, \tag{A-19}$$

which is the situation considered. Thus, when subregion I exists,

$$u^2 < (av-cw)^2 < \frac{v^2+m(v^2-w^2)}{m^2} \Rightarrow \sqrt{m^2u^2-m(v^2-w^2)} < v. \qquad (A-20)$$

In order that subregions II and III contribute to the integrations, u must be in the range

$$u > av-cw, \qquad (A-21)$$

and av-cw is greater than w/m when v > w so that

$$u > av-cw > w/m \Rightarrow mu > w. \qquad (A-22)$$

With these considerations the evaluation of the ν integration is complete and by substituting equation A-14 into equation A-12, P(w→v) becomes, letting $(m+1)^2v/(4m^2w) = A$,

$$P = 2A \int_{\sqrt{\frac{v^2-w^2}{m}}}^{av-cw} du \frac{M(u)}{u} \sqrt{m^2u^2-m(v^2-w^2)}$$

$$+ A \int_{av-cw}^{av+cw} du \frac{M(u)}{u} \left[v+w+ \sqrt{m^2u^2-m(v^2-w^2)} -mu \right] \qquad (A-23)$$

$$+ 2Aw \int_{av+cw}^{\infty} du \frac{M(u)}{u} \qquad \text{if } v > w .$$

When cv > aw, subregion I does not exist and the first integral of A-23 must be omitted.

Neutron Speed Loss v ≤ w

When v ≤ w the positive sections of the hyperbola of equation A-3 are shown in figure 2. The lines (A-2) intersect the ν axis at $\nu \leq 0$ (point (f)). The lines (A-2) intersect the hyperbola (A-3) at the positive values of u,

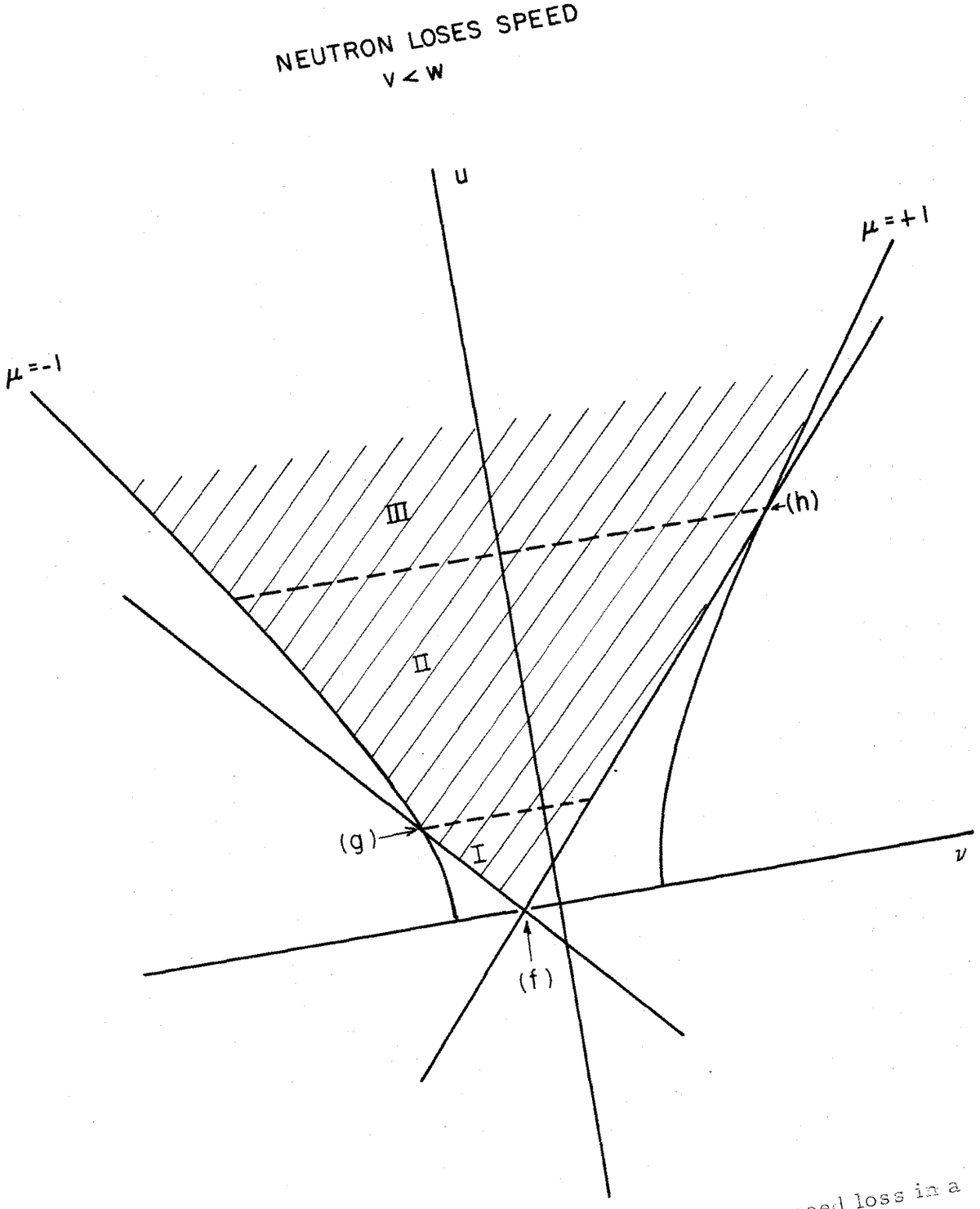

Figure 2. Domain of integration for neutron speed loss in a collision

$$\begin{array}{lllll} \text{point (g)} & \mu = -1 & u = av-cw & \text{if } av > cw, & \\ & \mu = +1 & u = cw-av & \text{if } av < cw, & \text{(A-24)} \\ \text{point (h)} & \mu = +1 & u = av+cw\ . & & \end{array}$$

If $av < cw$ the line $\mu = -1$ does not intersect the hyperbola at positive u and the subregion I does not exist. The u boundaries of the subregions are:

$$\begin{array}{ll} \text{I:} & 0 \le u \le av-cw \\ \text{II:} & |av-cw| \le u \le av+cw \\ \text{III:} & av+cw \le u \le \infty\ . \end{array} \qquad \text{(A-25)}$$

The boundaries of ν are the lines (A-4) in subregion I, the hyperbola and the line $\mu = +1$ in subregion II, and the branches of the hyperbola in subregion III. These values of ν are

$$\begin{array}{ll} \text{I:} & -2m[uw-c(v^2-w^2)] \le \nu \le 2m[uw+c(v^2-w^2)] \\ \text{II:} & -2v\sqrt{m^2u^2-m(v^2-w^2)} \le \nu \le 2m[uw+c(v^2-w^2)] \\ \text{III:} & -2v\sqrt{m^2u^2-m(v^2-w^2)} \le \nu \le 2v\sqrt{m^2u^2-m(v^2-w^2)}\ . \end{array} \qquad \text{(A-26)}$$

The results of the ν integration are very similar to equation A-14 except that the regions are labeled differently. They are

$$\begin{array}{ll} \text{I:} & w + mu - |w-mu| \\ \text{II:} & w + mu - \left|\sqrt{m^2u^2-m(v^2-w^2)} - v\right| \\ \text{III:} & v + \sqrt{m^2u^2-m(v^2-w^2)} - \left|\sqrt{m^2u^2-m(v^2-w^2)} - v\right|\ . \end{array} \qquad \text{(A-27)}$$

Again the relative magnitudes of the quantities which may be negative in A-27 must be determined. In subregion I, when it exists, the integration on u contributes when u is in the range

$$u < av-cw\,, \tag{A-28}$$

and $av-cw < w/m$ when $v < w$ which is the situation here considered. Thus

$$u < av-cw < w/m \Rightarrow mu < w\,. \tag{A-29}$$

In order that subregions II and III contribute to the integrations u must be in the range $u > |av-cw|$. Now $(av-cw)^2$ is greater than $[v^2+m(v^2-w^2)]/m^2$ when

$$(aw-cv)^2 > 4v^2, \tag{A-30}$$

and aw is always greater than cv when $w > v$ so that A-30 becomes $aw-cv > 2v$, or $w > v$. Thus the inequality

$$\frac{v^2+m(v^2-w^2)}{m^2} < (av-cw)^2 < u^2, \tag{A-31}$$

determines that

$$v < \sqrt{m^2u^2-m(v^2-w^2)}\,. \tag{A-32}$$

Therefore the ordering of the magnitudes of the expressions in equation A-27 is as written and the substitution of the evaluated v integration into equation A-12 gives

$$P = 2mA\int_0^{av-cw} du M(u) + A\int_{|av-cw|}^{av+cw} \frac{du M(u)}{u}\left[v+w+mu-\sqrt{m^2u^2-m(v^2-w^2)}\right] \tag{A-33}$$

$$+ 2vA\int_{av+cw}^{\infty} du\,\frac{M(u)}{u} \qquad \text{if } v < w\,,$$

where the first integral is omitted if $av < cw$.

It is apparent that a symmetry exists between the relations for

$v \leq w$ and $v \geq w$. A possibility that is not apparent is that the vanishing of the subregions I may not affect the non-zero values of $P(w \to v)$. However, the vanishing of the subregions does determine the point at which P becomes zero. These observations are made more specific in the following sections.

II-A. $P(w \to v)$ FOR A MONATOMIC GAS ATOM SPEED DISTRIBUTION

The normalized distribution of atom speeds for a monatomic gas is a Maxwellian:

$$M_o(u) = \frac{4m^{3/2}}{\sqrt{\pi}} b^3 u^2 e^{-mu^2 b^2} \qquad b^2 = \frac{1}{2kT} \qquad (A\text{-}34)$$

$$0 \leq u \leq \infty .$$

With this speed distribution the first integral of equation A-23 is, writing $B = 2/(\sqrt{\pi}\, A)$,

$$4m^{3/2} b^3 B \int_{\sqrt{\frac{v^2-w^2}{m}}}^{av-cw} du\, u e^{-mu^2 b^2} \sqrt{m^2 u^2 - m(v^2-w^2)}\,, \qquad (A\text{-}35)$$

which with the change of variable,

$$mu^2 - (v^2 - w^2) = t^2/b^2 ,$$

becomes

$$4mB\, e^{-b^2(v^2-w^2)} \int_0^{\sqrt{m}\, b(aw-cv)} dt\, t^2 e^{-t^2} , \qquad (A\text{-}36)$$

and the integral contributes only when $aw > cv$ when subregion I exists. The remaining integrals of equation A-23 are, after the same or simpler changes of variable,

$$2mBe^{-b^2(v^2-w^2)}\int_{\sqrt{mb}|aw-cv|}^{\sqrt{mb}(aw+cv)} dt\, t^2 e^{-t^2} + 2B(v+w)\sqrt{mb}\int_{\sqrt{mb}(av-cw)}^{\sqrt{mb}(av+cw)} dt\, te^{-t^2}$$

$$+ 4Bw\sqrt{mb}\int_{\sqrt{mb}(av+cw)}^{\infty} dt\, te^{-t^2} - 2Bm\int_{\sqrt{mb}(av-cv)}^{\sqrt{mb}(av+cv)} dt\, t^2 e^{-t^2} . \qquad \text{(A-37)}$$

The limits of integration are similar to expressions defined in the text of the thesis:

$$\begin{aligned} \alpha(v, w) &= b\sqrt{m}\,(av + cw) \\ \beta(v, w) &= b\sqrt{m}\,(aw + cv) \\ \varkappa(v, w) &= b\sqrt{m}\,(av - cw) \\ \lambda(v, w) &= b\sqrt{m}\,(aw - cv) . \end{aligned} \qquad \text{(A-38)}$$

The integral of equation A-36 is

$$2mBe^{-b^2(v^2-w^2)}\left[\int dte^{-t^2} - te^{-t^2}\right]_0^{\lambda} = 2mBe^{-b^2(v^2-w^2)}\left[I(\lambda) - \lambda e^{-\lambda^2}\right], \qquad \text{(A-39)}$$

where $I(\lambda)$ is an unnormalized error function. The integrations of equation A-37 give, in a similar fashion,

$$\begin{aligned} &mBe^{-b^2(v^2-w^2)}\left[I(\beta) - \beta e^{-\beta^2} + |\lambda|\, e^{-\lambda^2} - I(|\lambda|)\right] \\ &+ B(v+w)\sqrt{mb}\left[e^{-\varkappa^2} - e^{-\alpha^2}\right] + 2Bw\sqrt{mb}\, e^{-\alpha^2} \\ &- mB\left[I(\alpha) - I(\varkappa) - \alpha e^{-\alpha^2} + \varkappa e^{-\varkappa^2}\right] . \end{aligned} \qquad \text{(A-40)}$$

The expressions of A-39 and A-40 are to be combined when $\lambda > 0$, i.e., when $aw > cv$. Using the identities

$$\lambda^2 + b^2(v^2-w^2) = \varkappa^2$$
$$\beta^2 + b^2(v^2-w^2) = a^2 , \qquad \text{(A-41)}$$

the total is

$$P = mB\left\{e^{-b^2(v^2-w^2)}\left[I(\beta) + I(\lambda)\right] + I(\varkappa) - I(a)\right\}$$
$$+ Be^{-\varkappa^2}\left[\sqrt{m}b(v+w) - m(\lambda+\varkappa)\right] \qquad \text{(A-42)}$$
$$+ Be^{-a^2}\left[m(a-\beta) + \sqrt{m}b(w-v)\right] .$$

Since

$$m(\lambda+\varkappa) = \sqrt{m}\,b(v+w)$$
$$m(a-\beta) = \sqrt{m}\,b(v-w), \qquad \text{(A-43)}$$

equation A-42 is

$$P = mB\left\{e^{-b^2(v^2-w^2)}\left[I(\beta) + I(\lambda)\right] + I(\varkappa) - I(a)\right\} \qquad \text{(A-44)}$$

when $v > w$

and $cv < aw$.

Now if $cv > aw$ and $\lambda < 0$, only the expressions of equation A-40 need to be considered. These are

$$P = mB\left\{e^{-b^2(v^2-w^2)}\left[I(\beta) - I(-\lambda)\right] + I(\varkappa) - I(a)\right\}$$
$$+ Be^{-\varkappa^2}\left[\sqrt{m}\,b(v+w) - m(\lambda+\varkappa)\right] \qquad \text{(A-45)}$$
$$+ Be^{-a^2}\left[m(a-\beta) + \sqrt{m}\,b\,(w-v)\right]$$

or

$$P = mB\left\{e^{-b^2(v^2-w^2)}\left[I(\beta) - I(-\lambda)\right] + I(\varkappa) - I(a)\right\}, \qquad \text{(A-46)}$$

which is the same result as equation A-44 but only because the error function is an odd function. Thus the vanishing of subregion I does not affect the final result for P when the atom speed distribution $M_o(u)$ is used when $v > w$.

When $v < w$, the integrations of equation A-33 are very similar to those just performed. Again the first integral should be considered separately. It is

$$2mA \int_0^{av-cw} du\, M_o(u) \qquad \text{when } av > cw \quad (\varkappa > 0), \tag{A-47}$$

and when integrated is

$$2mB\left[I(\varkappa) - \varkappa e^{-\varkappa^2} \right]. \tag{A-48}$$

The remaining terms of equation A-33 are, when evaluated,

$$\begin{aligned} &-mBe^{-b^2(v^2-w^2)}\left[I(\beta) - \beta e^{-\beta^2} - I(\lambda) + \lambda e^{-\lambda^2} \right] \\ &+ B(v+w)\sqrt{m}b\left(e^{-\varkappa^2} - e^{-a^2} \right) + 2vB\sqrt{m}be^{-a^2} \\ &+ mB\left[I(a) - I(|\varkappa|) - ae^{-a^2} + |\varkappa|\, e^{-\varkappa^2} \right]. \end{aligned} \tag{A-49}$$

When $av > cw$ $(\varkappa > 0)$ combining A-48 and A-49 gives

$$\begin{aligned} &mB\left\{ I(\varkappa) + I(a) + e^{-b^2(v^2-w^2)}\left[I(\lambda) - I(\beta) \right] \right\} \\ &+ Be^{-\varkappa^2}\left[\sqrt{m}\, b(v+w) - m(\lambda+\varkappa) \right] \\ &+ Be^{-a^2}\left[m(\beta-a) + \sqrt{m}b(v-w) \right], \end{aligned} \tag{A-50}$$

or, with the terms multiplying exponentials vanishing,

$$P = mB\left\{ I(\varkappa) + I(\alpha) + e^{-b^2(v^2-w^2)}\left[I(\lambda) - I(\beta) \right] \right\}. \qquad \text{(A-51)}$$

When $\varkappa < 0$ equation A-49 alone is

$$P = mB\left\{ I(\alpha) - I(-\varkappa) + e^{-b^2(v^2-w^2)}\left[I(\lambda) - I(\beta) \right] \right\} \qquad \text{(A-52)}$$

which is the same value as equation A-51 because $-I(-\varkappa) = I(\varkappa)$, and the vanishing of subregion I does not change the result.

The total result for $P(w \to v)$ for the Maxwellian distribution of atom speeds is thus

$$P(w \to v) = \frac{2}{\sqrt{\pi}} ma^2 \frac{v}{w}\left\{ e^{-b^2(v^2-w^2)}\left[I(\beta)+I(\lambda) \right] + I(\varkappa) - I(\alpha) \right\} \quad \text{if } w \le v$$

$$= \frac{2}{\sqrt{\pi}} ma^2 \frac{v}{w}\left\{ I(\varkappa)+I(\alpha) + e^{-b^2(v^2-w^2)}\left[I(\lambda) - I(\beta) \right] \right\} \quad \text{if } w \ge v . \qquad \text{(A-53)}$$

The form of P is very much simpler when m=1. When m=1, a=1, c=0, $\alpha=\varkappa=bv$, and $\beta=\lambda=bw$. Equation A-53 above reduces to

$$P(w \to v) = \frac{4}{\sqrt{\pi}} \frac{v}{w} e^{-b^2(v^2-w^2)} I(bw) \qquad w \le v$$

$$P(w \to v) = \frac{4}{\sqrt{\pi}} \frac{v}{w} I(bv) \qquad w \ge v . \qquad \text{(A-54)}$$

Equations A-53 and A-54 agree with results given by Wigner and Wilkins (1).

III-A. $P(w \to v)$ FOR THE SINGLE ENERGY OSCILLATOR MODEL

The atom speed distribution for the single energy oscillator model is

$$M(u) = \frac{2}{\pi\sqrt{U^2-u^2}} \qquad \text{if } 0 \le u \le U$$
$$= 0 \qquad \text{if } U < u \,. \tag{A-55}$$

The finite upper bound U of the oscillator speed distribution restricts the integrations of equations A-23 and A-33. P(w→v) thus has different forms depending upon the magnitude of U relative to the u values which characterize the various subregions of integration. In addition, restrictions are placed on the w integration of the integral equation. For example, if $w < cv/a$, subregion I does not exist and P(w→v) = 0 if $U < av-cw$. That is, the lower limit of integration on w is $(av-U)/c$. The latter quantity is positive only as long as $av > U$ or $v > U/a$ so that the integral equation itself has different forms depending upon the magnitude of v relative to U and the atom mass. The detailed consideration of this fractionation is deferred until specific values of P(w→v) are obtained.

Three different integrations occur in equation A-23 and A-33. With the speed distribution A-55 these are

$$I_1 = \frac{2}{\pi}\int \frac{du}{\sqrt{U^2-u^2}} = \frac{2}{\pi}\sin^{-1}\frac{u}{U} \,, \tag{A-56}$$

$$I_2 = \frac{2}{\pi}\int \frac{du}{u\sqrt{U^2-u^2}} = -\frac{2}{\pi U}\operatorname{sech}^{-1}\frac{u}{U} \,, \tag{A-57}$$

and

$$I_3 = \frac{2}{\pi}\int \frac{du\sqrt{m^2u^2-m(v^2-w^2)}}{u\sqrt{U^2-u^2}} \,. \tag{A-58}$$

With the substitution

$$t = \sqrt{\frac{m^2u^2 - m(v^2-w^2)}{U^2-u^2}}, \qquad \text{(A-59)}$$

or

$$u^2 = \frac{t^2U^2 - m(v^2-w^2)}{t^2+m^2} .$$

I_3 becomes

$$I_3 = \frac{2}{\pi}\int dt\left[\frac{m^2}{t^2+m^2} - \frac{m(v^2-w^2)}{t^2U^2+m(v^2-w^2)}\right]$$

$$= \frac{2}{\pi}\left[m\,tg^{-1}\frac{t}{m} - \frac{\sqrt{m(v^2-w^2)}}{U}\,tg^{-1}\frac{tU}{\sqrt{m(v^2-w^2)}}\right]. \qquad \text{(A-60)}$$

The various forms of P are denoted by the following shorthand notation:

$\underline{w \le v}$

$P_{og}(\equiv 0)$: when $U \le av-cw$ if $w \le cv/a$

when $U \le \sqrt{\frac{v^2-w^2}{m}}$ if $w \ge cv/a$

P_{1g}: $\sqrt{\frac{v^2-w^2}{m}} \le U \le av-cw$ (A-61)

P_{2g}: $av-cw \le U \le av+cw$

P_{3g}: $av+cw \le U$

$\underline{w \ge v}$

$P_{o\ell}(\equiv 0)$: $U \le cw-av$ when $w \ge av/c$

$P_{1\ell}$: $0 \le U \le av-cw$ when $w \le av/c$ (A-62)

$P_{2\ell}$: $|av-cw| \le U \le av+cw$

$P_{3\ell}$: $av+cw \le U$.

In A-61 and A-62 the subscripts g and ℓ signify neutron speed gain and loss. Using equations A-23 and A-33 and the indefinite integrals I_1, I_2, and I_3 the terms of equation A-61 become

$$P_{1g} = 2AI_3 \Big|_{t=0}^{\infty} = 2A\left[m - \frac{\sqrt{m(v^2-w^2)}}{U}\right] \qquad \text{(A-63)}$$

$$P_{2g} = 2AI_3 \Big|_{t=0}^{t=\frac{m(aw-cv)}{\sqrt{U^2-(av-cw)^2}}} + AI_3 \Big|_{t=\frac{m|aw-cv|}{\sqrt{U^2-(av-cw)^2}}}^{t=\infty} \qquad \text{(A-64)}$$

$$+ A(v+w)I_2 \Big|_{u=av-cw}^{u=U} - mAI_1 \Big|_{u=av-cw}^{U} .$$

At this point the vanishing of subregion I for neutron speed gain must be considered. If the subregion does not contribute ($aw-cv < 0$) the term $2AI_3$ in A-64 should not appear. However, since I_3 contains only odd functions the remaining term in I_3 is, in effect,

$$AI_3 \Big|^{t=\frac{m(aw-cv)}{\sqrt{U^2-(av-cw)^2}}} + AI_3 \Big|^{t=\infty} . \qquad \text{(A-65)}$$

But this is just the contribution of both terms in I_3 when $aw-cv > 0$. Thus the vanishing of the subregion is accounted for by the change in sign in aw-cv. The same observations apply to P_{3g} below. When evaluated P_{2g} is

$$\frac{2A}{\pi}\left\{ m\,tg^{-1}\frac{aw-cv}{\sqrt{U^2-(av-cw)^2}} + m\,\sin^{-1}\frac{av-cw}{U}\right.$$

$$-\frac{\sqrt{m(v^2-w^2)}}{U}\left[tg^{-1}\frac{U\sqrt{m}\,(aw-cv)}{\sqrt{v^2-w^2}\,\sqrt{U^2-(av-cw)^2}}+\frac{\pi}{2}\right] \qquad \text{(A-66)}$$

$$\left.+\frac{v+w}{U}\,\mathrm{sech}^{-1}\frac{av-cw}{U}\right\}.$$

P_{3g} is, symbolically,

$$P_{3g}=2AI_3\Bigg|_{t=0}^{t=\frac{m(aw-cv)}{\sqrt{U^2-(av-cw)^2}}}+AI_3\Bigg|_{t=\frac{m|aw-cv|}{\sqrt{U^2-(av-cw)^2}}}^{t=\frac{m(aw+cv)}{\sqrt{U^2-(av+cw)^2}}} \qquad \text{(A-67)}$$

$$+A(v+w)I_2\Bigg|_{u=av-cw}^{u=av+cw}-mAI_1\Bigg|_{u=av-cw}^{u=av+cw}+2AI_2\Bigg|_{u=av+cw}^{u=U},$$

and when evaluated is

$$P_{3g}=\frac{2A}{\pi}\left\{ m\,tg^{-1}\frac{aw-cv}{\sqrt{U^2-(av-cw)^2}}+m\,\sin^{-1}\frac{av-cw}{U}+m\,tg^{-1}\frac{aw+cv}{\sqrt{U^2-(av+cw)^2}}\right.$$

$$-m\,\sin^{-1}\frac{av+cw}{U}-\frac{\sqrt{m(v^2-w^2)}}{U}\left[tg^{-1}\frac{U\sqrt{m}\,(aw-cv)}{\sqrt{v^2-w^2}\,\sqrt{U^2-(av-cw)^2}}\right.$$

$$\left.\left.+tg^{-1}\frac{U\sqrt{m}\,(av+cw)}{\sqrt{v^2-w^2}\,\sqrt{U^2-(av+cw)^2}}\right]+\frac{v+w}{U}\,\mathrm{sech}^{-1}\frac{av-cw}{U}+\frac{w-v}{U}\,\mathrm{sech}^{-1}\frac{av+cw}{U}\right\}. \qquad \text{(A-68)}$$

The expressions of equation A-62 are evaluated in a similar manner. Because w is now greater than v the indefinite integral I_3 should be

modified slightly.

$$I_3 = \frac{2}{\pi}\int dt\left[\frac{m^2}{t^2+m^2} - \frac{m(w^2-v^2)}{m(w^2-v^2)-t^2U^2}\right]$$

$$= \frac{2}{\pi}\left[m\,tg^{-1}\frac{t}{m} - \frac{\sqrt{m(w^2-v^2)}}{2U}\,\ell n\left|\frac{\sqrt{m(w^2-v^2)}+Ut}{\sqrt{m(w^2-v^2)}-Ut}\right|\right]. \qquad (A\text{-}60)$$

$P_{1\ell}$ is, using equation A-33,

$$P_{1\ell} = 2mAI_1\Big|_{u=0}^{u=U} = 2mA, \qquad (A\text{-}69)$$

and $P_{2\ell}$ is

$$P_{2\ell} = 2mAI_1\Big|_{u=0}^{u=(av-cw)} + mAI_1\Big|_{u=|av-cw|}^{u=U} + A(v+w)I_2\Big|_{u=|av-cw|}^{u=U} - AI_3\Big|_{t=\frac{m(aw-cv)}{\sqrt{U^2-(av-cw)^2}}}^{t=\infty}. \qquad (A\text{-}70)$$

Again, the vanishing of the subregion I does not affect the above expression when av-cw is allowed to change sign in the integral I_1. However, the modulus of av-cw must be used in the integral I_2 to keep the inverse hyperbolic secant defined. This is consistent since the integration for I_2 only occurs when $u \geq 0$. The same results hold for $P_{3\ell}$ below. Evaluating equation A-70 gives

$$P_{2\ell} = \frac{2A}{\pi}\left\{m\sin^{-1}\frac{av-cw}{U} + m\,tg^{-1}\frac{aw-cv}{\sqrt{U^2-(av-cw)^2}}\right. \qquad (A\text{-}71)$$

$$\left. + \frac{v+w}{U}\,\mathrm{sech}^{-1}\frac{|av-cw|}{U} - \frac{\sqrt{m(w^2-v^2)}}{2U}\,\ell n\left|\frac{\sqrt{m(w^2-v^2)}+\frac{Um(aw-cv)}{\sqrt{U^2-(av-cw)^2}}}{\sqrt{m(w^2-v^2)}-\frac{Um(aw-cv)}{\sqrt{U^2-(av-cw)^2}}}\right|\right\}.$$

The last term in equation A-71 can be arranged to compare more closely with P_{2g}. The inequality,

$$\sqrt{m(w^2-v^2)} < \frac{Um(aw-cv)}{\sqrt{U^2-(av-cw)^2}}, \tag{A-72}$$

holds because

$$m(w^2-v^2) < \frac{U^2m^2(aw-cv)^2}{U^2-(av-cw)^2} \tag{A-73}$$

is

$$-(av-cw)^2\, m(w^2-v^2) < U^2m^2(aw-cv)^2 - U^2m(w^2-v^2) = U^2m^2(av-cw)^2,$$

or

$$-(w^2-v^2) < U^2m. \tag{A-74}$$

Therefore the last term of equation A-71 may be written as

$$+i\,\frac{\sqrt{m(v^2-w^2)}}{U}\coth^{-1}\frac{-iUm(aw-cv)}{\sqrt{m(v^2-w^2)}\,\sqrt{U^2-(av-cw)^2}}, \tag{A-75}$$

and

$$i\coth^{-1}-it = \frac{i}{2}\ln\frac{it-1}{it+1} = \frac{i}{2}\ln\frac{1-it}{1+it} + \frac{i}{2}\ln(-1) = \tan^{-1}t - \frac{\pi}{2}. \tag{A-76}$$

Thus $P_{2\ell}$ may be written

$$P_{2\ell} = \frac{2A}{\pi}\left\{ m\sin^{-1}\frac{av-cw}{U} + m\,tg^{-1}\frac{aw-cv}{\sqrt{U^2-(av-cw)^2}} \right. \tag{A-77}$$

$$\left. + \frac{v+w}{U}\,\mathrm{sech}^{-1}\frac{|av-cw|}{U} - \frac{\sqrt{m(v^2-w^2)}}{U}\left[tg^{-1}\frac{U\sqrt{m}(aw-cv)}{\sqrt{(v^2-w^2)}\,\sqrt{U^2-(av-cw)^2}} - \frac{\pi}{2}\right]\right\}.$$

The last term is the same as if I_3 had been integrated without modification and is real.

$P_{3\ell}$ is symbolically

$$2mAI_1\Big|_{u=0}^{u=(av-cw)} + mAI_1\Big|_{u=|av-cw|}^{u=av+cw} + A(v+w)I_2\Big|_{u=|av-cw|}^{u=av+cw} \tag{A-78}$$

$$-AI_3\Big|_{t=\frac{m(aw-cv)}{\sqrt{U^2-(av-cw)^2}}}^{t=\frac{m(aw+cv)}{\sqrt{U^2-(av+cw)^2}}} + 2vAI_2\Big|_{u=av+cw}^{U},$$

and, when modifications are made as for $P_{2\ell}$, is

$$P_{3\ell} = \frac{2A}{\pi}\left\{ m\sin^{-1}\frac{(av-cw)}{U} + m\sin^{-1}\frac{av+cw}{U} + m\,tg^{-1}\frac{aw-cv}{\sqrt{U^2-(av-cw)^2}}\right.$$

$$-m\,tg^{-1}\frac{(aw+cv)}{\sqrt{U^2-(av+cw)^2}} + \frac{v+w}{U}\,\mathrm{sech}^{-1}\frac{|av-cw|}{U} + \frac{v-w}{U}\,\mathrm{sech}^{-1}\frac{av+cw}{U} \tag{A-79}$$

$$\left. -\frac{\sqrt{m(v^2-w^2)}}{U}\left[tg^{-1}\frac{U\sqrt{m}\,(aw-cv)}{\sqrt{v^2-w^2}\sqrt{U^2-(av-cw)^2}} - tg^{-1}\frac{U\sqrt{m}(aw+cv)}{\sqrt{v^2-w^2}\sqrt{U^2-(av+cw)^2}}\right]\right\}.$$

The P expressions above are all continuous at their various boundary points.

To determine where the P expressions are applicable in the integral equation a trial and error process is necessary. The process is systematized below, but much of the initial confusion in such a process is not indicated by the analysis. In general there are two ranges of w relative to v in which the forms of P vary. These are

$$0 \le w \le v$$
$$v \le w \le 0 . \qquad \text{(A-80)}$$

In these ranges the relative magnitude of U and the u limits of integration determine ranges of v in which the integral equation is applicable as well as intermediate ranges of integration on w. By trial and error five ranges of v are found that make the inequalities in the subsequent analysis determinate. These ranges are:

$$\begin{aligned} &\text{(a)}\ 0 \le v \le U, \\ &\text{(b)}\ U \le v \le U/a, \\ &\text{(c)}\ U/a \le v \le amU, \\ &\text{(d)}\ amU \le v \le mU, \\ &\text{(e)}\ mU \le v \le \infty . \end{aligned} \qquad \text{(A-81)}$$

The analysis is begun for $w < v$ and completed for the five ranges of v before the analysis for $w > v$ is executed.

(1) $\underline{0 \le w \le v}$

(a) $\underline{0 \le v \le U}$

If U is greater than av + cw the applicable expression of P is P_{3g}.

$$U \ge av+cw \Longrightarrow \quad w \le \frac{U-av}{c}, \qquad \text{(A-82)}$$

but $w \le v$, and

$$v \le \frac{U-av}{c} \Longrightarrow \quad v \le U . \qquad \text{(A-83)}$$

Further $U \ge av$ when $v \le U/a$, but $U/a \ge U$ so that this inequality is satisfied. Summarizing,

$$w \le v \le \frac{U-av}{c} \quad \text{when } v \le U, \qquad \text{(A-84)}$$

so that $U \geq av+cw$ and P_{3g} is the correct expression for $0 \leq w \leq v$. Symbolically this is

$$\int_0^v dw\, n(w) P_{3g} \,. \tag{A-85}$$

(b) $\underline{U \leq v \leq U/a}$

In this region, again,

$$U \geq av+cw \Longrightarrow \quad w \leq \frac{U-av}{c} \,, \tag{A-86}$$

but

$$\frac{U-av}{c} \leq v \qquad \text{when } U \leq v, \tag{A-87}$$

so that now P_{3g} is restricted to $0 \leq w \leq (U-av)/c$. Now when $w \geq (U-av)/c$, $U \leq av+cw$ so that P_{2g} is applicable if $U \geq av-cw$. The last relation implies $w \geq (av-U)/c$ which is valid $v < U/a$. Thus the contribution to the integral equation in the range of v and w is

$$\int_0^{\frac{U-av}{c}} dw\, n(w) P_{3g} + \int_{\frac{U-av}{c}}^{v} dw\, n(w) P_{2g} \,. \tag{A-88}$$

(c) $\underline{U/a \leq v \leq amU}$

In this range of v,

$$U \geq av+cw \Longrightarrow \quad w \leq \frac{U-av}{c} \leq 0, \tag{A-89}$$

so there is no contribution from P_{3g}.

$$U \geq av-cw \Longrightarrow \quad w \geq \frac{av-U}{c} \geq 0, \tag{A-90}$$

and

$$\frac{av-U}{c} \leq v \Longrightarrow \qquad v \leq mU. \tag{A-91}$$

But

$$v \leq amU \leq mU. \tag{A-92}$$

Finally,

$$U \leq av-cw \Longrightarrow \quad w \leq \frac{av-U}{c} , \tag{A-93}$$

and

$$\frac{av-U}{c} \leq \frac{cv}{a} \Longrightarrow \quad v \leq amU. \tag{A-94}$$

So that in the range of v considered the values of w provided by equation A-93 are $\leq cv/a$ which is the criterion for the vanishing of subregion I so that for $U \leq av-cw$ there is no contribution to the integral equation from P_{1g}. In this range of v and w the total contribution is

$$\int_{\frac{av-U}{c}}^{v} dw\, n(w) P_{2g} . \tag{A-95}$$

(d) $\underline{amU \leq v \leq mU}$

In this range subregion I is present which contributes (P_{1g}) when

$$\sqrt{\frac{v^2-w^2}{m}} \leq U \leq av-cw . \tag{A-96}$$

Equation A-96 determines a range of w,

$$\sqrt{v^2-mU^2} \leq w \leq \frac{av-U}{c} , \tag{A-97}$$

and $v^2 > mU^2$ when $v^2 \geq (amU)^2 \geq mU^2$ where amU is the lower limit of the range of v considered. Now if

$$U \geq av-cw , \tag{A-98}$$

then $w \geq \frac{av-U}{c}$ and $\frac{av-U}{c} \leq v$ when $v \leq mU$ so that P_{2g} contributes to the integral equation. U cannot be greater than av+cw for

$$U \geq av+cw \Rightarrow \quad w \leq \frac{U-av}{c} \leq 0 . \tag{A-99}$$

The total of the neutron gain terms of the integral equation in this range of v is then

$$\int_{\sqrt{v^2-mU^2}}^{\frac{av-U}{c}} dw\, n(w) P_{1g} + \int_{\frac{av-U}{c}}^{v} dw\, n(w) P_{2g} . \tag{A-100}$$

(e) $\underline{mU \leq v \leq \infty}$

In this range $\frac{av-U}{c} \geq v \geq w$ and thus $U \leq av-cw$ and the only contribution is from P_{1g} in the limits of equation A-97. This is

$$\int_{\sqrt{v^2-mU^2}}^{v} dw\, n(w) P_{1g} . \tag{A-101}$$

(2) $\underline{v \leq w \leq \infty}$

The fractionation for this range of w is somewhat simpler and a general discussion permits quick formulation of the integral equation.

$P_{3\ell}$ contributes only when $0 \leq v \leq U$. That is

$$U \geq av+cw \Rightarrow \quad w \leq \frac{U-av}{c} , \tag{A-102}$$

and

$$\frac{U-av}{c} \geq v \quad \text{only when } v \leq U . \tag{A-103}$$

$P_{2\ell}$ contributes to all ranges of v. An upper bound for the w integration of $P_{2\ell}$ is determined when av < cw since

$$U \geq |av-cw| \rightarrow U \geq cw-av \Rightarrow \quad w < \frac{U-av}{c} . \tag{A-104}$$

The lower bound of the w integration is determined by

$$U \leq av+cw \Rightarrow \quad w \geq \frac{U-av}{c} \tag{A-105}$$

when $v \leq U$ only, and by

$$U \geq av-cw \Rightarrow \quad w \geq \frac{av-U}{c} \tag{A-106}$$

when $v \geq U$. But

$$\frac{av-U}{c} \geq v \text{ only if } v \geq mU . \tag{A-107}$$

Thus for $U \leq v \leq mU$ the lower limit of the $P_{2\ell}$ integration on w is v.

$P_{1\ell}$ contributes only when $w < av/c$ and the condition

$$U \leq av-cw \Rightarrow \quad w \leq \frac{av-U}{c} \tag{A-108}$$

determines that $P_{1\ell}$ occurs only when $(av-U)/c \geq v$ which is only when $v \geq mU$.

The portion of the integral equation for $w > v$ is represented symbolically below.

(a) $\underline{0 \leq v \leq U}$

$$\int_{v}^{\frac{U-av}{c}} dw\, n(w) P_{3\ell} + \int_{\frac{U-av}{c}}^{\frac{U+av}{c}} dw\, n(w) P_{2\ell} \tag{A-109}$$

(b)(c)(d) $\underline{U \le v \le mU}$

$$\int_{v}^{\frac{U+av}{c}} dw\, n(w) P_{2\ell} \tag{A-110}$$

(e) $\underline{mU < v < \infty}$

$$\int_{v}^{\frac{av-U}{c}} dw\, n(w) P_{1\ell} + \int_{\frac{av-U}{c}}^{\frac{U+av}{c}} dw\, n(w) P_{2\ell} \; . \tag{A-111}$$

The entire integral equation is summarized in Table I in the text of the thesis.

IV-A. V(v) AND P(w→v) FOR THE AVERAGED ENERGY OSCILLATOR MODEL

As is pointed out in the text of the thesis, V(v) and P(w→v) for the averaged energy model may be calculated by integrating the corresponding expressions for the single energy oscillator model over the normalized distribution of atom energies

$$P(E_o)dE_o = \frac{2}{\sqrt{\pi}} \frac{\sqrt{E_o}}{(kT)^{3/2}} e^{-E_o/kT} dE_o. \tag{A-112}$$

The process is cumbersome but relatively straightforward provided due caution is exercised in choosing the limits of integration. When P(w→v) is calculated, a decided simplification occurs if a certain integration by parts is performed. The simplification is outlined below.

V(v) is calculated first. The integration to be executed is

$$V(v) = \frac{2}{\sqrt{\pi}} \frac{1}{(k/T)^{3/2}} \int_0^\infty dE_o V(v, E_o) \sqrt{E_o}\, e^{-E_o/kT} . \qquad \text{(A-113)}$$

It is most convenient to introduce the quantity

$$\epsilon = E_o/kTm , \qquad \text{(A-114)}$$

and the dimensionless speed

$$x = v/\sqrt{2kT} . \qquad \text{(A-115)}$$

In terms of these variables V of the single energy oscillator model given in Section II of the thesis is

$$U = \sqrt{2kT}\sqrt{\epsilon}$$

$$\sqrt{2kT}\, V(x) = \frac{\sqrt{2kT}}{3\pi}\left[5\sqrt{\epsilon - x^2} + \left(6x + \frac{\epsilon}{x}\right)\sin^{-1}\frac{x}{\sqrt{\epsilon}} + \frac{2x^2}{\sqrt{\epsilon}}\,\mathrm{sech}^{-1}\frac{x}{\sqrt{\epsilon}}\right] \qquad \text{(A-116)}$$

$$0 \le x \le \sqrt{\epsilon}$$

$$= \sqrt{2kT}\left(x + \frac{\epsilon}{6x}\right) \qquad \sqrt{\epsilon} \le x \le \infty .$$

Equation A-113 is then,

$$V(x) = \frac{2m^{3/2}}{\sqrt{\pi}}\left\{\int_0^{x^2} d\epsilon \sqrt{\epsilon}\, e^{-m\epsilon}\left(x + \frac{\epsilon}{6x}\right) + \frac{1}{3\pi}\int_{x^2}^\infty d\epsilon \sqrt{\epsilon}\, e^{-m\epsilon}\left[5\sqrt{\epsilon - x^2} + \left(6x + \frac{\epsilon}{x}\right)\right.\right.$$

$$\left.\left. \times \sin^{-1}\frac{x}{\sqrt{\epsilon}} + \frac{2x^2}{\sqrt{\epsilon}}\,\mathrm{sech}^{-1}\frac{1}{\sqrt{\epsilon}}\right]\right\}, \qquad \text{(A-117)}$$

or with the change of variable $\epsilon = t^2$

$$V(x) = \frac{2m^{3/2}}{\sqrt{\pi}} \left\{ 2 \int_0^x dt\, t^2 e^{-mt^2} \left(x + \frac{t^2}{6x} \right) \right. \tag{A-118}$$

$$\left. + \frac{2}{3\pi} \int_x^\infty dt\, t^2 e^{-mt^2} \left[5\sqrt{t^2 - x^2} + \left(6x + \frac{t^2}{x} \right) \sin^{-1} \frac{x}{t} + \frac{2x^2}{t} \operatorname{sech}^{-1} \frac{x}{t} \right] \right\}.$$

Both integrals are integrated by parts, integrating te^{-mt^2} and differentiating the remaining terms. Since the integrals are continuous at $t = x$, and since the integrated terms vanish at $x = 0$ and ∞, only integrals remain.

$$V(x) = \frac{2m^{1/2}}{\sqrt{\pi}} \left\{ \int_0^x dt\, e^{-mt^2} \left(x + \frac{t^2}{2x} \right) + \frac{1}{\pi} \int_x^\infty dt\, e^{-mt^2} \left[3\sqrt{t^2 - x^2} + 2\left(x + \frac{t^2}{2x} \right) \sin^{-1} \frac{x}{t} \right] \right\} \tag{A-119}$$

If the first integral is extended to ∞ and the contribution from x to ∞ subtracted from the second integral the expression becomes

$$V(x) = \frac{2}{\sqrt{\pi}} \left\{ \frac{\sqrt{\pi}}{2} \left(x + \frac{1}{4mx} \right) + \frac{\sqrt{m}}{\pi} \int_x^\infty dt\, e^{-mt^2} \left[3\sqrt{t^2 - x^2} - 2\left(x + \frac{t^2}{2x} \right) \cos^{-1} \frac{x}{t} \right] \right\}, \tag{A-120}$$

which is, within a constant, the expression given in the text of the thesis. The expression of the thesis is consistent with the constants appearing in $P(y-x)$ there given.

To calculate $P(w-v)$, the expressions derived in Section III of this appendix are to be averaged over the energy distribution of equation A-112. The process can be accomplished by starting with Table I of the thesis and determining the limits of integration E_o from the boundaries of v and w, that is, by inverting the determination of the limits of the

single energy oscillator model integral equation; or the various expressions for P derived in this appendix can be integrated in their ranges of validity. The latter procedure is outlined below.

Before integrating, it is convenient to change to dimensionless variables. Let

$$t^2 = \epsilon = E_o/kT, \quad x = v/\sqrt{2kT}, \quad y = w/\sqrt{2kT}, \qquad \text{(A-121)}$$

and define

$$\begin{aligned} \alpha(x, y) &= \sqrt{m}\,(ax+cy) \\ \beta(x, y) &= \sqrt{m}\,(ay+cx) \\ \varkappa(x, y) &= \sqrt{m}\,(ax-cy) \\ \lambda(x, y) &= \sqrt{m}\,(ay-cx)\,. \end{aligned} \qquad (54)$$

The various expressions for P for the single energy oscillator model can be written

$$P_{1g} = 2Am\left[1 - \frac{\sqrt{x^2-y^2}}{t}\right] \qquad \text{(A-63)}$$

$$\text{if } \sqrt{x^2-y^2} \le t \le \varkappa \quad \text{and} \quad \frac{cx}{a} \le y \le x$$

$$P_{2g} = \frac{2Am}{\pi}\left[tg^{-1}\frac{\lambda}{\sqrt{t^2-\varkappa^2}} + tg^{-1}\frac{\varkappa}{\sqrt{t^2-\varkappa^2}} + \frac{(x+y)}{t\sqrt{m}}\,\text{sech}^{-1}\frac{\varkappa}{t} - \frac{\sqrt{x^2-y^2}}{t}\left(tg^{-1}\frac{t\lambda}{\sqrt{x^2-y^2}\sqrt{t^2-\varkappa^2}} + \frac{\pi}{2}\right)\right] \qquad \text{(A-66)}$$

$$\text{if } \varkappa \le t \le a$$

$$P_{3g} = \frac{2Am}{\pi}\left[tg^{-1}\frac{\lambda}{\sqrt{t^2-\varkappa^2}} + tg^{-1}\frac{\varkappa}{\sqrt{t^2-\varkappa^2}} + tg^{-1}\frac{\beta}{\sqrt{t^2-a^2}} - tg^{-1}\frac{a}{\sqrt{t^2-a^2}}\right.$$

$$\left. - \frac{\sqrt{x^2-y^2}}{t}\left(tg^{-1}\frac{t\lambda}{\sqrt{x^2-y^2}\sqrt{t^2-\varkappa^2}} + tg^{-1}\frac{t\beta}{\sqrt{x^2-y^2}\sqrt{t^2-a^2}}\right)\right. \qquad \text{(A-68)}$$

$$\left. + \frac{(x+y)}{t\sqrt{m}}\,\text{sech}^{-1}\frac{\varkappa}{t} + \frac{(y-x)}{t\sqrt{m}}\,\text{sech}^{-1}\frac{a}{t}\right] \qquad \text{if } a \le t \le \infty$$

$$P_{1\ell} = 2mA \qquad \text{if } 0 \le t \le \lambda \qquad \text{(A-69)}$$

$$\text{and } x \le y \le ax/c$$

$$P_{2\ell} = \frac{2Am}{\pi}\left[tg^{-1}\frac{\varkappa}{\sqrt{t^2-\varkappa^2}} + tg^{-1}\frac{\lambda}{\sqrt{t^2-\varkappa^2}}\right.$$

$$\left. + \frac{(x+y)}{t\sqrt{m}}\,\text{sech}^{-1}\frac{|\varkappa|}{t} - \frac{\sqrt{x^2-y^2}}{t}\left(tg^{-1}\frac{t\lambda}{\sqrt{x^2-y^2}\sqrt{t^2-\varkappa^2}} - \frac{\pi}{2}\right)\right] \qquad \text{(A-77)}$$

$$\text{if } \varkappa \le t \le a$$

$$P_{3\ell} = \frac{2Am}{\pi}\left[tg^{-1}\frac{\varkappa}{\sqrt{t^2-\varkappa^2}} + tg^{-1}\frac{\lambda}{\sqrt{t^2-\varkappa^2}} + tg^{-1}\frac{a}{\sqrt{t^2-a^2}} - tg^{-1}\frac{\beta}{\sqrt{t^2-a^2}}\right.$$

$$\left. + \frac{(x+y)}{t\sqrt{m}}\,\text{sech}^{-1}\frac{|\varkappa|}{t} + \frac{(x-y)}{t\sqrt{m}}\,\text{sech}^{-1}\frac{a}{t}\right. \qquad \text{(A-79)}$$

$$\left. - \frac{\sqrt{x^2-y^2}}{t}\left(tg^{-1}\frac{t\lambda}{\sqrt{x^2-y^2}\sqrt{t^2-\varkappa^2}} - tg^{-1}\frac{t\beta}{\sqrt{x^2-y^2}\sqrt{t^2-a^2}}\right)\right]$$

$$\text{if } a \le t \le \infty\,.$$

A in the above expressions is a^2x/y and the limits on t were determined from equations A-61 and A-62.

There are four regions of y in which the integration on t (E_o) is to be performed. The integrations and the ranges of y are indicated below, omitting a common factor $2/\sqrt{\pi}$.

$$2\int_{x}^{a} dt\, t^2 e^{-t^2} P_{2g} + 2\int_{a}^{\infty} dt\, t^2 e^{-t^2} P_{3g} \qquad \text{if } 0 \le y \le \frac{cx}{a}, \qquad \text{(A-122)}$$

$$2\int_{\sqrt{x^2-y^2}}^{x} dt\, t^2 e^{-t^2} P_{1g} + 2\int_{x}^{a} dt\, t^2 e^{-t^2} P_{2g} + 2\int_{a}^{\infty} dt\, t^2 e^{-t^2} P_{3g} \qquad \text{(A-123)}$$

$$\text{if } cx/a \le y \le x,$$

$$2\int_{0}^{x} dt\, t^2 e^{-t^2} P_{1\ell} + 2\int_{x}^{\infty} dt\, t^2 e^{-t^2} P_{2\ell} + 2\int_{a}^{\infty} dt\, t^2 e^{-t^2} P_{3\ell} \qquad \text{(A-124)}$$

$$\text{if } x \le y \le ax/c,$$

$$2\int_{|x|}^{\infty} dt\, t^2 e^{-t^2} P_{2\ell} + 2\int_{a}^{\infty} dt\, t^2 e^{-t^2} P_{3\ell} \qquad \text{if } ax/c \le y \le \infty. \qquad \text{(A-125)}$$

Equations A-122 and A-125 are not applicable when m = 1 for then c = 0 and the domains of integration disappear. However, if the integrations are performed and then m is set equal to unity, the equations describing thermalization by hydrogen are recovered. For a check on the accuracy of expressions, the case of m=1 was derived independently and compared with the results of the above integrations for m = 1.

The integrations above are more tedious than difficult. The integrations for $y \le x$ and $y \ge x$ are almost identical except for some

changes of numerical sign. Equation A-123 differs from A-122 only by one term and equation A-124 differs from A-125 by a similar term. Since all the P_{ij} expressions in the integrands are continuous at the limits of t, integrations by parts are indicated. In fact a single integration by parts will suffice to evaluate all the equations, at least in terms of integrals which cannot be further simplified. This will be illustrated in the case of equation A-122 which is typical of the remainder of the equations.

Both integrals in equation A-122 are integrated by parts, integrating te^{-t^2} and differentiating tP_{2g} and tP_{3g}. Now tP_{2g} vanishes at $t = \varkappa$ (remembering that λ is negative for $y < cx/a$); and at $t = \infty$, e^{-t^2} controls the remaining terms. At $t = a$, $P_{2g} = P_{3g}$ and the contributions are of opposite sign. Thus only terms that survive differentiation contribute to the final expression. A surprising cancellation occurs when tP_{2g} and tP_{3g} are differentiated. This is illustrated below for tP_{2g}.

$$tP_{2g} = \frac{2Am}{\pi}\left[t\,tg^{-1}\frac{\lambda}{\sqrt{t^2-\varkappa^2}} + t\,tg^{-1}\frac{\varkappa}{\sqrt{t^2-\varkappa^2}} \right. \qquad \text{(A-126)}$$

$$\left. + \frac{(x+y)}{\sqrt{m}}\,\text{sech}^{-1}\frac{\varkappa}{t} - \sqrt{x^2-y^2}\left(tg^{-1}\frac{t\lambda}{\sqrt{x^2-y^2}\sqrt{t^2-\varkappa^2}} + \frac{\pi}{2} \right) \right]$$

$$\frac{d}{dt}(tP_{2g}) = \frac{2Am}{\pi}\left[tg^{-1}\frac{\lambda}{\sqrt{t^2-\varkappa^2}} + tg^{-1}\frac{\varkappa}{\sqrt{t^2-\varkappa^2}}\right]$$

$$+\frac{2Am}{\pi}\left\{ t\left[\frac{-\varkappa}{t\sqrt{t^2-\varkappa^2}} - \frac{\lambda t}{(t^2-\varkappa^2+\lambda^2)\sqrt{t^2-\varkappa^2}}\right]\right. \tag{A-127}$$

$$\left. +\frac{(x+y)}{\sqrt{m}}\frac{1}{\sqrt{t^2-\varkappa^2}} + \frac{\varkappa^2\lambda(x^2-y^2)}{\left[(x^2-y^2)(t^2-\varkappa^2)+\lambda^2t^2\right]\sqrt{t^2-\varkappa^2}}\right\} .$$

The expression in the curly brackets is

$$\frac{2Am}{\pi\sqrt{t^2-\varkappa^2}}\left[-\varkappa - \frac{\lambda t^2}{(t^2-\varkappa^2+\lambda^2)} + \frac{(x+y)}{\sqrt{m}} + \frac{\varkappa^2\lambda(x^2-y^2)}{(x^2-y^2)(t^2-\varkappa^2)+\lambda^2t^2}\right], \tag{A-128}$$

or with

$$-\varkappa + \frac{(x+y)}{\sqrt{m}} = \lambda \tag{A-129}$$

$$\frac{2Am}{\pi\sqrt{t^2-\varkappa^2}}\left[\frac{\lambda^3-\varkappa^2\lambda}{t^2-\varkappa^2+\lambda^2} + \frac{\varkappa^2\lambda(x^2-y^2)}{(x^2-y^2)(t^2-\varkappa^2)+\lambda^2t^2}\right] . \tag{A-130}$$

Now

$$\lambda^2-\varkappa^2 = y^2-x^2 , \tag{A-131}$$

so that equation A-130 becomes

$$\frac{2Am\lambda(y^2-x^2)}{\pi\sqrt{t^2-\varkappa^2}}\left[\frac{1}{t^2-\varkappa^2+\lambda^2} - \frac{\varkappa^2}{(x^2-y^2)(t^2-\varkappa^2)+\lambda^2t^2}\right] \tag{A-132}$$

which is

$$\frac{2Am\lambda(y^2-x^2)}{\pi\sqrt{t^2-\varkappa^2}}\left[\frac{(x^2-y^2)(t^2-\varkappa^2)+(t^2-\varkappa^2)(\lambda^2-\varkappa^2)}{\text{Denominator}}\right] = 0 \tag{A-133}$$

Therefore the contribution from the integral of P_{2g} is

$$\frac{2Am}{\pi}\int_{\kappa}^{a} dt\, e^{-t^2}\left[tg^{-1}\frac{\lambda}{\sqrt{t^2-\kappa^2}}+tg^{-1}\frac{\kappa}{\sqrt{t^2-\kappa^2}}\right]. \qquad \text{(A-134)}$$

The same sort of cancellation occurs in the differentiation of P_{3g} although the algebra is lengthier because there are three more arctangents in P_{3g} than in P_{2g}. The result for P_{3g} is

$$\frac{2Am}{\pi}\int_{a}^{\infty} dt\, e^{-t^2}\left[tg^{-1}\frac{\lambda}{\sqrt{t^2-\kappa^2}}+tg^{-1}\frac{\kappa}{\sqrt{t^2-\kappa^2}}+tg^{-1}\frac{\beta}{\sqrt{t^2-a^2}}-tg^{-1}\frac{a}{\sqrt{t^2-a^2}}\right].$$

(A-135)

A-134 and A-135 combine to give

$$P(y\to x)=\frac{2ma^2x}{\pi y}\int_{\kappa}^{\infty} dt\, e^{-t^2}\left[tg^{-1}\frac{\lambda}{\sqrt{t^2-\kappa^2}}+tg^{-1}\frac{\kappa}{\sqrt{t^2-\kappa^2}}\right]$$

$$+\frac{2ma^2x}{\pi y}\int_{a}^{\infty} dt\, e^{-t^2}\left[tg^{-1}\frac{\beta}{\sqrt{t^2-a^2}}-tg^{-1}\frac{a}{\sqrt{t^2-a^2}}\right] \qquad \text{(A-136)}$$

$$\text{if } 0\le y\le cx/a$$

which is the expression given in the text of the thesis. The factor $2/\sqrt{\pi}$ omitted in writing equations A-122 to A-125 is canceled by multiplying the integral equation by $\sqrt{\pi}/2$.

All the other integrals for the other ranges of y can be evaluated in the manner shown above. The drastic simplification by a proper integration by parts is typical of all the expressions. It is to be noted

that when $y > cx/a$, $P_{2g}(t=x) \neq 0$ but is continuous with P_{1g}. This not only serves as a good check on the algebra of the expressions but makes the distinction between the averaged energy model and the gas model more evident. That is, the vanishing of subregion I in either the neutron speed gain or loss case significantly changes the form of $P(y \rightarrow x)$ in the averaged energy oscillator model when $m > 1$.

APPENDIX B

THERMALIZATION BY MONATOMIC GASES

In this appendix, the equations describing thermalization by a monatonic gas are summarized. The basic work is due to Wigner and Wilkins (1, 2). Although the work is the basis for much current work in thermalization, the original papers are available only as AEC reports. The notation used in the appendix is that adopted for the thesis which is somewhat different from that used in the original work.

The normalized distribution of atom speeds for a monatomic gas is

$$M_o(u) = \frac{4m^{3/2}b^3}{\sqrt{\pi}} u^2 e^{-m u^2 b^2} \qquad b = \frac{1}{\sqrt{2kT}} \qquad \text{(A-34)}$$

$$\text{if } 0 \le u \le \infty .$$

The integral equation describing thermalization is

$$\int_0^\infty dy\, n(y) P(y \to x) = n(x) \left[V(x) + \Delta \right], \qquad \text{(B-1)}$$

with

$$x = v/\sqrt{2kT}, \qquad y = w/\sqrt{2kT}, \qquad \Delta = \frac{\sqrt{\pi}}{2} \frac{\sigma_a(v) v}{\sigma_s \sqrt{2kT}}, \qquad \text{(B-2)}$$

and

$$V(x) = \left(x + \frac{1}{2mx} \right) I(\sqrt{m}\, x) + \frac{e^{-mx^2}}{2\sqrt{m}}, \qquad \text{(B-3)}$$

where I is an unnormalized error function

$$I(x) = \int_0^x dt\, e^{-t^2}. \qquad \text{(B-4)}$$

With the notation of the thesis,

$$a = \frac{m+1}{2m} \qquad c = \frac{m-1}{2m}$$

$$\begin{aligned} \alpha(x,y) &= \sqrt{m}\,(ax+cy) \\ \beta(x,y) &= \sqrt{m}\,(ay+cx) \\ \varkappa(x,y) &= \sqrt{m}\,(ax-cy) \\ \lambda(x,y) &= \sqrt{m}\,(ay-cx), \end{aligned} \tag{54}$$

the kernel $P(y\to x)$ is, when the expression derived in Appendix A is multiplied by $\sqrt{\pi}/2$,

$$P(y\to x) = \frac{ma^2x}{y}\left\{e^{y^2-x^2}\left[I(\beta)+I(\lambda)\right] + I(\varkappa) - I(\alpha)\right\} \qquad \text{if } 0 \le y \le x \tag{A-53}$$

$$= \frac{ma^2x}{y}\left\{I(\varkappa) + I(\alpha) + e^{y^2-x^2}\left[I(\lambda) - I(\beta)\right]\right\} \qquad \text{if } x \le y \le \infty .$$

For hydrogen (m=1), the equation simplifies, as partially indicated in Appendix A, to

$$2xe^{-x^2}\int_0^x dy\,\frac{n(y)}{y}\,e^{y^2}I(y) + 2xI(x)\int_x^\infty dy\,\frac{n(y)}{y} = n(x)\left[\left(x+\frac{1}{2x}\right)I(x) + \frac{e^{-x^2}}{2} + \Delta\right]. \tag{B-5}$$

A comparison of the expressions of this equation with those of the averaged energy hydrogen oscillator model of the thesis* is given below.

---

* Thesis expressions have been rearranged for closer comparison.

$P(y \to x) \quad 0 \le y \le x$

$$\frac{2x}{y} e^{y^2-x^2} \int_0^x dt\, e^{-t^2} \qquad \text{Wigner-Wilkins}$$

$$\frac{2x}{y} e^{y^2-x^2} \left[\int_0^x \frac{dt\, e^{-t^2} t}{\sqrt{t^2+x^2-y^2}} + \frac{2}{\pi} \int_y^\infty \frac{dt\, e^{-t^2} t}{\sqrt{t^2+x^2-y^2}} \sin^{-1} \frac{y}{t} \right] \qquad \text{Thesis} \qquad (B\text{-}6)$$

$P(y \to x) \quad x \le y \le \infty$

$$\frac{2x}{y} I(x) \qquad \text{Wigner-Wilkins}$$

$$\frac{2x}{y} \left[I(x) + \frac{2}{\pi} \int_x^\infty dt\, e^{-t^2} \sin^{-1} \frac{x}{t} \right] \qquad \text{Thesis} \qquad (B\text{-}7)$$

$V(x)$

$$\left(x + \frac{1}{2x}\right) I(x) + e^{-x^2}/2 \qquad \text{Wigner-Wilkins}$$

$$\left(x + \frac{1}{4x}\right) \left[I(x) + \frac{2}{\pi} \int_x^\infty dt\, e^{-t^2} \sin^{-1} \frac{x}{t} \right] + \frac{1}{2\pi} \int_x^\infty dt\, e^{-t^2} \frac{6t^2-6x^2-1}{\sqrt{t^2-x^2}} \qquad (B\text{-}8)$$

Thesis

The Wigner-Wilkins kernel A-53 may be written in symmetric form by introducing

$$\nu(x) = \frac{n(x) e^{x^2/2}}{x}. \qquad (B\text{-}9)$$

For m = 1 the kernel of equation B-5 is a product of functions of x and functions of y and thus may be reduced to a differential equation by

applying the theory of Green's functions. The self adjoint form of the differential equation is

$$\frac{d}{dx} p \frac{d}{dx} [(V+\Delta)\nu(x)] + [2+r(V+\Delta)]\nu(x) = 0, \qquad \text{(B-10)}$$

with boundary conditions

$$\nu(0) = 0 \qquad \text{(B-11)}$$
$$\nu(\infty) = \text{finite} .$$

The terms appearing in the equation are

$$1/p(x) = e^{-x^2} + 2xI(x)$$
$$r(x) = p(x)\left[p(x)e^{-x^2} - x^2\right] \qquad \text{(B-12)}$$
$$V(x) = \left(x + \frac{1}{2x}\right) I(x) + e^{-x^2}/2 .$$

Wigner and Wilkins treated B-10 by working with the associated Riccati equation. Finding series expansions for large and small x, they calculated n(x) for four values of Δ. With $\Delta' = (2/\sqrt{\pi})\Delta$, they give

$$n(x) \approx \frac{1}{x^2} \frac{e^{-2\Delta'/x}}{1+\Delta'/x + 1/2x^2 \ldots} \quad x >> 1 . \qquad \text{(B-13)}$$

This expression, with $e^{-2\Delta'/x} \approx (1+\Delta'/x)^{-2}$, is approximately

$$n(x) \approx \frac{x}{(x+\Delta')^3} . \qquad \text{(B-14)}$$

Wilkins (2), expanded $P(y \rightarrow x)$ and $V(x)$ of A-53 and B-3 in inverse powers of the atomic mass to provide an approximation for a heavy monatomic gas. The expansion of P is not straightforward. The

symmetric form of P is expanded as a delta function plus an inverse mass series and the independent variable $\nu(y)$ of B-9 is expanded about y=x. Wilkins discusses the technique in a separate mathematical treatise (28) in which the expression P(y-x) is used as an example. The result is the differential equation

$$x\frac{d^2n}{dx^2} + (2x^2-1)\frac{dn}{dx} + (4x-2m\Delta')n = 0 \qquad m \gg 1. \tag{B-15}$$

For large m, ξ is approximately 2/m so that

$$2m\Delta' \approx \frac{4\Delta'}{\xi} = \frac{4\sigma_a(v)v}{\xi\sigma_s\sqrt{2kT}}, \tag{B-16}$$

so that the single parameter describing the thermalizing material is the combination above.

An identical approximation was derived in a different manner by Hurwitz (23) considering the neutron flux as the independent variable and the neutron energy as the dependent variable. That is,

$$E = kTx^2 \tag{B-17}$$

$$\phi(E) = c_9 n(x).$$

The differential equation is, in these variables,

$$EkT\frac{d^2\phi}{dE^2} + E\frac{d\phi}{dE} + \left[1 - \frac{m\sigma_a(E)}{2\sigma_s}\right]\phi = 0. \tag{B-18}$$

The approximation of Hurwitz neglects terms of order smaller than 1/m (18). The physical parameters $\sigma_a/\xi\sigma_s$ appear explicitly in this equation. In terms of the dimensionless energy

$$\epsilon = E/kT, \tag{B-19}$$

this equation is, for 1/v absorption,

$$\epsilon \frac{d^2\phi}{d\epsilon^2} + \epsilon \frac{d\phi}{d\epsilon} + \left[1 - \frac{m\Delta'}{2\sqrt{\epsilon}} \right] \phi = 0. \tag{B-20}$$

The operator,

$$H = \epsilon \frac{d^2}{d\epsilon^2} + \epsilon \frac{d}{d\epsilon} + 1, \tag{B-21}$$

has eigenvunctions

$$\begin{aligned} H\phi_n(\epsilon) &= -n\phi_n(\epsilon) \\ \phi_n &= \epsilon e^{-\epsilon} L_n^{(1)}(\epsilon), \end{aligned} \tag{B-22}$$

where the $L_n^{(1)}$ are the associated Laguerre polynomials (cf. reference (29) page 784). Because of this fact, many thermalization problems have been treated in the heavy gas approximation using eigenvalue expansions. In time dependent problems, the time dependence enters as a $1/\sqrt{\epsilon}$ energy dependence as does 1/v absorption. (If the absorption is a constant the equation is solved by $\epsilon e^{-\epsilon} F(c \mid 2 \mid \epsilon)$ where F is a confluent hypergeometric function and $c = \frac{m}{2} \frac{\sigma_a}{\sigma_s}$, but constant absorption is an unlikely physical situation in the thermal energy range.)

For T near zero, that is, for the rest atom case, B-18 reduces to the Fermi age equation (18), (23).

APPENDIX C

COEFFICIENTS OF THE EXPANSION $\sum_{r=1}^{\infty} \frac{a_r}{x^r}$

As is indicated in equation 78 of Section II of the thesis, the equation describing thermalization by a single energy hydrogen oscillator may be written, for $x \geq \sqrt{2}$, as

$$\int_{\sqrt{x^2-1}}^{x} dy \frac{n(y)}{y}\left[1 - \sqrt{x^2-y^2}\right] + \int_{x}^{\infty} dy \frac{n(y)}{y} = \frac{n(x)}{2}\left[1 + \frac{1}{6x^2} + \frac{\Delta}{x}\right]. \tag{C-1}$$

A solution of the form

$$n(x) = \sum_{r=1}^{\infty} \frac{a_r}{x^r} \tag{C-2}$$

is assumed. Substituting equation C-2 into C-1 and integrating the simple terms gives

$$\sum_{r=1}^{\infty} a_r\left[\frac{1}{r(x^2-1)^{r/2}} + f(x, r)\right] = \frac{1}{2}\left[1 + \frac{1}{6x^2} + \frac{\Delta}{x}\right] \sum_{r=1}^{\infty} \frac{a_r}{x^r}, \tag{C-3}$$

where

$$f(x, r) = -\int_{\sqrt{x^2-1}}^{x} \frac{dy \sqrt{x^2-y^2}}{y^{r+1}}. \tag{C-4}$$

Changing the integration variable in C-4 to $t^2 = x^2 - y^2$ the integral is

$$f(x, r) = -\int_{0}^{1} \frac{dt\, t^2}{(x^2-t^2)^{r/2+1}}, \tag{C-5}$$

Integrating f(x, r) by parts once gives

$$f(x, r) = -\frac{1}{r(x^2-1)^{r/2}} + \frac{1}{r}\int_0^1 \frac{dt}{(x^2-t^2)^{r/2}} , \qquad (C-6)$$

so that the term multiplying a_r on the left of equation C-3 is

$$f(x, r) + \frac{1}{r(x^2-1)^{r/2}} = \frac{1}{rx^r}\int_0^1 \frac{dt}{(1-t^2/x^2)^{r/2}} . \qquad (C-7)$$

For x larger than 1 (and x must be larger than $\sqrt{2}$ before equation C-1 is valid),

$$\left(1 - \frac{t^2}{x^2}\right)^{-r/2} = \sum_{k=0}^{\infty} \frac{\Gamma(r/2+k)}{\Gamma(\frac{r}{2})\Gamma(k+1)} \left(\frac{t}{x}\right)^{2k} \qquad r \geq 1, \qquad (C-8)$$

which when substituted in C-7, integrated and evaluated at t=0 and t=1 gives

$$\frac{1}{rx^r} \sum_{k=0}^{\infty} \frac{\Gamma(r/2+k)}{\Gamma(\frac{r}{2})\, k!\, (2k+1)} \frac{1}{x^{2k}} , \qquad (C-9)$$

as the coefficient of a_r, so that equation C-3 becomes

$$\sum_{r=1}^{\infty} \frac{a_r}{2x^r} \sum_{k=0}^{\infty} \frac{\Gamma(r/2+k)}{\Gamma(\frac{r}{2}+1)k!(2k+1)} \frac{1}{x^{2k}} = \frac{1}{2}\left[1 + \frac{1}{6x^2} + \frac{\Delta}{x}\right] \sum_{r=1}^{\infty} \frac{a_r}{x^r} . \qquad (C-10)$$

Equating coefficients of the first two powers of x on each side gives

$$\frac{a_1}{x} \frac{\Gamma(\frac{1}{2})}{2\Gamma(\frac{3}{2})\,(1)(1)} = \frac{a_1}{2x} \quad \text{or} \quad \frac{a_1}{x} = \frac{a_1}{2x} , \qquad (C-11)$$

$$\frac{a_2}{2x^2} \frac{\Gamma(1)}{\Gamma(2)\,(1)(1)} = \frac{a_2}{2x^2} \quad \text{or} \quad \frac{a_2}{2x^2} = \frac{a_2}{2x^2} ,$$

so that a_1 is taken to be zero and a_2 is arbitrary. In C-10 the coefficients of $1/x^{10}$, say, on the left involve a_{10}, a_8, a_6, a_4 and a_2, that is, values for which $2k+r = 10$. Making the change of indices

$$\begin{aligned} 2k+r &= j \\ i &= k, \end{aligned} \tag{C-12}$$

on the left and k=j on the right, C-10 becomes, with $a_1 = 0$,

$$\sum_{j=2}^{\infty} \frac{\Gamma(\frac{j}{2})}{x^j} \sum_{i=0}^{[j/2-1]} \frac{a_{j-2i}}{\Gamma(\frac{j}{2}-i+1)i!(2i+1)} = \sum_{j=2}^{\infty} a_j \left[\frac{1}{xj} + \frac{1}{6x^{j+2}} + \frac{\Delta}{x^{j+1}} \right], \tag{C-13}$$

where the sum on i is truncated so that only the coefficients a_j, $a_{j-2}, \ldots a_2$ contribute. That is, from C-12, i=0, 1... until

$$i = \frac{j-r}{2} \Big|_{r=2} = j/2 - 1, \tag{C-14}$$

and i is an integer so that the sum on i contributes only up to the integer closest to j/2-1. Extracting coefficients of $1/x^2$ and $1/x^3$ from both sides, and rearranging the indices gives

$$\frac{a_2}{x^2} + \frac{2a_3}{3x^3} + \sum_{j=2}^{\infty} \frac{\Gamma(\frac{j+2}{2})}{x^{j+2}} \sum_{i=0}^{[j/2]} \frac{a_{j+2-2i}}{\Gamma(\frac{j}{2}-i+2)i!(2i+1)}$$

$$= \frac{a_2}{x^2} + \frac{a_3}{x^3} + \frac{\Delta a_2}{x^3} + \sum_{j=2}^{\infty} \frac{1}{x^{j+2}} \left[a_{j+2} + \Delta a_{j+1} + \frac{a_j}{6} \right]. \tag{C-15}$$

Thus, equating coefficients of powers of x,

$$a_3 = -3\Delta a_2, \tag{C-16}$$

$$a_{j+2} = -\Delta a_{j+1} - \frac{a_j}{6} + \Gamma\left(\frac{j+2}{2}\right) \sum_{i=0}^{[j/2]} \frac{a_{j+2-2i}}{\Gamma\left(\frac{1}{2}-i+2\right) i!\,(2i+1)} \quad \text{if } j \geq 2. \qquad \text{(C-17)}$$

To express coefficients in terms of preceding coefficients the first two terms are removed from the i sum.

$$a_{j+2} = -\Delta a_{j+1} - \frac{a_j}{6} + \frac{2a_{j+2}}{j+2} + \frac{a_j}{3} + \Gamma\left(\frac{j+2}{2}\right) \sum_{i=2}^{[j/2]} \frac{a_{j+2-2i}}{\Gamma\left(\frac{1}{2}-i+2\right) i!\,(2i+1)}, \qquad \text{(C-18)}$$

with empty sums taken to be zero. After collecting terms C-18 becomes

$$a_{j+2} = \frac{-\Delta(j+2)a_{j+1}}{j} + \frac{(j+2)a_j}{6j} + \frac{(j+2)\Gamma\left(\frac{j}{2}\right)}{2} \sum_{i=2}^{[j/2]} \frac{a_{j+2-2i}}{\Gamma\left(\frac{1}{2}-i+2\right) i!\,(2i+1)} \qquad \text{(C-19)}$$

$$j \geq 2 .$$

For even $j=2r$ this relation becomes

$$a_{2r+2} = \frac{-\Delta(r+1)a_{2r+1}}{r} + \frac{(r+1)a_{2r}}{6r} + (r+1)(r-1)! \sum_{i=2}^{r} \frac{a_{2r+2-2i}}{(r+1-i)!\; i!\; (2i+1)} \qquad \text{(C-20)}$$

$$r \geq 1 .$$

Or, letting $r = r-1$

$$a_{2r} = \frac{-\Delta r a_{2r-1}}{r-1} + \frac{r a_{2r-2}}{6(r-1)} + \frac{1}{r-1} \sum_{i=2}^{r-1} \frac{a_{2r-2i}}{(2i+1)} \binom{r}{i} \qquad r \geq 2, \qquad \text{(C-21)}$$

where the term in brackets in the sum is a binomial coefficient. A similar transformation, $r = 2r-1$, gives the odd coefficients

$$a_{2r+1} = \frac{-\Delta(2r+1)a_{2r}}{2r-1} + \frac{(2r+1)a_{2r-1}}{6(2r-1)} + \frac{2}{2r-1}\sum_{i=2}^{r-1} \frac{a_{2r-2i+1}}{2i+1}\binom{r+\frac{1}{2}}{i} \qquad (C\text{-}22)$$

$$r \geq 1,$$

where the upper limit on the i sum has been changed from $r - \frac{1}{2}$ to r-1 without affecting the summation. Equation C-22 recovers the term a_3,

$$a_3 = -3\Delta a_2 , \qquad (C\text{-}23)$$

since $a_1 = 0$.

The first few terms of $\sum_{r=2}^{\infty} \frac{a_r}{x^r}$ are given in the text of the thesis in equation 91.

APPENDIX D

ERROR ESTIMATE FOR THE NEUTRON CONSERVATION CONDITION

In Section IV of the thesis an approximate neutron conservation condition is used to adjust the neutron source to maintain a steady state neutron distribution. The error caused by this approximation in the numerical solution of the integral equation describing thermalization by a single energy harmonic oscillator is estimated below. If the integral equation for neutron balance is

$$\int_0^{x_o} dy\, n(y)P(y\to x) + S(x) = n(x)\,[V(x)+\Delta], \tag{D-1}$$

the approximate relation to be examined is

$$\int_0^{x_o} dx S(x) = \Delta \int_0^{x_o} dx\, n(x) + \int_0^{x_o} dx\, n(x)V(x) - \int_0^{x_o} dx \int_0^{x_o} dy\, n(y)P(y\to x) \approx \Delta \int_0^{x_o} dx\, n(x). \tag{D-2}$$

The approximation arises because $x_o \neq \infty$. Otherwise the two neglected terms cancel. Both $P(y\to x)$ and $V(x)$ for the single energy oscillator model have different forms for $x < 1$ and $x > 1$ which are temporarily denoted with the subscripts 1 and 2, respectively. Also, for $y < x$ in $P(y\to x)$ the subscript g is used and for $y > x$ the subscript ℓ is used. The ranges for which $P(y\to x)$ is not zero are, for the single energy oscillator model,

$$\begin{aligned} &P_{1g} && 0 \le y \le x \\ &P_{1\ell} && x \le y \le x_o \\ &P_{2g} && \sqrt{x^2-1} \le y \le x \\ &P_{2\ell} && x \le y \le x_o . \end{aligned} \tag{D-3}$$

With this notation, the integral

$$I = \int_0^{x_o} dx \int_0^{x_o} dy\, n(y)\, P(y \to x) \tag{D-4}$$

is for $x_o > 1$,

$$I = \int_0^1 dx \int_0^x dy\, n(y) P_{1g} + \int_0^1 dx \int_x^{x_o} dy\, n(y) P_{1\ell}$$

$$+ \int_1^{x_o} dx \int_{\sqrt{x^2-1}}^{x} dy\, n(y) P_{2g} + \int_1^{x_o} dx \int_x^{x_o} dy\, n(y) P_{2\ell} \qquad 0 \le x \le x_o . \tag{D-5}$$

Interchanging the order of integration, D-5 becomes

$$I = \int_0^1 dy\, n(y) \int_y^1 dx P_{1g} + \int_0^1 dy\, n(y) \int_0^y dx P_{1\ell} + \int_1^{x_o} dx\, n(y) \int_0^1 dx P_{1\ell}$$

$$+ \int_0^1 dy\, n(y) \int_1^{\sqrt{1+y^2}} dx P_{2g} + \int_1^{x_o} dy\, n(y) \int_y^{\sqrt{1+y^2}} dx P_{2g} - \int_{\sqrt{x_o^2-1}}^{x_o} dy\, n(y) \int_{x_o}^{\sqrt{1+y^2}} dx P_{2g} \tag{D-6}$$

$$+ \int_1^{x_o} dy\, n(y) \int_1^y dx P_{2\ell} .$$

The integration of $P(y \to x)$ with respect to x can now be accomplished.

The various expressions for $P(y \to x)$ and their integrals are

$$P_{1g} = \frac{4x}{\pi y}\left[\mathrm{tg}^{-1} \frac{y}{\sqrt{1-x^2}} - \sqrt{x^2-y^2}\, \mathrm{tg}^{-1} \frac{y}{\sqrt{x^2-y^2}\sqrt{1-x^2}} + y\, \mathrm{sech}^{-1} x \right] \tag{D-7}$$

$$\int_{y}^{1} dx P_{1g} = \frac{1}{3\pi}\left[4\sqrt{1-y^2} - \frac{2\pi}{y}(1-y^2)^{3/2} + \frac{2}{y}\sin^{-1}y - 2y^2\,\mathrm{sech}^{-1}y + \pi\left(\frac{2}{y} - 3y\right)\right] \tag{D-8}$$

$$P_{1\ell} = \frac{4x}{\pi y}\left(\sin^{-1}x + x\,\mathrm{sech}^{-1}x\right) \tag{D-9}$$

$$\int_{0}^{y} dx P_{1\ell} = \frac{1}{3\pi}\left[\left(6y - \frac{1}{y}\right)\sin^{-1}y + \sqrt{1-y^2} + 4y^2\,\mathrm{sech}^{-1}y\right] \tag{D-10}$$

$$\int_{0}^{1} dx P_{1\ell} = \frac{5}{6y} \tag{D-11}$$

$$P_{2g} = \frac{2x}{y}\left[1 - \sqrt{x^2-y^2}\right] \tag{D-12}$$

$$\int_{1}^{\sqrt{1+y^2}} dx P_{2g} = \frac{1}{3\pi}\left[-\pi\left(\frac{2}{y} - 3y\right) + \frac{2\pi}{y}(1-y^2)^{3/2}\right] \tag{D-13}$$

$$\int_{y}^{\sqrt{1+y^2}} dx P_{2g} = \frac{1}{3y} \tag{D-14}$$

$$\int_{x_o}^{\sqrt{1+y^2}} dx P_{2g} = -\left[y + \frac{1}{3y} - \frac{x_o^2}{y} + \frac{2}{3}\,\frac{(x_o^2-y^2)^{3/2}}{y}\right] \tag{D-15}$$

$$P_{2\ell} = \frac{2x}{y} \tag{D-16}$$

$$\int_{1}^{y} dx P_{2\ell} = y - \frac{1}{y}\ . \tag{D-17}$$

In equation D-6, the integrals D-8, D-10 and D-13 may be combined since the integrations on y are all for $0 \le y \le 1$. This combination is

$$\int_0^1 dy\, n(y) \left[\frac{1}{3\pi} \left(5\sqrt{1-y^2} + (6y + \frac{1}{y}) \sin^{-1} y + 2y^2 \operatorname{sech}^{-1} y \right) \right]. \qquad \text{(D-18)}$$

The combination in the integrand is just the expression of the single energy oscillator model for V(y), $0 \le y \le 1$. Thus D-18 is

$$\int_0^1 dy\, n(y) V_1(y) . \qquad \text{(D-19)}$$

In the same manner, the integrals D-11, D-14 and D-17 in equation D-6 are combined to give

$$\int_1^{x_o} dy\, n(y) \left(y + \frac{1}{6y}\right) = \int_1^{x_o} dy\, n(y)\, V_2(y), \qquad \text{(D-20)}$$

where V_2 is the single energy oscillator model expression for V(y) when $y \ge 1$. Combining D-19 and D-20 and the one remaining term D-15, equation D-6 becomes

$$I = \int_0^{x_o} dy\, n(y) V(y) - \frac{\int_0^{x_o} dy\, n(y) \left[y + \frac{1}{3y} - \frac{x_o^2}{y} + \frac{2}{3} \frac{(x_o^2 - y^2)^{3/2}}{y} \right]}{\sqrt{x_o^2 - 1}}. \qquad \text{(D-21)}$$

The error in the approximate relation D-2 is

$$\epsilon(x_o) = \int_0^{x_o} dx\, n(x) V(x) - I = \frac{\int_0^{x_o} dy\, n(y) \left[y + \frac{1}{3y} - \frac{x_o^2}{y} + \frac{2}{3} \frac{(x_o^2 - y^2)^{3/2}}{y} \right]}{\sqrt{x_o^2 - 1}}. \qquad \text{(D-22)}$$

In Section II of the thesis (equations 80 and 84) it is shown that $n(x)$ approaches $1/x^2$ for large x. Using $1/y^2$ as an approximation for $n(y)$ in D-22 and integrating gives

$$\epsilon(x_o) = \frac{1}{2} \ell n \frac{x_o^2}{x_o^2 - 1} - \frac{1}{6x_o^2} + 1 - x_o \tanh^{-1} \frac{1}{x_o}, \qquad \text{(D-23)}$$

which, when expanded in inverse powers of x_o, is

$$\epsilon(x_o) = \sum_{n=0}^{\infty} \frac{1}{(2n+4)(2n+5)x_o^{2n+4}}. \qquad \text{(D-24)}$$

As $x_o \to \infty$, $\epsilon(x_o) \to 0$, confirming that the relation D-2 is exact when $x_o \to \infty$. More precisely, when $x_o = \infty$ is used as an upper limit of integration in D-2, the interchange of limits of integration in D-5 does not produce the integral D-15 so that $\int_0^\infty dx P(y-x) = V(y)$ exactly, in accordance with the general properties of V and P discussed in Section I of the thesis. The fact that $\int_0^\infty dx\, P(y-x) = V(y)$ serves as incidental check that the integrations producing P and V themselves are performed correctly since P and V are determined from separate relations.

APPENDIX E

NUMERICAL ANALYSIS AND COMPUTER PROGRAMS

Numerical Analysis

The numerical solution of thermalization equations by the method outlined in Section IV of the thesis is not suitable for equations describing thermalization in non-absorbing media because the parameter containing absorption (Δ) is used as a divisor. For the monatomic gas model of Wigner and Wilkins (1), this is not a serious deficiency since the solution of the equations for $\sigma_a = 0$ is known to be Maxwellian. For the models employed in the thesis, however, the solution for $\sigma_a = 0$ is not known. This section of the appendix is devoted to a discussion of various numerical methods that were attempted, with varying degrees of success, to solve the problem for $\sigma_a = 0$.

The typical equation to be solved is

$$\int_0^{x_o} dy\, n(y)P(y\to x) + S(x) = n(x)V(x), \qquad \text{(E-1)}$$

with

$$S(x) = \int_{x_o}^{\infty} dy\, n_o(y)P(y\to x) \qquad \text{(E-2)}$$

computed from an assumed form of $n(x)$ for $x \geq x_o$ and the known form of $P(y\to x)$. Defining, in matrix notation, with a mesh spacing h for the variables,

$x = ih \quad y = ij$

$\vec{n}$ column vector $\quad n_i = n(ih)$

$\vec{s}$ column vector $\quad s_i = s(ih)$

P square matrix $P_{ij} = P(jn \rightarrow ih)w_j$

V diagonal matrix $V_{ij} = V(ih)\delta_{ij}$,

where the w_j are suitable quadrature coefficients; the integral equation E-1 becomes the discrete system

$$P\vec{n} + \vec{s} = V\vec{n} , \tag{E-3}$$

in which the size of the system is given by x_o/h. Defining

$$A = P-V , \tag{E-4}$$

equation E-3 becomes

$$A\vec{n} = -\vec{s}, \tag{E-5}$$

which is a system of inhomogeneous linear equations. The system E-5 is of a type for which numerous standard programs of solution exist in computer libraries. The most common type of solution is a row reduction of the augmented matrix

$$[A \mid -\vec{s}] \tag{E-6}$$

in which the row reduction is carried out by a procedure which eliminates division by small numbers. The discussion below outlines the difficulties encountered in using standard row reduction programs for the single energy oscillator model of the thesis.

For the single energy oscillator model of the thesis, the matrix A is found to be nearly singular. That is, det A is very small compared to a row sum of A. Qualitatively this may be seen from the fact that for large x_o, $S(x)$ is very small. Thus $\vec{s}$ is almost zero, and if $\vec{s}$ were zero A would have to be singular to provide non-trivial solutions to E-5.

After anomalous results for row reduction of E-5, it was numerically verified that det A was nearly zero with consequent loss of accuracy in solving E-5 by row reduction. The anomalous solutions of E-5 were not detected in first attempts to solve E-1 for the single energy oscillator model. As the mesh spacing h was decreased solutions remained apparently stable and qualitatively much as presented in the results of the thesis until at a small h a solution partially negative in the range $0 \leq x \leq x_o$ appeared. The appearance of a radically different solution suggested that subtraction of nearly equal small quantities was occurring in the row reduction process and that almost all accuracy was being lost. Therefore the row reduction method of solution was discarded and iterative schemes were attempted.

Equation E-3 may be solved iteratively in a number of ways after an initial guess for $\vec{n}$ is made. Two possibilities are:

$$\vec{n}^{(k+1)} = P^{-1}(V\vec{n}^{(k)} - \vec{s}), \qquad \text{(E-7)}$$

and

$$\vec{n}^{(k+1)} = V^{-1}(P\vec{n}^{(k)} + \vec{s}). \qquad \text{(E-8)}$$

Equation E-8 is the simplest procedure because the inverse of V is simply computed. For convergence of an iterative scheme the largest eigenvalue of the iteration matrix must be less than one. By using computer routines, the largest eigenvalue of $V^{-1}P$ for the single energy oscillator model was shown to be slightly larger than one. A modification of E-8, obtained by adding or subtracting integer multiples of $V\vec{n}$ to both sides of E-3, that is,

$$P\vec{n} + \vec{s} + mV\vec{n} = (V\vec{n})(m+1)$$

$$\vec{n}^{(k+1)} = \frac{1}{m+1} V^{-1} (P+mV)\vec{n}^{(k)} + \vec{s} \qquad m=\pm 1, \pm 2, \ldots, \qquad \text{(E-9)}$$

did not succeed in reducing the largest eigenvalue of the iteration matrix below one although it appeared possible to approach one as closely as desired from above.

At this point it was suggested by Dr. Franklin of the California Institute of Technology, that the scheme E-8 be used with a normalization of $\vec{n}$ after each iteration to keep one element of $\vec{n}$ a constant. This procedure resulted in slow convergence of the iteration scheme E-8. The scheme in effect allows the shape of n(x) to change without allowing the amplitude of n(x) to increase without bound. The procedure was used to calculate n(x) for the single energy oscillator model with $\Delta = 0$.

The method of iterate normalization used for $\sigma_a \neq 0$ ($\Delta \neq 0$), that is, neutron conservation, is discussed in Section IV of the thesis. The method is commonly used in numerical solution of thermalization problems (see references (15) and (9)). It not only insures that the neutron density is normalized to be compatible with the source rate of introduction of neutrons, but greatly speeds convergence. For example, for $\Delta \neq 0$, the averaged energy hydrogen oscillator model solutions converged in roughly 200 iterations for fixed element normalization and in approximately 10 iterations for neutron conservation normalization. The fixed element normalization technique is not as accurate as the neutron conservation normalization because fixed element normalization modifies the source slightly with each iteration. That is

if the fixed element is n_p and

$$n_p^{(k+1)} = [1+\epsilon(k)]\, n_p^{(k)} , \qquad \text{(E-10)}$$

the equation E-3 is divided by 1+ε at each normalization and the effect on $\vec{s}$ for r iterations is

$$(1+\epsilon)^{-r}\, \vec{s} . \qquad \text{(E-11)}$$

For the single energy oscillator model ($\Delta=0$), $\epsilon(k)$ was typically 0.001 so that the effect is relatively small. A procedure in which $\vec{s}$ was not modified as iteration continued affected only the asymptotic amplitude of n(x) for the single energy oscillator model, $\Delta=0$. The amplitude of $n(x), 0 \le x \le 1.5$, was not changed. If $\vec{s}$ is not modified the fixed element normalization is not mathematically rigorous, but convergence of the $n^{(k)}$ does produce a solution of E-3. It is for this reason that the results displayed in figure 9 are not felt to be as reliable as those results for which $\Delta \neq 0$ since $\vec{s}$ was not modified to produce n(x) in figure 9.

Computer Programs

The remainder of the appendix displays the programs used for solution of n(x), $\Delta \neq 0$. Three of the programs are for m=1. These three are the single energy oscillator model, the averaged energy oscillator model, and the Wigner-Wilkins monatomic gas model. The remaining program was used for $m > 1$ and the averaged energy oscillator model. Because of the simplifications for m=1, a ten fold saving of computing time was gained by separately programming the averaged energy oscillator equations for m=1 and $m > 1$.

```
      DIMENSION  RA(150),RB(150),RC(150),RD(150),RE(150),RF(150)
      DIMENSION P(150,150),V(150),S(150)
    1 FORMAT (I5)
    2 FORMAT (5E14.7)
    3 FORMAT (10H NO. EQNS=I5, 6H MESH=E14.7, 16H MAX ABSORPTION=E14.7,
     X7H RANGE=E14.7)
    4 FORMAT (8H ENERGY=E14.7,11H AMPLITUDE=E14.7,
     X16H DEL ABSORPTION=E14.7)
    5 FORMAT (12H ABSORPTION=E14.7)
    6 FORMAT (1HO)
    7 FORMAT (3H X=E14.7,3H N=E14.7,4H NN=E14.7,5H DEL=E14.7,
     X3H E=E14.7,5H PHI=E14.7)
      FREQUENCY 10(1,0,3),14(1,0,1),41(1,0,3),18(2,0,1),21(1,0,3),
     X24(1,0,0),34(1,0,5),37(10,0,1)
      READ 1,M
      READ 2, H,Z,EN,AM,DA,ABM,W
      PRINT 3, M,H,ABM,Z
      PRINT 4, EN,AM,DA
      PRINT 5, W
      PI=3.1415927
      DO 27 I=1,M
      X=FLOATF(I)*H
      U=X*X
      T=X+1.0/X/6.0
      R=2.0*((Z+W)**2)
   10 IF (X-1.0) 11,12,12
   11 A=SQRTF(1.0-U)
      B=ATANF(X/A)
      C=LOGF((1.0+A)/X)
      V(I)=(5.0*A+6.0*T*B+2.0*U*C)/3.0/PI
      D=4.0*X*(B+X*C)/PI
      S(I)=D/R
      GO TO 13
   12 V(I)=T
      E=2.0*X
      S(I)=E/R
   13 DO 26 J=1,M
      Y=FLOATF(J)*H
      F=Y*Y
   14 IF (Y-X) 15,21,21
   15 G=SQRTF(U-F)
   41 IF (X-1.0) 16,17,17
   16 P(I,J)=4.0*X*(ATANF(Y/A)-G*ATANF(Y/G/A)+Y*C)*H/(Y*PI)
      GO TO 24
   17 Q=SQRTF(U-1.0)
   18 IF (Y-Q) 19,19,20
   19 P(I,J)=0.0
      GO TO 24
   20 P(I,J)=E*H*(1.0-G)/Y
      GO TO 24
   21 IF (X-1.0) 22,23,23
   22 P(I,J)=D*H/Y
      GO TO 24
   23 P(I,J)=E*H/Y
   24 IF (J-M) 26,25,26
   25 P(I,J)=.5*P(I,J)
```

Single energy oscillator model, m = 1 (Page 1).

```
26 CONTINUE
   RD(I)=X
   RE(I)=EN*U
   RA(I)=U*EXPF(-U)
27 CONTINUE
   G=0.0
   MM=M-1
   DO 28 I=1,MM
   G=G+RA(I)
28 CONTINUE
   G=W*H*(G+.5*RA(M))
   F=(Z*Z-1.0/6.0)/(2.0*((Z+W)**2))
   T=F/G
   DO 29 I=1,M
   RA(I)=T*RA(I)
29 CONTINUE
   DO 31 I=1,M
   RB(I)=0.0
   DO 30 J=1,M
   RB(I)=RB(I)+P(I,J)*RA(J)
30 CONTINUE
   RB(I)=(RB(I)+S(I))/(V(I)+W)
31 CONTINUE
   G=0.0
   DO 32 I=1,MM
   G=G+RB(I)
32 CONTINUE
   G=W*H*(G+.5*RB(M))
   T=F/G
   B=0.0
   DO 33 I=1,M
   RB(I)=T*RB(I)
   RC(I)=1.0-RA(I)/RB(I)
   B=MAX1F(B,ABSF(RC(I)))
   RA(I)=RB(I)
33 CONTINUE
34 IF(B-.00001) 35,35,29
35 A=W/F
   DO 36 I=1,M
   RB(I)=RB(I)*A
   RF(I)=AM*RA(I)
36 CONTINUE
   PRINT 6
   PRINT 5,W
   PRINT 6
   PRINT 7, (RD(I),RA(I),RB(I),RC(I),RE(I),RF(I), I=1,M)
   WA=W
   W=W+DA
37 IF (W-ABM) 38,38,40
38 DO 39 I=1,M
   S(I)=S(I)*((Z+WA)**2)/((Z+W)**2)
39 CONTINUE
   GO TO 27
40 CALL EXIT
   END
```

Single energy oscillator model, m = 1 (Page 2).

```
      DIMENSION R1(150),R2(150),R3(150),R4(150),R5(150),R6(150)

      DIMENSION P(150,150),V(150),S(150)
    1 FORMAT (I5)
    2 FORMAT (5E14.7)
    3 FORMAT (10H NO. EQNS=I5, 6H MESH=E14.7, 16H MAX ABSORPTION=E14.7,
     X7H RANGE=E14.7)
    4 FORMAT (8H ENERGY=E14.7,11H AMPLITUDE=E14.7,
     X16H DEL ABSORPTION=E14.7)
    5 FORMAT (12H ABSORPTION=E14.7)
    6 FORMAT (1HC)
    7 FORMAT (3H X=E14.7,3H N=E14.7,4H NN=E14.7,5H DEL=E14.7,
     X3H E=E14.7,5H PHI=E14.7)
      FREQUENCY 10(0,1,1),13(1,0,0),17(1,0,1),19(0,1,1),22(0,0,1),
     X24(1,0,0),29(1,0,0),39(0,0,1),42(0,0,1)
      READ 1,M
      READ 2, H,ABSM,Z,EN,AM,DELAB,W
      PRINT 3, M,H,ABSM,Z
      PRINT 4, EN,AM,DELAB
      PRINT 5, W
      WA=.8862269*W
      DO 32 I=1,M
      X=FLOATF(I)*H
      U=X*X
      L=0
      A=0.0
      B=0.0
      C=X
      DO 16 K=1,80
      L=L+1
      C=C+.05
      D=C*C
      E=D/U
      F=SQRTF(E-1.0)
      G=EXPF(-D)
      Q=ATANF(F)
      R=G*G
      T=-R*(2.0+E)+3.0*F*G
   10 IF(L-1) 11,11,12
   11 R=4.0*R
      T=4.0*T
      GO TO 13
   12 R=2.0*R
      T=2.0*T
      L=0
   13 IF (K-80) 15,14,15
   14 R=R/2.0
      T=T/2.0
   15 A=A+R
      B=B+T
   16 CONTINUE
      V(I)=.8862269*(X+.25/X)+B*X/188.49556
      A=2.0*X*(.8862269-A/94.247781)
      C=2.0*((Z+W)**2)
      S(I)=A/C
      CALL SAVE
      DO 31 J=1,M
```

Averaged energy oscillator model m = 1 (Page 1).

```
      Y=FLOATF(J)*H
   17 IF (Y-X) 18,28,28
   18 L=0
      AA=0.0
      B=0.0
      C=X
      CA=SQRTF(U-Y*Y)
      DO 27 K=1,80
      L=L+1
      C=C+.05
      D=C*C
      R=EXPF(-CA**2)
      F=SQRTF(D-U)
      T=ATANF(F/Y)*EXPF(-D)
   19 IF (L-1) 20,20,21
   20 R=2.0*R
      T=4.0*T
      GO TO 22
   21 R=4.0*R
      T=2.0*T
      L=0
   22 IF (K-1) 24,23,24
   23 R=R/2.0
      GO TO 26
   24 IF (K-80) 26,25,26
   25 T=T/2.0
   26 AA=AA+R
      B=B+T
      CA=CA+.05
   27 CONTINUE
      P(I,J)=X*H*(AA-.6366198*B)/(30.0*Y)
      GO TO 29
   28 P(I,J)=A*H/Y
   29 IF (J-M) 31,30,31
   30 P(I,J)=.5*P(I,J)
   31 CONTINUE
      R1(I)=U*EXPF(-U)
      CALL SAVE
   32 CONTINUE
      MM=M-1
      G=0.0
      B=0.0
      DO 33 I=1,MM
      G=G+S(I)
      B=B+R1(I)
   33 CONTINUE
      G=G+.5*S(M)
      B=WA*(B+.5*R1(M))
      C=G/B
      DO 34 I=1,M
      R1(I)=C*R1(I)
   34 CONTINUE
      CALL SAVE
      DO 36 I=1,M
      R2(I)=0.0
      DO 35 J=1,M
```

Averaged energy oscillator model m = 1 (Page 2).

```
      R2(I)=R2(I)+P(I,J)*R1(J)
   35 CONTINUE
      R2(I)=(R2(I)+S(I))/(V(I)+WA)
   36 CONTINUE
      B=0.0
      DO 37 I=1,MM
      B=B+R2(I)
   37 CONTINUE
      B=WA*(B+.5*R2(M))
      C=G/B
      D=0.0
      DO 38 I=1,M
      R2(I)=C*R2(I)
      R3(I)=1.0-R1(I)/R2(I)
      D=MAXLF(D,ABSF(R3(I)))
      R1(I)=R2(I)
   38 CONTINUE
   39 IF (D-.00001) 40,40,34
   40 F=WA/B/G
      DO 41 I=1,M
      R2(I)=R2(I)*F
      R4(I)=FLOATF(I)*H
      R5(I)=C*(R4(I)**2)
      R6(I)=AM*R1(I)
   41 CONTINUE
      PRINT 6
      PRINT 5, W
      PRINT 6
      PRINT 7, (R4(I),R1(I),R2(I),R3(I),R5(I),R6(I), I=1,M)
      WC=W
      W=W+DELAB
      WA=.8062269*W
   42 IF (ABSM-W) 45,43,43
   43 DO 44 I=1,M
      S(I)=S(I)*((Z+WC)**2)/((Z+W)**2)
   44 CONTINUE
      GO TO 32
   45 CALL EXIT
      END
```

Averaged energy oscillator model m = 1 (Page 3).

```
      DIMENSION R1(150),R2(150),R3(150),R4(150),R5(150),R6(150)
      DIMENSION P(150,150),V(150),S(150)
      DIMENSION RG(150)
    1 FORMAT (I5)
    2 FORMAT (5E14.7)
    3 FORMAT (10H NO. EQNS=I5, 6H MESH=E14.7, 16H MAX ABSORPTION=E14.7,
     X7H RANGE=E14.7)
    4 FORMAT (8H ENERGY=E14.7,11H AMPLITUDE=E14.7,
     X16H DEL ABSORPTION=E14.7)
    5 FORMAT (12H ABSORPTION=E14.7)
    6 FORMAT (1H0)
    7 FORMAT (3H X=E14.7,3H N=E14.7,4H NN=E14.7,5H DEL=E14.7,
     X3H E=E14.7,5H PHI=E14.7)
      FREQUENCY  12(1,0,1),15(1,0,0),39(0,0,1),42(0,0,1)
      READ 1,M
      READ 2, H,ABSM,Z,EN,AM,DELAB,W
      PRINT 3, M,H,ABSM,Z
      PRINT 4, EN,AM,DELAB
      PRINT 5, W
      PK=.8862269
      WA=PK*W
      L=59
      DEL=.05
      DO 11 I=1,M
      X=FLOATF(I)*H
      A=0.0
      R=X
      DO 10 K=1,L
      R=R+DEL
      S=EXPF(-R*R)
      A=A+S
   10 CONTINUE
      E=.5*(EXPF(-X*X)+EXPF(-(X+3.0)**2))
      RG(I)=PK-DEL*(A+E)
   11 CONTINUE
      DO 32 I=1,M
      X=FLOATF(I)*H
      U=X*X
      D=EXPF(-U)
      V(I)=(X+.5/X)*RG(I)+.5*D
      S(I)=X*RG(I)/((Z+W)**2)
      B=2.0*X*H
      C=B*RG(I)
      DO 17 J=1,M
      Y=FLOATF(J)*H
   12 IF (Y-X) 13,14,14
   13 P(I,J)=B*RG(J)*D*EXPF(Y*Y)/Y
      GO TO 15
   14 P(I,J)=C/Y
   15 IF (J-M) 17,16,17
   16 P(I,J)=.5*P(I,J)
   17 CONTINUE
      R1(I)=U*D
   32 CONTINUE
      MM=M-1
      G=0.0
```

Wigner-Wilkins monatomic gas model, m = 1 (Page 1).

```
      B=0.0
      DO 33 I=1,MM
      G=G+S(I)
      B=B+R1(I)
   33 CONTINUE
      G=G+.5*S(M)
      B=WA*(B+.5*R1(M))
      C=G/B
      DO 34 I=1,M
      R1(I)=C*R1(I)
   34 CONTINUE
      CALL SAVE
      DO 36 I=1,M
      R2(I)=0.0
      DO 35 J=1,M
      R2(I)=R2(I)+P(I,J)*R1(J)
   35 CONTINUE
      R2(I)=(R2(I)+S(I))/(V(I)+WA)
   36 CONTINUE
      B=0.0
      DO 37 I=1,MM
      B=B+R2(I)
   37 CONTINUE
      B=WA*(B+.5*R2(M))
      C=G/B
      D=0.0
      DO 38 I=1,M
      R2(I)=C*R2(I)
      R3(I)=1.0-R1(I)/R2(I)
      D=MAX1F(D,ABSF(R3(I)))
      R1(I)=R2(I)
   38 CONTINUE
   39 IF (D-.00001) 40,40,34
   40 F=WA/H/G
      DO 41 I=1,M
      R2(I)=R2(I)*F
      R4(I)=FLOATF(I)*H
      R5(I)=EN*(R4(I)**2)
      R6(I)=AM*R1(I)
   41 CONTINUE
      PRINT 6
      PRINT 5, W
      PRINT 6
      PRINT 7, (R4(I),R1(I),R2(I),R3(I),R5(I),R6(I), I=1,M)
      WC=W
      W=W+DELAB
      WA=.8862269*W
   42 IF (ABSM-W) 45,43,43
   43 DO 44 I=1,M
      S(I)=S(I)*((Z+WC)**2)/((Z+W)**2)
   44 CONTINUE
      GO TO 32
   45 CALL EXIT
      END
```

Wigner-Wilkins monatomic gas model, m = 1 (Page 2).

```
      DIMENSION R1(150),R2(150),R3(150),R4(150),R5(150),R6(150)
      DIMENSION P(150,150),V(150),S(150)
400   FORMAT (14H TOTAL SOURCE=E14.7)
401   FORMAT (4(3H K(I3,1H,I3,2H)=E14.7))
  1   FORMAT (3I5)
  2   FORMAT (5E14.7)
  3   FORMAT (10H NO. EQNS=I5, 6H MESH=E14.7, 16H MAX ABSORPTION=E14.7,
     X7H RANGE=E14.7)
  4   FORMAT (8H ENERGY=E14.7,11H AMPLITUDE=E14.7,
     X16H DEL ABSORPTION=E14.7)
  5   FORMAT (12H ABSORPTION=E14.7)
  6   FORMAT (1H0)
  7   FORMAT (3H X=E14.7,3H N=E14.7,4H NN=E14.7,5H DEL=E14.7,
     X3H E=E14.7,5H PHI=E14.7)
  8   FORMAT (6H MASS=E14.7,6H DEL1=E14.7,6HDEL2=E14.7,4H K1=I4,
     X4H K2=I4)
  9   FORMAT(4(8H SOURCE(I3,2H)=E14.7))
      FREQUENCY 10(0,1,1),13(1,0,0),90(1,0,1),91(1,0,1),20(0,1,1),
     X23(0,0,1),25(1,0,0),92(1,0,1),31(1,0,0),93(1,0,2),94(1,0,0),
     X45(1,0,5),48(1,0,10)
      FREQUENCY 201(3,0,1),204(1,0,3),207(3,0,1),211(1,0,3)
      READ 1, M,KA,KB
      READ 2, H,ABSM,Z,EN,AM,DELAB,W,HA,D1,D2
      PRINT 3, M,H,ABSM,Z
      PRINT 4, EN,AM,DELAB
      PRINT 5,W
      PRINT 8, HA,D1,D2,KA,KB
      PI=3.1415927
      PJ=2.0/3.0/PI
      PK=.8862269
      HB=SQRTF(HA)
      WA=PK*W
      A=HA+1.0
      C=HA-1.0
      B=.5*A/HB
      D=.5*C/HB
      AC=A/C
      CA=C/A
      CB=CA*CA
      XI=1.0+CB*LOGF(CB)/(1.0-CB)
      XJ=2.0/XI
      AA=.5*A*A/HA
      MM=M-1
      DO 34 I=1,M
      CALL SAVE
      X=FLOATF(I)*H
      U=X*X
      L=0
      E=0.0
      F=X
      DO 16 K=1,KB
      L=L+1
      F=F+D2
      G=F*F
      Q=G/U
      R=SQRTF(Q-1.0)
```

Averaged energy oscillator model, m > 1 (Page 1).

```
      T=(3.0*R-ATANF(R)*(2.0+Q))*EXPF(-G*HA)
   10 IF (L-1) 11,11,12
   11 T=2.0*T
      GO TO 13
   12 L=0
   13 IF (K-KB) 15,14,15
   14 T=.5*T
   15 E=E+T
   16 CONTINUE
      V(I)=PK*(X+.25/X/HA)+E*X*D2*PJ*HB
      BA=B*X
      DA=D*X
      DO 33 J=1,M
      Y=FLOATF(J)*H
      BB=B*Y
      DB=D*Y
      AL=BA+DB
      BE=BB+DA
      GA=BA-DB
      DE=BB-DA
      L=0
      GM=GA*GA
      AP=AL*AL
      E=0.0
      EA=0.0
      EB=0.0
      F=ABSF(GA)
      FA=AL
      RR=Y-X
      RC=Y-CA*X
      RA=Y-AC*X
   90 IF(RR) 17,18,18
   17 FB=SQRTF(U-Y*Y)
   18 DO 28 K=1,KA
      L=L+1
      F=F+D1
      FA=FA+D1
      RB=SQRTF(FA*FA-AP)
      TA=(ATANF(BE/RB)-ATANF(AL/RB))*EXPF(-FA*FA)
      R=SQRTF(F*F-GM)
      T=ATANF(DE/R)+ATANF(GA/R)
      RD=EXPF(-F*F)
   91 IF(RR) 201,204,204
  201 IF(RC) 202,202,203
  202 T=T*RD
      GO TO 20
  203 T=(T-PI)*RD
      TB=EXPF(-FB*FB)
      FB=FB+D1
      GO TO 20
  204 IF (RA) 205,206,206
  205 T=(T-PI)*RD
      GO TO 20
  206 T=T*RD
   20 IF (L-1) 21,21,22
   21 T=2.0*T
```

Averaged energy oscillator model, m > 1 (Page 2).

```
      TA=2.0*TA
      GO TO 23
   22 TB=2.0*TB
      L=0
   23 IF (K-1) 25,24,25
   24 TB=.5*TB
      GO TO 27
   25 IF (K-KA) 27,26,27
   26 T=.5*T
      TA=.5*TA
   27 E=E+T
      EA=EA+TA
      EB=EB+TB
   28 CONTINUE
      RE=AA*X*H/Y
      RF=RE*D1
      RG=RF*PJ
   92 IF (RR) 207,211,211
  207 IF (RC) 208,209,210
  208 R=RG*(E+EA)
      GO TO 215
  209 R=RG*(E+EA+.25*PI*EXPF(-GM))
      GO TO 215
  210 R=RF*(2.0*EB/3.0+(E+EA)*PJ)
      GO TO 215
  211 IF (RA) 212,213,214
  212 R=RE*(PK+(E-EA)*D1*PJ)
      GO TO 215
  213 R=RG*(E-EA+.25*PI)
      GO TO 215
  214 R=RG*(E-EA)
  215 P(I,J)=R
   31 IF (J-M) 33,32,33
   32 P(I,J)=.5*P(I,J)
      CALL SAVE
   33 CONTINUE
      R4(I)=X
      R5(I)=EN*U
      R1(I)=U*EXPF(-U)
   34 CONTINUE
      IF (EN) 216,200,200
  216 PRINT 401, ((I,J,P(I,J), J=1,M),I=1,M)
  200 G=W*XJ
      Q=W*G*(XJ-1.0)
      E=AA/(XI*Q)
      F=((Z/(Z+W))**XJ)*(1.0+G/Z)
      EA=0.0
      EB=0.0
      DO 39 I=1,M
      X=FLOATF(I)*H
      XM=X/CA
   93 IF (XM-Z) 36,36,35
   35 R=((XM/(XM+W))**XJ)*(1.0+G XM)-F
      S(I)=E*X*R*AM
      GO TO 37
   36 S(I)=0.0
```

Averaged energy oscillator model, m > 1 (Page 3).

```
 37 EA=EA+S(I)
    EB=EB+R1(I)
 94 IF (I-M) 39,38,39
 38 EA=EA-.5*S(I)
    EB=EB-.5*R1(I)
 39 CONTINUE
    EB=W*EB
    EE=EA/EB
    DO 40 I=1,M
    R1(I)=EE*R1(I)
 40 CONTINUE
100 DO 42 I=1,M
    R2(I)=0.0
    DO 41 J=1,M
    R2(I)=R2(I)+P(I,J)*R1(J)
 41 CONTINUE
    R2(I)=(R2(I)+PK*S(I))/(V(I)+WA)
 42 CONTINUE
    EB=0.0
    DO 43 I=1,MM
    EB=EB+R2(I)
 43 CONTINUE
    EB=W*(EB+.5*R2(M))
    EE=EA/EB
    DEL=0.0
    DO 44 I=1,M
    R2(I)=EE*R2(I)
    R3(I)=1.0-R1(I)/R2(I)
    DEL=MAX1F(DEL,ABSF(R3(I)))
    R1(I)=R2(I)
 44 CONTINUE
 45 IF (DEL-.00001) 46,46,100
 46 EF=W/H/EA
    DO 47 I=1,M
    R2(I)=R2(I)*EF
    R6(I)=AM*R1(I)
 47 CONTINUE
    PRINT 6
    PRINT 5,W
    PRINT 6
    PRINT 7, (R4(I),R1(I),R2(I),R3(I),R5(I),R6(I),I=1,M)
    PRINT 6
    PRINT 9, (I,S(I),  I=1,M)
    PRINT 400, EA
    CALL SAVE
    W=W+DELAB
    WA=PK*W
 48 IF (ABSM-W) 49,200,200
 49 CALL EXIT
    END
```

Averaged energy oscillator model, m > 1 (Page 4).

APPENDIX F

THERMALIZATION BY A MONATOMIC GAS WITH A SPEED DEPENDENT CROSS SECTION

In this appendix is displayed the equation describing thermalization by a monatomic hydrogen gas for which the intrinsic microscopic scattering cross section is assumed to be inversely proportional to the neutron-atom relative speed.

$$\sigma_s(v_r) = \sigma_s^o / v_r \ . \tag{F-1}$$

With this one exception, all the assumptions of the thesis are used to derive the thermalization equation using a Maxwellian distribution of atom speeds.

The thermalization equation is

$$2x \int_0^x dy \frac{n(y)}{y} \left[x e^{y^2-x^2} I_1(y,x) - y I_2(x,y) \right]$$

$$+ 2x \int_x^\infty dy \frac{n(y)}{y} \left[y I_1(x,y) - x e^{y^2-x^2} I_2(y,x) \right] = n(x)[1+\Delta] , \tag{F-2}$$

where

$$x = v/\sqrt{2kT}, \qquad y = w/\sqrt{2kT}, \qquad \Delta = \frac{\sigma_a x}{\sigma_s^o} , \tag{F-3}$$

and

$$I_1(a,b) = \frac{2}{\sqrt{\pi}} \int_0^a \frac{dt\, e^{-t^2}}{t^2+b^2} \tag{F-4}$$

$$I_2(a,b) = \frac{2}{\sqrt{\pi}} \int_a^\infty \frac{dt\, e^{-t^2}}{t^2+b^2} \ .$$

The solution to equation F-2 for $\Delta = 0$ is a Maxwellian distribution of neutron speeds

$$n(x) = c_{10} x^2 e^{-x^2} . \qquad (F\text{-}5)$$

as may be verified, with some labor, by substituting in equation F-2.

However, the assumed scattering cross section is not physically plausible for large neutron speed because it goes to zero rapidly. This effect is reflected in the asymptotic solution to F-2

$$n(x) \approx \frac{c_{11} x}{x^{2/(1+\Delta)}} \qquad x \gg 1 \qquad (F\text{-}6)$$

obtained by neglecting the neutron speed gain terms and approximating the speed loss terms for large x. Thus the density at high speeds is larger than in the presence of a non-zero cross section because there is little attenuation of the distribution due to scattering out of the speed range.

APPENDIX G

THERMALIZATION BY HYDROGEN ATOMS OF SPEED u_o

If all the hydrogen atoms in a medium can be described by a single speed u_o, the atom speed distribution is

$$M(u) = \delta(u-u_o) . \tag{G-1}$$

The above atom speed distribution clearly is not likely to represent a physical situation, yet it serves to introduce the energy of the atoms into the thermalizing system so that a neutron can both gain and lose speed in a collision. In addition the distribution G-1 is sufficiently simple that considerable familiarity can be acquired with the nature of the thermalization problem.

The expression V(v) defined in Section I of the thesis (equation 37) is, for the distribution G-1,

$$V(v) = \int_{-1}^{1} \frac{d\mu}{2} \int_{0}^{\infty} du\,\delta(u-u_o) \sqrt{v^2+u^2-2vu\mu}$$

$$= u_o + \frac{v^2}{2u_o} \qquad \text{if } 0 \le v \le u_o \tag{G-2}$$

$$= v + \frac{u_o^2}{3v} \qquad \text{if } u_o \le v \le \infty .$$

The expression P(w→v) is, for m = 1,

$$P(w\to v) = v \int_{-1}^{1} \frac{d\mu}{2} \int \frac{du\,\delta(u-u_o)}{\sqrt{w^2+u^2+2uw\mu}} . \tag{G-3}$$

By proceeding as outlined in Appendix A, P(w→v) is found to be

$0 \le v \le u_o$

$$P(w-v) = \frac{2v}{u_o} \qquad \text{if } 0 \le w \le v$$
$$= \frac{2v^2}{u_o w} \qquad \text{if } v \le w \le \infty , \tag{G-4}$$

$u_o \le v \le \infty$

$$P(w-v) = \frac{2v\sqrt{u_o^2 - v^2 + w^2}}{wu_o} \qquad \text{if } \sqrt{v^2 - u_o^2} \le w \le v$$
$$= \frac{2v}{w} \qquad \text{if } v \le w \le \infty . \tag{G-5}$$

The equation describing thermalization by hydrogen atoms with the speed distribution G-1 is, in terms of $x = v/u_o$, $y = w/u_o$,

$$2x \int_0^x dy\, n(y) + 2x^2 \int_x^\infty dy \frac{n(y)}{y} = n(x)\left[1 + \frac{x^2}{3} + \Delta\right] \qquad \text{if } 0 \le x \le 1, \tag{G-6}$$

and

$$2x \int_{\sqrt{x^2-1}}^x \frac{dy\, n(y)\sqrt{1-x^2+y^2}}{y} + 2x \int_x^\infty \frac{dy\, n(y)}{y} = n(x)\left[x + \frac{1}{3x} + \Delta\right] \qquad \text{if } 1 \le x \le \infty , \tag{G-7}$$

with $\Delta = \sigma_a x/\sigma_s^o$. The above pair of equations is similar to, but much simpler than, the equations describing thermalization by a single energy hydrogen oscillator.

Equation G-6 can be reduced to a second order differential equation in terms of $h(x) = n(x)/x$, by differentiating twice. The equation is

$$(1+\Delta+\frac{x^2}{3})\frac{d^2h}{dx^2} + \frac{4x}{3}\frac{dh}{dx} + \frac{8}{3}h = 0. \tag{G-8}$$

A power series expansion about the origin

$$h(x) = \sum_{n=0}^{\infty} a_n x^n , \tag{G-9}$$

gives the recursion relation,

$$a_{n+2} = \frac{-a_n(n^2+3n+8)}{3(1+\Delta)(n+2)(n+1)} , \tag{G-10}$$

for the coefficients a_n. From G-10

$$h(x) = a_o \sum_{n=0}^{\infty} \frac{(-1)^n x^{2n} 2^n \prod_{r=0}^{n-1}(2r^2+3r+4)}{3^n(1+\Delta)^n(2n)!} + a_1 \sum_{n=0}^{\infty} \frac{(-1)^n x^{2n+1} 2^n \prod_{r=0}^{n-1}(2r^2+5r+6)}{3^n(1+\Delta)^n(2n+1)!} . \tag{G-11}$$

The solution for n(x) that is parabolic (as is $x^2 e^{-x^2}$, a Maxwellian) near the origin is

$$n(x) = a_1 x^2 \sum_{n=0}^{\infty} \frac{(-1)^n x^{2n}}{(2n+1)!} \left[\frac{2}{3(1+\Delta)}\right]^n \prod_{r=0}^{n-1}(2r^2+5r+6) \qquad 0 \le x \le 1 . \tag{G-12}$$

If the term $x^2/3$ is neglected in G-6 for small x, the solution corresponding to G-12 above is

$$n(x) = a_1 x \sin\sqrt{\frac{2}{1+\Delta}}\, x . \tag{G-13}$$

The comparable solution to the Wigner-Wilkins equations (Appendix B) for thermalization by gaseous monatomic hydrogen, for small x, is

$$n(x) = a_1 x \sin\sqrt{\frac{2}{1+\frac{\sqrt{\pi}}{2}\Delta}}\, x \qquad x = v/\sqrt{2kT} \qquad \Delta = \sigma_a x/\sigma_s . \tag{G-14}$$

For $x \gg 1$, neglecting the neutron speed gain term and $n/3x$ in G-7 leads to the solution

$$n(x) \simeq \frac{c_{12}^{x}}{(x+\Delta)^{3}} \qquad x \gg 1 \,. \tag{G-15}$$

Although the same sort of approximations used in Section II of the thesis for the single energy oscillator model can be applied to equation G-7 to give approximate analytic solutions for large x, it has not been found possible to solve G-7 exactly. It is interesting that the extremely simple atom speed distribution G-1 produces an integral equation that is only slightly more susceptible to analytic solution than integral equations derived using much more complicated atom speed distributions.

REFERENCES

1. Wigner, E.P., and Wilkins, J.E., Atomic Energy Commission Report AECD 2275, (1944), "Effect of the Temperature of the Moderator on the Velocity Distribution of Neutrons with Numerical Calculations for H as Moderator".

2. Wilkins, J.E., Atomic Energy Commission Report CP-2481, (1944), "Effect of the Temperature of the Moderator on the Velocity Distribution of Neutrons for a Heavy Moderator".

3. Fermi, Enrico, Ricerca Scientifica, VII-2 (1936), "On the Motion of Neutrons in Hydrogenous Substances", pp. 13-52.

4. Nelkin, M.S., Proceedings of Symposia in Applied Mathematics, Vol. XI (1961), "Neutron Thermalization", pp. 20-42.

5. Nelkin, M.S., Physics Review, Vol. 119, Series 2 (1960), "Scattering of Slow Neutrons by Water", pp. 741-746.

6. Kottwitz, D.A., Nuclear Science and Engineering, Vol. 7 (1960), "Thermal Neutron Flux Spectrum in a Medium with a Temperature Discontinuity", pp. 345-54.

7. Michael, P., Nuclear Science and Engineering, Vol. 8 (1960), "Thermal Neutron Flux Distributions in Space and Energy", pp. 426-31.

8. Hurwitz, H. and Nelkin, M.S., Nuclear Science and Engineering, Vol. 3 (1958), "The Thermal Neutron Spectrum in a Diffusing Medium", pp. 1-10.

9. Honeck, H.C., Nuclear Science and Engineering, Vol. 8 (1960), "The Distribution of Thermal Neutrons in Space and Energy in Reactor Lattices. Part I: Theory", pp. 193-202.

10. Brown, H. and St. John, D., Report DP-33, (1954), "Neutron Energy Spectrum in D_2O".

11. Wigner, E.P., Proceedings of Symposia in Applied Mathematics, Vol. XI (1961), "Mathematical Problems of Nuclear Reactor Theory", pp. 89-104.

12. Chapman, S. and Cowling, T.G., The Mathematical Theory of Non Uniform Gases (1952). See also reference 37 below.

13. Meghreblian, R.V. and Holmes, D.K., Reactor Theory (1960).

14. Weinberg, A.M. and Wigner, E.P., The Physical Theory of Neutron Chain Reactors, (1958).

15. Poole, M.J., et al., Progress in Nuclear Energy, Vol. II, Series I (1958), "The Measurement and Theory of Reactor Spectra", pp. 91-164.

16. McReynolds, et. al., Proceedings of the Second International Conference on the Peaceful Uses of Atomic Energy, Vol. 16 (1958), "Neutron Thermalization by Bound Hydrogen and Carbon", pp. 297-313.

17. Cohen, E.R. and Vaughan, E.U., Report: North American Aviation - SR-3377, (1959), "Thermal Neutron Spectrum In Harmonically Bound Hydrogen Moderators".

18. Cohen, E.R., Proceedings of the International Conference on the Peaceful Uses of Atomic Energy, Vol. 6 (1955), "Survey of Neutron Thermalization Theory", pp. 405-416.

19. Morse, P.M. and Feshbach, H., Methods of Theoretical Physics, Part II (1953), pp. 1092-1100.

20. Dwight, H.B., Tables of Integrals and Other Mathematical Data, (1961), Fourth Edition.

21. Bateman, H., Tables of Integral Transforms, Vol. I (1954).

22. Grobner, W. and Hofreiter, N., Integraltafel, Part II (1950), page 57.

23. Hurwitz, H., et al, Nuclear Science and Engineering, Vol. 1 (1956), "Neutron Thermalization by a Heavy Gaseous Moderator", pp. 280-312.

24. Beyster, J.R., et al., Nuclear Science and Engineering, Vol. 9, (1961), "Measurements of Neutron Spectra in Water, Polyethylene, and Zirconium Hydride", pp. 168-184.

25. Brown, D.H. and Nelkin, N.S., General Atomic Report GAMD-1176, undated, "B-Spectrum Code or Thermalization".

26. Lamb, W.E., Physics Review, Vol. 55 (1939), "Capture of Neutrons by Atoms in a Crystal", pp. 190-197.

27. Dresner, L., Resonance Absorption in Nuclear Reactors, (1960), p. 33.

28. Wilkins, J.E., Annals of Mathematics, Vol. 49 (1948), "A Note on the General Summability of Functions", pp. 189-199.

29. Morse, P.M. and Feshbach, H., Methods of Theoretical Physics, Part I (1953).

30. Hildebrand, F.B., Introduction to Numerical Analysis, (1956).

31. Cohen, E.R., Nuclear Science and Engineering, Vol. 2 (1957), "The Neutron Velocity Spectrum in a Heavy Moderator", pp. 227-45.

32. Nelkin, M.S., Nuclear Science and Engineering, Vol. 2 (1957), "Neutron Thermalization. II. Heavy Crystalline Moderator", pp. 199-212.

33. Osborn, R.K., Nuclear Science and Engineering, Vol. 3 (1958), "Some Characteristics of the Thermal Neutron Scattering Probability", pp. 29-37.

34. Nelkin, M.S. and Cohen, E.R., Progress in Nuclear Energy, Vol. III, Series I (1959), "Recent Work in Neutron Thermalization", pp. 179-193.

35. Corngold, N., Annals of Physics, Vol. 6 (1959), "Thermalization of Neutrons in Infinite Homogeneous Systems", pp. 368-398.

36. Corngold, N., Annals of Physics, Vol. 11 (1960), "Chemical Binding Effects in the Thermalization of Neutrons", pp. 338-358.

37. Landau, L.D. and Lifshitz, E.M., Quantum Mechanics, Vol. 3 of Course of Theoretical Physics (1958).

38. Nelkin, M.S., Nuclear Science and Engineering, Vol. 7 (1960), "The Decay of a Thermalized Pulse", pp. 210-216.

39. Kothari, L.S. and Khubchandani, P.G., Nuclear Science and Engineering, Vol. 7 (1960), "Slowing Down of Neutrons in Graphite Close to Thermal Equilibrium", pp. 240-244.

40. Conkie, W.R., Nuclear Science and Engineering, Vol. 7 (1959), "Velocity Dependent Neutron Transport Theory", pp. 295-303.

41. Purohit, S.N., Nuclear Science and Engineering, Vol. 9 (1961), "Neutron Thermalization and Diffusion in Pulsed Media", pp. 157-167.

42. Purohit, S.N., Nuclear Science and Engineering, Vol. 9 (1961), "Time Dependent Thermal Neutron Energy Spectra in a Monatomic Heavy Gas", pp. 305-313.

43. Corngold, N. and Zamie, L., Nuclear Science and Engineering, Vol. 9 (1961), "The Effect of Diffusion upon the Initial Phases of the Thermalization of Neutrons", pp. 367-9.

44. Parks, D.E., Nuclear Science and Engineering, Vol. 9 (1961), "The Effects of Atomic Motions on the Moderation of Neutrons", pp. 430-441.

45. De Sobrino, L. and Clark, M., Nuclear Science and Engineering, Vol. 10 (1961), "Comparison of the Wilkins Equation with Experiments on Water Systems", pp. 367-71.

46. De Sobrino, L. and Clark, M., Nuclear Science and Engineering, Vol. 10 (1961), "Comparison of the Wilkins Equation and Higher Order Approximations for Solid Moderators", pp. 372-376.

47. De Sobrino, L. and Clark, M., Nuclear Science and Engineering, Vol. 10 (1961), "A Study of Wilkins Equation", pp. 377-383.

48. Devooght, J., Nuclear Science and Engineering, Vol. 11 (1961), "Neutron Thermalization in Plane Lattices", pp. 7-18.

49. Kladnik, R. and Kuscer, I., Nuclear Science and Engineering, Vol. 11 (1961), "Milne's Problem for Thermal Neutrons in a Nonabsorbing Medium", pp. 116-120.

50. Egelstaff, P.A., Nuclear Science and Engineering, Vol. 12 (1962), "The Scattering of Thermal Neutrons by Moderators", pp. 250-259.

51. Egelstaff, P.A. and Schofield, P., Nuclear Science and Engineering, Vol. 12 (1962), "On the Evaluation of the Thermal Neutron Scattering Law", pp. 260-270.